

**Peptidergic control of reproduction and development in dipteran
insects (*Drosophila spp.* and the mosquitoes, *Aedes aegypti* and
Anopheles gambiae)**

Zatul-'Iffah Abu Hasan

Submitted in accordance with the requirements for the degree of
Doctor of Philosophy

The University of Leeds
School of Biology

September, 2016

The candidate confirms that the work submitted is his/her own and that appropriate credit has been given where reference has been made to the work of others.

This copy has been supplied on the understanding that it is copyright material and that no quotation from the thesis may be published without proper acknowledgement.

The right of Zatul-'Iffah Abu Hasan to be identified as Author of this work has been asserted by her in accordance with the Copyright, Designs and Patents Act 1988.

Acknowledgements

Principally, I would like to thank my supervisor and mentor Prof. Dr. R. Elwyn Isaac for his unwavering guidance and moral support throughout my project. Your enthusiasm and moral support kept me positive and allowed me to grow in an atmosphere of openness, where I was free to discuss new ideas. Working with you has been a privilege.

Many people helped on different projects that form this thesis. Special thanks go to:

Dr. Dusan Žitňan and Dr. Ivana Daubnerová (Institute of Zoology, Slovak Academy of Sciences, Bratislava, Slovakia) who were very helpful in teaching me the technique of *in-situ* hybridization. Thank you for being a part of my PhD and I hope many more projects in the future. To their lab members for a great hospitality during my attachment in their lab.

Professor Young-Joon Kim and lab members (GIST, Republic of Korea) for generously sharing their endless resources and ideas for this project.

Dr. Neil Audsley who was helpful since the beginning of my study and contributing in the mass-spectrum data for this thesis. Prof. Dr. Christian Wegener for valuable discussion regarding the sNPF.

Dr. Susanne Neupert for being a wonderful companion during the conference in Bagan, Myanmar and for contributing to the single-cell analysis within this thesis.

Prof. Dr. Angela Lange and Prof. Dr. Christopher J. H. Elliott who were invaluable during the bioassay contractions methods. Dr. Robert Holbrook for his advice on the contractions assay video recording.

Prof. Dr. Ian Hope, Dr. Andrew Peel, Dr. Stephanie Wright, Assoc. Prof. Dr. Glenn McConkey, and all School of Biology lecturers for generously sharing facilities and providing continuous support, you made the university feel like home for me.

Personal thanks also go to:

Firstly, to my family for their unconditional love and support, you always believed in me and allowed me to pursue my interest.

Also to my wonderful friends (no particular order) who were constantly with me throughout my PhD journey, David, Rahul, Rob, Francis, Ellie, Petra, Isra, Brittany, Elpi, Noha, Charlotte, Dayah, Helen, Fir, Ikhmal Hisyam, Mark, Nazlah, Suhana, Jiji, Anna, Caliph, Suhaila, Ella, Sherry, Zana, Tim, Jue, Rahida, Caroline, Martha, Lucy, Shafa, Deng, Ina, Umami, Areej, Noraini, Steven Laird, and those I have forgotten to mention. Thank you very much for all your support and fun times.

Abstract

Peptides and biogenic amines are important regulators of muscle activity in reproductive tissues, and therefore can play important roles in the reproductive success of insects. The role of neuropeptides was investigated in regulating contractions of the male accessory gland (MAG) and the ejaculatory duct (ED). The FlyAtlas tissue expression database indicated that *DMS*, dromyosuppressin (DMS) pro-hormone, is highly expressed in the MAGs of *D. melanogaster*. However, DMS, could not be found using HPLC and mass spectrometry, but was detected by immunohistochemistry which revealed extensive staining of neuronal processes on the surface of MAGs and ED of *Drosophila melanogaster*, *D. yakuba*, *D. erecta*, *D. virilis*, *D. simulans*, and the pest species *D. suzukii*. The GAL4-UAS expression system revealed DMS neuronal fibres descending from the abdominal ganglion onto the surface of the MAG, ED, and seminal vesicles. A pair of rectal cells and a single cell, that we have called the ejaculatory duct cell because of its projections to the ED, also contain DMS. The rectal and ED cells were isolated and subjected to MALDI-TOF mass spectrometry. Molecular ions of several neuropeptides were detected, and the identity of DMS and sNPF⁴⁻¹¹ were confirmed by fragmentation sequencing. Both DMS and sNPF⁴⁻¹¹ reduced the frequency of contractions of the MAG and ED, suggesting that these peptides are involved in regulating ejaculation of seminal fluid and spermatozoa. Furthermore, the finding of DMS-R1 and DMS-R2 expression in the epitracheal cells suggested that both receptors might be involved in adult ecdysis. The silencing of *DMS* expression using *nSyb-GAL4/UAS-dicr2>DMS-RNAi* (108760), shows abnormal abdomen phenotype and mortality at day 5 post-emergence. Inhibitors of neuropeptide metabolism were shown to be larvicidal when fed to two species of mosquitoes (*Anopheles gambiae* and *Aedes aegypti*) identifying an enzyme target for the development of novel control chemicals.

Table of Contents

| | |
|--|------|
| Acknowledgements | iii |
| Abstract | iv |
| Table of Contents | v |
| List of Tables | x |
| List of Figures | xi |
| List of Abbreviations | xvi |
| Amino acids | xxii |
| Chapter 1 General Introduction | 1 |
| 1.1 Introduction | 2 |
| 1.2 Peptidomics in <i>Drosophila</i> | 3 |
| 1.2.1 Peptide characterisation by LC-MS | 4 |
| 1.2.2 Peptide characterisation by direct peptide profiling of tissues | 5 |
| 1.2.3 Peptide characterisation in single cells or enriched neuronal populations | 6 |
| 1.2.4 Disagreements with peptide predictions and limitations of peptidomics in <i>Drosophila</i> | 6 |
| 1.3 Peptide processing in <i>Drosophila</i> | 7 |
| 1.4 Peptide receptors | 9 |
| 1.5 Neuropeptide inactivation | 10 |

| | | |
|------------------|---|----|
| 1.6 | <i>Drosophila melanogaster</i> male reproductive system | 11 |
| Chapter 2 | Materials and Methods | 15 |
| 2.1 | Source of materials | 16 |
| 2.2 | Mosquito culture | 17 |
| 2.3 | Fly culture | 17 |
| 2.4 | Fly strains | 18 |
| 2.5 | High-performance liquid chromatography (HPLC) and matrix-assisted laser desorption ionization time of flight mass spectrometry (MALDI-TOF-MS) | 19 |
| 2.6 | Immunohistochemistry | 22 |
| 2.7 | Phalloidin staining | 27 |
| 2.8 | <i>In-situ</i> hybridization | 27 |
| 2.9 | Contraction assays | 29 |
| 2.10 | Development study | 30 |
| 2.11 | Effect of ACE inhibitors on <i>Ae. aegypti</i> and <i>An. gambiae</i> enzymes | 31 |
| 2.11.1 | Preparation of mosquito enzyme | 31 |
| 2.11.2 | Assay of peptidyl dipeptidase activity | 31 |
| 2.11.3 | Behavioural and mortality effect of ACE inhibitors on <i>Ae. aegypti</i> and <i>An. gambiae</i> larvae | 32 |
| Chapter 3 | Signalling Pathways of <i>Drosophila</i> spp. : RFa peptides and Serotonin | 33 |
| 3.1 | Introduction | 34 |

| | | |
|------------------|---|-----------|
| 3.1.1 | Peptides and protein signaling molecules of the male seminal fluid | 35 |
| 3.1.2 | Sex peptide | 37 |
| 3.1.3 | RFa peptides | 39 |
| 3.1.4 | Dromyosuppressin | 42 |
| 3.1.5 | Serotonin | 42 |
| 3.1.6 | Chapter aims | 44 |
| 3.2 | Results | 45 |
| 3.2.1 | High-performance liquid chromatography-mass spectrometry (HPLC-MS) of peptides extracted from <i>D. melanogaster</i> MAGs | 45 |
| 3.2.2 | RFa immunoreactivity associated with the reproductive tissues of <i>Drosophila spp.</i> | 48 |
| 3.2.2.1 | RFa neurons innervate the MAG, ED, and SV of <i>D. melanogaster</i> | 48 |
| 3.2.2.2 | Single cells associated with male reproductive tissue and the rectum | 60 |
| 3.2.3 | Serotonin immunoreactivity associated with the reproductive tissue of <i>Drosophila spp.</i> | 63 |
| 3.2.4 | RFa-like peptide is not co-localised with serotonin in the male reproductive tissues of <i>D. melanogaster</i> and <i>D. sukuzii</i> | 68 |
| 3.3 | Discussion | 75 |
| Chapter 4 | Spatial Expression and Function of the <i>Dromyosuppressin</i> gene (<i>DMS</i>) in Male Reproductive Structures of <i>Drosophila melanogaster</i> | 80 |

| | | |
|------------------|--|-----|
| 4.1 | Introduction | 81 |
| 4.1.1 | Chapter aims | 84 |
| 4.2 | Results | 85 |
| 4.2.1 | <i>Dromyosuppressin</i> neurons of the male reproductive tract in <i>DMS>GFP</i> flies | 85 |
| 4.2.2 | No co-localisation of GFP and 5-HT in <i>DMS >GFP</i> male flies | 89 |
| 4.2.3 | <i>Dromyosuppressin</i> expression in the male abdominal ganglion, ejaculatory duct cell, and a pair of rectal cells | 92 |
| 4.2.4 | Single-cell peptidomics of <i>Drosophila melanogaster</i> ejaculatory duct cell | 96 |
| 4.2.5 | <i>DMS>GFP</i> in rectal cells of the 3 rd instar wandering larvae and adult female | 100 |
| 4.2.6 | <i>Dromyosuppressin</i> control of muscular activity of the ejaculatory duct and male accessory glands in <i>Drosophila melanogaster</i> | 102 |
| 4.2.7 | <i>Dromyosuppressin</i> receptor expression in the male reproductive tissue | 108 |
| 4.3 | Discussion | 115 |
| Chapter 5 | RNAi Silencing of <i>Dromyosuppressin</i> Expression Generates an Ecdysis Wing Phenotype | 121 |
| 5.1 | Introduction | 122 |
| 5.1.1 | Chapter aims | 124 |
| 5.2 | Results | 125 |

| | | |
|------------------|---|-----|
| 5.2.1 | Development and phenotypic effects of RNAi silencing of <i>DMS</i> expression | 125 |
| 5.2.2 | Expression of DMS-R1 and DMS-R2 in the epitracheal gland cells | 131 |
| 5.2.3 | Expression of DMS-R2 in midgut enteroendocrine cells | 140 |
| 5.3 | Discussion | 150 |
| Chapter 6 | The toxicity of angiotensin converting enzyme (ACE) inhibitors to larvae of the dengue fever mosquito, <i>Aedes aegypti</i> and malaria fever mosquito, <i>Anopheles gambiae</i> | 154 |
| 6.1 | Introduction | 155 |
| 6.1.1 | Mosquito vectors of disease | 155 |
| 6.1.2 | Angiotensin converting enzyme (peptidyl dipeptidase A, ACE) | 156 |
| 6.1.3 | Chapter aims | 159 |
| 6.2 | Results | 161 |
| 6.2.1 | Inhibition of the soluble peptidyl dipeptidase (iACE) activity from whole larvae of <i>Ae. aegypti</i> and <i>An. gambiae</i> | 161 |
| 6.2.2 | The toxicity of captopril and fosinopril to larval instars of <i>Ae. aegypti</i> and <i>An. gambiae</i> | 166 |
| 6.3 | Discussion | 169 |
| Chapter 7 | General Discussion | 171 |
| Chapter 8 | Conclusion | 179 |
| | List of References | 180 |
| | Appendix A Attempted crosses | 210 |

List of Tables

| | | |
|----------|--|-----|
| Table 1 | Details of <i>DMS-GAL4</i> and <i>DMS-R-GAL4</i> fly stocks from the Bloomington Stock Centre in Janelia Research Campus, Ashburn, Virginia, U.S.A. | 20 |
| Table 2 | Stock numbers and associated genes of fly stocks that were obtained from Bloomington Stock Centre and Vienna Drosophila Resource Centre (VDRC) via Gwangju Institute of Science and Technology, Republic of Korea. | 23 |
| Table 3 | Fly saline composition for dissection of <i>Drosophila</i> tissues. | 24 |
| Table 4 | Antibodies that were used for immunohistochemistry. | 25 |
| Table 5 | Combinations of parental flies for development study. | 30 |
| Table 6 | Peptides with C-terminal Arg-Pheamide (RFa) identified in <i>Drosophila melanogaster</i> . | 41 |
| Table 7 | The <i>DMS-R</i> expression in male reproductive tissues of <i>DMS-R1</i> and <i>DMS-R2-GAL4</i> lines from Janelia Research Campus. | 109 |
| Table 8 | A screen of Janelia Research Campus GAL4 lines for enhancers that drive expression in epitracheal cells. | 132 |
| Table 9 | IC ₅₀ values for the inhibition of larval peptidyl dipeptidase. | 165 |
| Table 10 | Larvicidal activity of captopril and fosinopril against <i>Aedes aegypti</i> larvae. | 167 |
| Table 11 | Larvicidal activity of captopril and fosinopril against <i>Anopheles gambiae</i> larvae. | 168 |

List of Figures

| | | |
|-----------|--|----|
| Figure 1 | The amino acid sequence of the myosuppressin preprohormone of <i>D. melanogaster</i> translated from nucleic acid sequences (FlyBase). | 8 |
| Figure 2 | <i>Drosophila melanogaster</i> reproductive tissue. | 13 |
| Figure 3 | Striated and smooth muscles surround <i>D. melanogaster</i> male reproductive tissues. | 14 |
| Figure 4 | The structure of <i>D. melanogaster</i> sex peptide. | 38 |
| Figure 5 | The structure of serotonin or 5-hydroxytryptamine (5-HT). | 43 |
| Figure 6 | HPLC traces (214 nm) from the reverse-phase chromatography of an extract of 75 <i>D. melanogaster</i> MAGs. | 47 |
| Figure 7 | Distribution of RFa immunoreactivity on the surface of <i>D. melanogaster</i> MAGs and ED. | 50 |
| Figure 8 | RFa expression in a cross-section of the <i>D. melanogaster</i> ED using a confocal microscope. | 51 |
| Figure 9 | RFa immunoreactivity in the CNS of <i>D. melanogaster</i> wandering larvae. | 53 |
| Figure 10 | RFa expression in <i>D. erecta</i> reproductive tissues. | 55 |
| Figure 11 | RFa expression in <i>D. yakuba</i> tissues. | 56 |
| Figure 12 | RFa expression (white arrows) in <i>D. virilis</i> reproductive tissue detected with RFa antiserum. | 59 |
| Figure 13 | RFa expression in <i>D. simulans</i> reproductive tissue detected with RFa antiserum. | 59 |

| | | |
|-----------|---|----|
| Figure 14 | Single bright cell detected with RFa antiserum close to the <i>D. melanogaster</i> ED (see white arrow). | 60 |
| Figure 15 | The single ED cell of (A) <i>D. melanogaster</i> (B) <i>D. erecta</i> , and (C) <i>D. yakuba</i> detected with RFa antiserum. | 61 |
| Figure 16 | Bright cells detected with RFa antiserum at different plane of the <i>D. simulans</i> rectum tissue. | 62 |
| Figure 17 | Serotonergic processes at <i>D. melanogaster</i> MAGs, SV, and ED detected with 5-HT antibody. | 63 |
| Figure 18 | Serotonergic processes in <i>D. erecta</i> MAG detected with 5-HT antibody. | 64 |
| Figure 19 | The serial optical section images of <i>D. erecta</i> serotonergic processes on MAG, ED, and SV from 16 images taken every 2.6 μm (40x magnification). | 67 |
| Figure 20 | Expression of serotonergic processes in <i>D. yakuba</i> MAGs and SV detected with 5-HT antibody (40x magnification). | 67 |
| Figure 21 | Confocal microscopy of the double-labelling staining of RFa and 5-HT of <i>D. melanogaster</i> ED and MAG (40x magnification). | 68 |
| Figure 22 | The serial optical section images of RFa (red) and 5-HT (green) IHC (40x magnification) confirm the absence of co-localisation of these neurotransmitters in neurites on the surface of the ED and MAG. | 69 |
| Figure 23 | Cross section of <i>D. melanogaster</i> RFa (red) and 5-HT (green) staining (40x magnification). | 70 |
| Figure 24 | RFa and 5-HT expression in the CNS of wandering larvae of <i>D. melanogaster</i> . | 71 |
| Figure 25 | RFa and 5-HT expressions at <i>D. sukuzii</i> MAG detected with RFa and 5-HT antisera. | 73 |

| | | |
|-----------|---|-----|
| Figure 26 | RFa (red) and 5-HT (green) neurons in <i>D. suzukii</i> MAG and ED. | 74 |
| Figure 27 | The <i>GAL4</i> fly line (61H01) uses a 1413bp intergenic promoter region that extends into the first exon of <i>DMS</i> to drive expression of the yeast transcriptional activator <i>GAL4</i> . | 83 |
| Figure 28 | Characterisation of RFa immunoreactivity on the surface of the ED in <i>DMS>GFP</i> male flies. | 86 |
| Figure 29 | Ejaculatory bulb (EB) auto-fluorescent expression in <i>UAS-pJFRC81</i> male flies (4x magnification). | 87 |
| Figure 30 | <i>DMS</i> neurons in the adult male <i>DMS>GFP</i> in crop. | 88 |
| Figure 31 | The <i>DMS-GAL4</i> transgene generates GFP expression in the MAG, ED, and SV tissues. | 91 |
| Figure 32 | Male <i>DMS-GAL4</i> neurons of the AbG that innervate abdominal organs. | 94 |
| Figure 33 | A cartoon describing the innervation of male abdominal organs by <i>DMS</i> neurons. | 95 |
| Figure 34 | MALDI-TOF mass spectra obtained from a single ED cell of <i>DMS>GFP</i> adult male fly. | 97 |
| Figure 35 | The <i>sNPF-GAL4</i> transgene generates GFP expression in the ED cell. | 99 |
| Figure 36 | The <i>DMS-GAL4</i> transgene generates GFP expression in the rectal cells of adult female and 3 rd instar larvae. | 101 |
| Figure 37 | <i>DMS</i> inhibits the frequency of ED contractions. | 103 |
| Figure 38 | <i>DMS</i> inhibits the number of ED contractions in a dose dependent manner, with EC_{50} of 1.5×10^{-8} M. | 104 |
| Figure 39 | <i>sNPF</i> ⁴⁻¹¹ inhibits the frequency of ED contractions. | 106 |

| | | |
|-----------|---|-----|
| Figure 40 | DMS and sNPF ⁴⁻¹¹ inhibit the frequency of MAG contractions. | 107 |
| Figure 41 | GFP in the secondary cells of <i>DMS-R1</i> and <i>DMS-R2</i> present in two short fragments of the respective receptors. | 111 |
| Figure 42 | Characterisation of <i>DMS-R1 (48230)>GFP</i> on the surface of the male reproductive tissues. | 113 |
| Figure 43 | Characterisation of myofibres expression in the MAGs and ED of tagged GFP myosin flies. | 114 |
| Figure 44 | Diagram of transgenic RNAi in <i>Drosophila</i> adapted from the VDRC. | 122 |
| Figure 45 | Janelia Research Campus GAL4 lines <i>DMS-R</i> gene map | 123 |
| Figure 46 | Epitracheal cells in <i>D. melanogaster</i> larvae. | 124 |
| Figure 47 | Phenotype of adult <i>D. melanogaster</i> OR R wild-type, adult <i>nSyb-GAL4/UAS-dicr2</i> , adult <i>DMS-RNAi</i> (108760), and adult <i>nSyb-GAL4/UAS-dicr2>DMS-RNAi</i> (108760) flies. | 127 |
| Figure 48 | Morphology of the wings in flies lacking <i>DMS</i> function. | 128 |
| Figure 49 | The <i>nSyb-GAL4/UAS-dicr2>DMS-RNAi</i> (108760) adult male shows no expression of RFa (DMS) in reproductive tissue. | 130 |
| Figure 50 | Double-labelling with anti-GFP (green) and anti-ETH (red) antibodies in <i>DMS-R2 (39399)>GFP</i> 3 rd instar larvae. | 136 |
| Figure 51 | ETH-GFP reporter activity in epitracheal cells (stained green) on 3 rd instar <i>ETH>GFP</i> larvae. | 137 |
| Figure 52 | Double-labelling with anti-GFP and anti-ETH antibodies of the trachea from 3 rd instar larvae of <i>D. melanogaster DMS-R1 (48230)>GFP</i> . | 139 |

| | | |
|-----------|--|-----|
| Figure 53 | The <i>DMS-R2</i> (39399)- <i>GAL4</i> transgene generates GFP expression in epitracheal cells, brain, and midgut endocrine cells. | 141 |
| Figure 54 | GFP and ETH expression in 3 rd instar larvae of <i>DMS-R2</i> (46556)>GFP. | 143 |
| Figure 55 | GFP fluorescence in the brain and proventriculus area of <i>DMS-R2</i> (46556)> <i>GFP</i> 3 rd instar larvae. | 144 |
| Figure 56 | <i>DMS-R2</i> localisation in <i>DMS-R2</i> > <i>GFP</i> 3 rd instar larvae. | 147 |
| Figure 57 | The GFP expression in the corpora cardiaca (CC) of <i>DMS-R2</i> > <i>GFP</i> 3 rd instar larvae. | 149 |
| Figure 58 | Chemical structures of inhibitors of mosquito larval peptidyl dipeptidase activity. | 160 |
| Figure 59 | The relative activity of peptidyl dipeptidase in a homogenate of mosquito larvae before and after high-speed centrifugation. | 162 |
| Figure 60 | Inhibition of the peptidyl dipeptidase activity of <i>Ae. aegypti</i> larvae. | 163 |
| Figure 61 | Inhibition of the peptidyl dipeptidase activity of <i>An. gambiae</i> larvae. | 164 |

List of Abbreviations

| | |
|------------------|--|
| μl | Microliter |
| 5-HT | Serotonin or 5-hydroxytryptamine |
| AbG | Abdominal ganglion |
| ACE | Angiotensin converting enzyme |
| <i>Aea-HP-1</i> | <i>Aedes aegyti</i> head peptide |
| AKH | Adipokinetic hormone |
| AnCE | <i>Drosophila melanogaster</i> angiotensin converting enzyme |
| <i>AnoACE</i> | <i>Anopheles gambiae</i> ACE gene |
| AP | Alkaline phosphatase buffer |
| BLAST | Basic Local Alignment Search Tool |
| BPP-12b | Bradykinin-potentiating peptide |
| BSA | Bovine serum albumin |
| Ca^{2+} | Calcium ions |
| CaCl_2 | Calcium chloride |
| cAMP | Cyclic adenosine monophosphate |
| CAPA | Capability neuropeptide |

| | |
|------------------|--|
| CapHPLC | Capillary high-performance liquid chromatography |
| CC | Corpora cardaica |
| CCAP/CAP2b | Crustacean cardioactive peptide |
| cDNA | Complementary DNA |
| Cm | Centimetre |
| CNS | Central nervous system |
| CO ₂ | Carbon dioxide |
| DAPI | 4',6-diamidino-2-phenylindole |
| dFMRFamides | <i>Drosophila</i> FMRFamide |
| DH31 | Diuretic hormone 31 |
| DMS | Dromyosuppressin |
| DMS-R1 | Dromyosuppressin receptor 1 |
| DMS-R2 | Dromyosuppressin receptor 2 |
| DSK | Drosulfakinin |
| EB | Ejaculatory bulb |
| EC ₅₀ | Half maximal effective concentration |
| ED | Ejaculatory duct |
| EH | Eclosion hormone |
| ESI-Q-TOF MS/MS | Electrospray ionisation quadrupole time-of-flight mass spectrometry |
| ETH | Ecdysis triggering hormone |

| | |
|------------------|---|
| ETH-1 | Ecdysis triggering hormone-1 |
| ETH-2 | Ecdysis triggering hormone-2 |
| FaRPs | FMRFamide-related peptides |
| FERA | Food and Environment Research Agency |
| <i>Fru</i> | <i>Fruitless</i> |
| FT | Fourier transform |
| GAL4 | Galactose-responsive transcription factor |
| GD | P-Element RNAi Stocks |
| GFP | Green fluorescent protein |
| GIST | Gwangju Institute of Science and Technology |
| GPCR | G protein coupled receptor class |
| GTX-PBS | Goat serum in Triton X-100 phosphate buffer saline |
| H ₂ O | Water |
| HEPES | 4-(2-hydroxyethyl)-1-piperazineethanesulfonic acid |
| HG | Hindgut |
| hP | 4-hydroxyproline |
| HPLC | High-performance liquid chromatography |
| hpRNAs | hairpin RNA |
| HS | Hybridization solution |
| iACE | Insect angiotensin converting enzyme |
| IC ₅₀ | Half maximal response of an inhibitor concentration |

| | |
|-------------------|---|
| IgG | Immunoglobulin G |
| IHC | Immunohistochemistry |
| ISH | <i>In-situ</i> hybridization |
| KCl | Potassium chloride |
| kDa | Kilo dalton |
| KK | Phic31 RNAi Stocks |
| KO | Knockout |
| L1 | Larval instars 1 |
| L2 | Larval instars 2 |
| L3 | Larval instars 3 |
| LC-MS | Liquid chromatography–mass spectrometry |
| LK | Leucokinin |
| m/z | Mass/charge number of ions |
| MAG | Male accessory gland |
| MALDI | Matrix-assisted laser desorption ionization |
| MALDI-TOF-MS | Matrix-assisted laser desorption ionization time of flight mass spectrometry |
| Mg | Milligram |
| MgCl ₂ | Magnesium Chloride |
| ml | Millilitre |

| | |
|--------------------|---|
| mM | Milimolar |
| MOL | Muscle of Lawrence |
| MS | Mass spectrometry |
| NaCl | Sodium Chloride |
| NaHCO ₃ | Sodium bicarbonate |
| NBT-BCIP | Nitroblue tetrazolium salt/5-bromo-4-chloro-3-indolyl-phosphate |
| NPF | Neuropeptide F |
| °C | Degrees Celsius |
| PBS | Phosphate buffer saline |
| PBST20 | Phosphate buffer saline 0.2% Tween 20 |
| pE | Pyroglutamic acid |
| PETH | Pre-ecdysis triggering hormone |
| PK | Proteinase K |
| RFa | C-terminal Arg-Pheamide |
| RH | Relative humidity |
| RNA | Ribonucleic acid |
| RNAi | RNA interference |
| RP-HPLC | Reverse phase high performance liquid chromatography |
| SFPs | Seminal fluid proteins or peptides |

| | |
|-------------------|---|
| sNPF | Short neuropeptide F |
| SP | Sex peptide |
| SV | Seminal vesicle |
| TFA | Trifluoroacetic acid |
| TMOF | Trypsin-modulating oostatic factor |
| Trp | Tryptophan |
| TX-PBS | Triton X-100 in phosphate buffer saline |
| U.K. | United Kingdom |
| U.S.A. | United State of America |
| UAS | Upstream activation sequence |
| v/v | Volume per volume |
| VD | Vas deferens |
| VDRC | Vienna Drosophila Resource Centre |
| VNC | Ventral nerve cord |
| w/v | Weight per volume |
| ZnCl ₂ | Zinc Chloride |

Amino acids

| Amino acid | Three Letter Abbreviation | One Letter Abbreviation |
|---|---------------------------|-------------------------|
| Nonpolar Amino Acids (hydrophobic) | | |
| Alanine | Ala | A |
| Glycine | Gly | G |
| Isoleucine | Ile | I |
| Leucine | Leu | L |
| Methionine | Met | M |
| Phenylalanine | Phe | F |
| Proline | Pro | P |
| Tryptophan | Trp | W |
| Valine | Val | V |
| Polar Amino Acids (hydrophilic) | | |
| Asparagine | Asn | N |
| Cysteine | Cys | C |
| Glutamine | Gln | Q |
| Serine | Ser | S |
| Threonine | Thr | T |
| Tyrosine | Tyr | Y |
| Electrically Charged (negative and hydrophilic) | | |
| Aspartic acid | Asp | D |
| Glutamic acid | Glu | E |
| Electrically Charged (positive and hydrophilic) | | |
| Arginine | Arg | R |
| Histidine | His | H |
| Lysine | Lys | K |

Chapter 1

General Introduction

1.1 Introduction

Neuropeptides are neuronal signalling molecules that modulate the activity of the brain and body. Neuropeptides can act as neuromodulators in the central nervous system (CNS) and as peptide hormones released from neurohemal sites or endocrine cells into the circulation to regulate body functions. These body functions include any biological processes from basal physiology, such as carbohydrate metabolism and control of diuresis, to complex behaviours, such as courtship and learning. In some of the cases, peptides serve as both neuronal modulators/chemical transmitters and as circulating hormones. Hence, it is possible that this structurally diverse group of signalling molecules represent the first messengers used by the CNS and endocrine systems to communicate between cells and coordinate physiology and behaviour in animals. Both neuropeptides and peptide hormones (regulatory peptides) are synthesized from larger precursor molecules by the same sets of specific enzymes to generate bioactive molecules (Pauls *et al.*, 2014).

The study on these regulatory peptides in insects have made important contributions to the detailed understanding of systems critical for development and ecdysis, the productions and release of other peptide hormones, modulation of feeding-related behaviours, metabolic homeostasis and reproduction and fertility (Nässel and Winther, 2010b). Mass spectrometry combined with HPLC techniques to chemically characterise the regulatory peptides, the so-called peptidome, has provided the fundamental knowledge for the functional studies of insect neuropeptides. A major step forward was the sequencing of the first insect genome, which for the first time allowed systematic analysis of pro-hormone genes for known peptides and the

prediction of novel peptides (Adams *et al.*, 2000). The peptidomics approach is still the most reliable way to identify the regulatory peptides since the genome prediction software is not always accurate and the way in which pro-hormones are processed and peptides undergo posttranslational modification (e.g. hydroxylation of Pro as in sex peptide) is not completely predictable (Pauls *et al.*, 2014). The prediction is difficult as the neuropeptide sequences are small and fairly variable in structure. The data can only be retrieved when there is an amino acid sequence available from a homolog from previously identified neuropeptides or a number of very similar peptide sequences separated by putative convertase processing sites (Veenstra, 2016). Other methods such as IHC and ISH will confirm the outcome of the peptidomics study.

1.2 Peptidomics in *Drosophila*

In *Drosophila*, a total of 7 neuropeptides were biochemically characterised up to the year 2000 (Schaffer *et al.*, 1990; Nichols, 1992a; Nichols, 1992b; Terhzaz *et al.*, 1999) which were cited by Pauls *et al.* (2014). These cover the finding of adipokinetic hormone (AKH) (Schaffer *et al.*, 1990), drosulfakinin (DSK) (Nichols, 1992a), four FMRFa peptides (DPKQDFMRFa, TPAEDFMRFa, SDNFMRFa, and TDVDHVFLRFa) (Nichols, 1992b), and leucokinin (LK) (Terhzaz *et al.*, 1999). Concurrently, several dozens of peptides were sequenced in larger insect species such as cockroaches and locusts (Schoofs *et al.*, 1997; Predel *et al.*, 2001). The sequencing of the *Drosophila* genome (Adams *et al.*, 2000) alongside peptidomics techniques, LC/MS-MS (Tinoco and Saghatelian, 2011) and direct peptide profiling

of nervous and endocrine tissues (Wegener *et al.*, 2010) is proving powerful approach to obtain a complete *Drosophila* peptidome.

1.2.1 Peptide characterisation by LC-MS

The *Drosophila* peptidomics study started from the discovery of 28 neuropeptides characterised from a 50 *Drosophila* larvae CNS extract using one-dimensional capillary high-performance liquid chromatography (capHPLC)/electrospray ionisation quadrupole time-of-flight mass spectrometry (ESI-Q-TOF MS/MS) (Baggerman *et al.*, 2002). The study was improved by upgrading to two-dimensional capHPLC-separation, yielding 38 peptides from 50 larval CNS (Baggerman *et al.*, 2005). Over time, using different LC/MS/MS combination, more peptides were successfully identified. From *Drosophila* brain extracts, a total of 42 neuropeptides were characterised using LS/MS-MS MALDI- Fourier Transform (FT) MS and the full sequence of 26 peptides using ESI-QTOF MS/MS (Yew *et al.*, 2009). Also, some of these peptides were determined in a *Drosophila* midgut extract; this midgut area contains enteroendocrine cells. All 24 enteroendocrine peptides were identified using offline capHPLC combined with MALDI-TOF MS/MS (Reiher *et al.*, 2011) and classified as brain-gut peptides.

1.2.2 Peptide characterisation by direct peptide profiling of tissues

Direct peptide profiling has been successfully used to identify *Drosophila* peptides; this technique is related to MALDI-TOF imaging. It is carried out on dissected whole tissues such as neurohemal organ, for example the corpora cardiaca (CC), thoracic perisymphathetic organ, and abdominal perisymphathetic organ or part of the digestive tract. The tissue is transferred to a MALDI target plate and left to dry (Wegener *et al.*, 2010). The peptides are extracted by adding appropriate matrix solution and directly analysed by MALDI-MS. Compared to LC-MS analyses, this technique can also specifically characterise and identify single peptides of interest (Winther *et al.*, 2003; Audsley *et al.*, 2011). However, the major advantage of this technique is peptide loss during LC and adsorption to plastic-ware can be avoided (Pauls *et al.*, 2014). The on-plate extraction gives broad selective extractions of regulatory peptides, but not peptides present in the cytosol, mitochondria, and/or nucleus (intracellular peptides) (Ferro *et al.*, 2014), and it avoids cell disruption compared to the conventional method. This technique was first used in insects to characterise the adult neuropeptidome from neurohemal organs and brain tissue revealing 32 different neuropeptides in adult *D. melanogaster* (Predel *et al.*, 2004). Later by using the same approach, 23 different peptides have been identified in larval neurohemal organ and the endocrine/epitracheal cells (Wegener *et al.*, 2006). This technique led to the discovery of a differential processing of the CAPA neuropeptides between neurohemal organs of the brain and the ventral ganglion (Predel *et al.*, 2004; Wegener *et al.*, 2006).

1.2.3 Peptide characterisation in single cells or enriched neuronal populations

A single-cell analysis is an approach to isolate single identified fly neurons for mass spectrometric analysis. The targeted neurons can be detected using GAL4 promotor lines to drive expression of a green fluorescent protein (GFP) under upstream activating sequence (UAS) control. These neurons isolated under the fluorescence microscope are subjected to MALDI-TOF mass spectrometry. This technique is difficult but it is a valuable method to master, as it can isolate single neurons of interest for MS analysis, hence eliminate any neurons that may overlay on top of the targeted neurons. The analysis not only shows peptides expressed from specific peptides precursors, but it will also reveal information about co-localisation with other neuropeptides in the targeted GFP neurons (Neupert *et al.*, 2007).

1.2.4 Disagreements with peptide predictions and limitations of peptidomics in *Drosophila*

The improvement of peptide processing prediction and development of new bioinformatics tools and pipelines have contributed to the expanding genomic and peptidomic data. The nearly complete data obtained allows bioinformatic comparison of the pro-hormone obtained from the genome data with a large set of actually made peptides (Pauls *et al.*, 2014). However, up till now the prediction technique is still not precise. For example, sNPF-1 is predicted long form with 11 amino acids (AQRSPSLRLRFa) (Broeck, 2001; Clynen *et al.*, 2009), the sNPF⁴⁻¹¹

and sNPF-2¹²⁻¹⁹ (SPSLRLRFa) are more abundant compared to sNPF-1 (Pauls *et al.*, 2014).

1.3 Peptide processing in *Drosophila*

The processing of peptide pro-hormones in insects appears to be very similar to what occurs in other animals (Veenstra *et al.*, 2008). Pro-hormones are made as prepro-hormones with a classical N-terminal hydrophobic signal peptide sequence for entry into the secretory pathway. This signal peptide is cleaved by a signal peptidase to the pro-hormone which then undergoes limited proteolysis by the action of trypsin-like enzymes known as pro-hormone convertases. These enzymes recognise pairs or sometimes single basic residues and therefore peptide sequences are usually flanked by basic amino acids in the pro-hormone (Figure 1). It is not unusual for pro-hormones to contain several peptide sequences separated by basic residues. These reactions take place in secretory vesicles and generate peptides with Arg or Lys at the C-terminus. These peptides are then trimmed back from the C-terminus by carboxypeptidases, such as carboxypeptidase E. Many mature insect neuropeptides possess an α -amidated C-terminus rather than a charged carboxyl group. The amide group is formed by the action of amidating enzymes on the α -NH₂ of glycine (Eipper *et al.*, 1992) and therefore pro-hormone sequences of amidated peptides can often be recognised by a motif similar to Gly-Lys-Arg (Figure 1).

MSFAQFFVACCLAIVLLAVSNTRAAVQGPPLCQSGIVEEMPPHIRKVCQALENSDQLTS
*ALKSYINNEASALVANSDDLKKNYNKRTDVDHVFLRF***GKRR**

Figure 1 The amino acid sequence of the myosuppressin prepro-hormone of *D. melanogaster* translated from nucleic acid sequences (FlyBase). The signal peptide sequence is in italics, the dibasic cleavage motifs are in red, the Gly used for α amidation is in blue and the sequence of the mature myosuppressin peptide is in bold.

1.4 Peptide receptors

The majority of insect neuropeptides and hormones act through high-affinity binding to cell surface receptors of the G protein coupled receptor class (GPCR). The receptors and their ligands are often evolutionarily conserved so that they can readily be identified in insect genomes by BLAST (Basic Local Alignment Search Tool) homology searches (Hauser *et al.*, 2008). Most have been characterised pharmacologically by expression in mammalian cells with suitable signal transduction mechanisms that link ligand binding to a cellular response such as changes in intracellular Ca^{2+} levels. The structure of insect GPCRs remain to be elucidated, but they appear to have 7 transmembrane domains and are coupled to trimeric G proteins that transduce the signal downstream to increase intracellular Ca^{2+} or elevate or decrease levels of cAMP. The de-orphanisation of *D. melanogaster* GPCRs has been a major step forward in understanding the mechanism of action of neuropeptides and has permitted the use of targeted genetic techniques to study the physiological role of the signalling pathways (Claeys *et al.*, 2005; Poels *et al.*, 2007).

1.5 Neuropeptide inactivation

Once released from a nerve or endocrine cell, peptides will be subjected to attack by extra-cellular peptidases, either on the surface of cell membranes or in the soluble extracellular environment. Peptide hormones released into the circulation will be vulnerable to haemolymph peptidases as well as those on the surface of tissues such as fat body that have large surface areas. Neprilysins and angiotensin converting enzymes (ACE) are two endopeptidase families that have been implicated in insect peptide metabolism (Isaac and Shirras, 2013).

Neuropeptides and peptide hormones are protected to some extent from exo-peptidase attack at the C-terminus by α -amidation and at the N-terminus by the presence of a cyclic pyroglutamate or Pro as the second amino acid. The positioning of Pro as the second residue makes the first N-terminal peptide bond metabolically stable because of the cyclic nature of the Pro side-chain (Cottrell *et al.*, 2012). These structural properties of many insect peptides are therefore not only important for receptor binding but also for protection from metabolic inactivation.

1.6 *Drosophila melanogaster* male reproductive system

The *D. melanogaster* male reproductive system consists of paired testes, paired vas deferens (VD) dilated in the posterior part to form paired seminal vesicles (SV), paired accessory gland (MAG), and unpaired ejaculatory duct (ED) with an appended ejaculatory bulb (EB) (see Figure 2). In recently emerged flies, all the organs are colourless. However, the testes and the SV gradually become bright-yellow. The colour fades in fixed material. The testes are in a compact coil shape and filled with male sex cells (spermatozoa) in various stages of development. The mature sperm are present as early as when the fly emerges from the pupal case. SVs of newly emerged flies contain no sperm, and subsequently each is filled with a compact mass of spermatozoa.

The ED contains two portions; a dilated thick-walled anterior ED extending to the EB, and a slender thin-walled posterior ED extending from the bulb to the aedeagus. The aedeagus is a chitinised tube that is morphologically different between *Drosophila* species. At the beginning of the copulation process, this chitinised tube can be pushed out through the genital opening between the lower ends of the genital arch. The MAGs are a pair of elongated sacs that open separately into the common anterior ED. The glands contain colourless cloudy fluid that is rich in proteins, carbohydrate and lipid and which forms the bulk of the seminal fluid that is important for the egg fertilisation (reviewed in (Wolfner, 1997)). It has been reported that the sperm that are taken from the SVs and injected into the female reproductive tissue produce fewer offspring compared to the normally ejaculated sperm carried in the seminal fluid.

The *D. melanogaster* male reproductive tissues apart from testes are surrounded by distinct mononucleated or multinucleated striated muscle sheath. In testes, the tissue is covered by pigment cells, followed by smooth muscle sheath. By using phalloidin F-actin dye, the muscle of the ED (Figure 3A), MAG (Figure 3C), and SV (Figure 3D) can be visualised. The EB has thick linear muscle fibers (Figure 3B). At the MAG muscle sheath, interconnections of different muscles can be seen (arrowheads in Figure 3C) (Susic-Jung *et al.*, 2012). More detailed introduction to the molecules found in the seminal fluid and the role of peptides and serotonin (5-HT) in male reproduction is provided in Chapter 3.

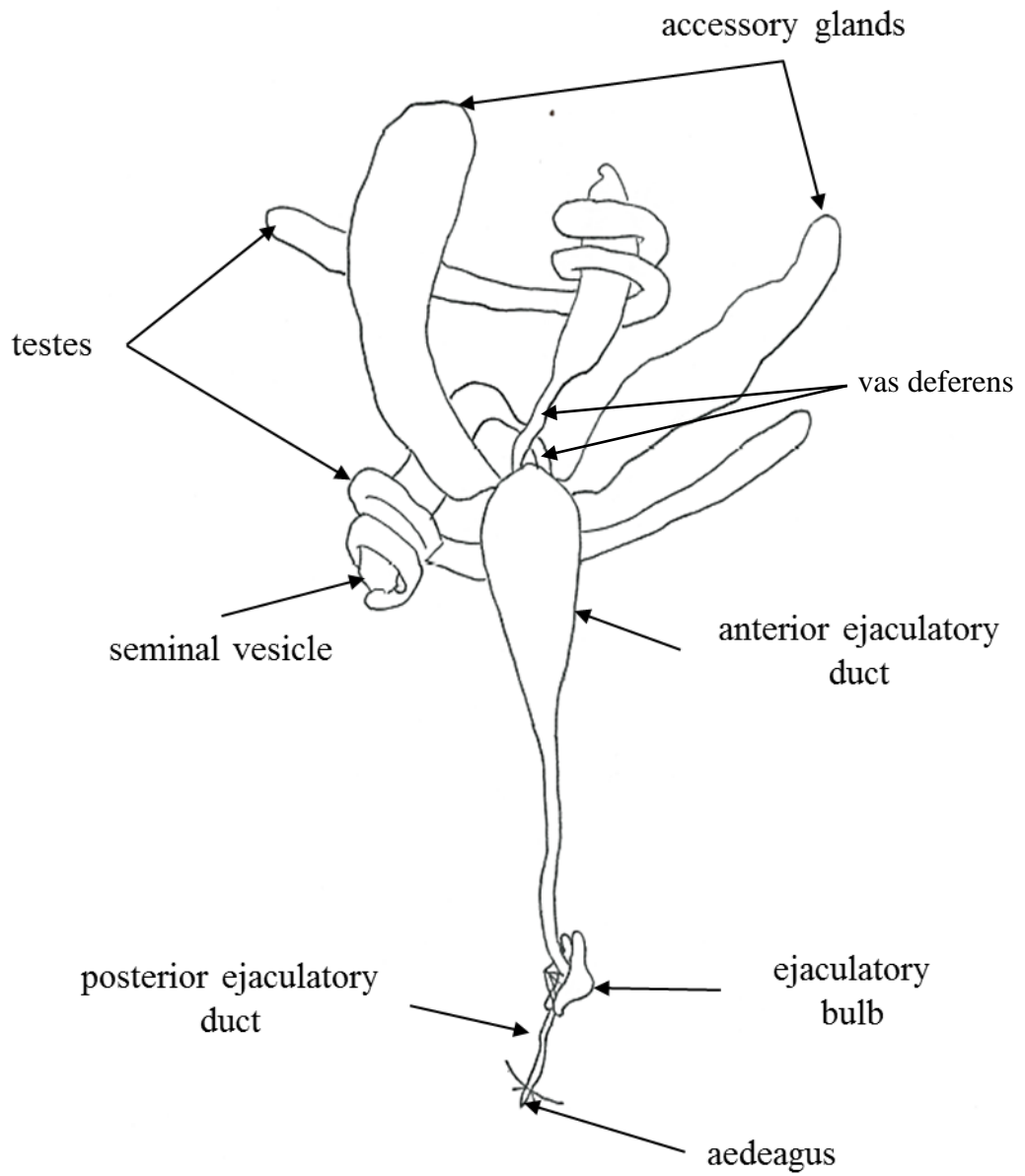


Figure 2 *Drosophila melanogaster* reproductive tissue.

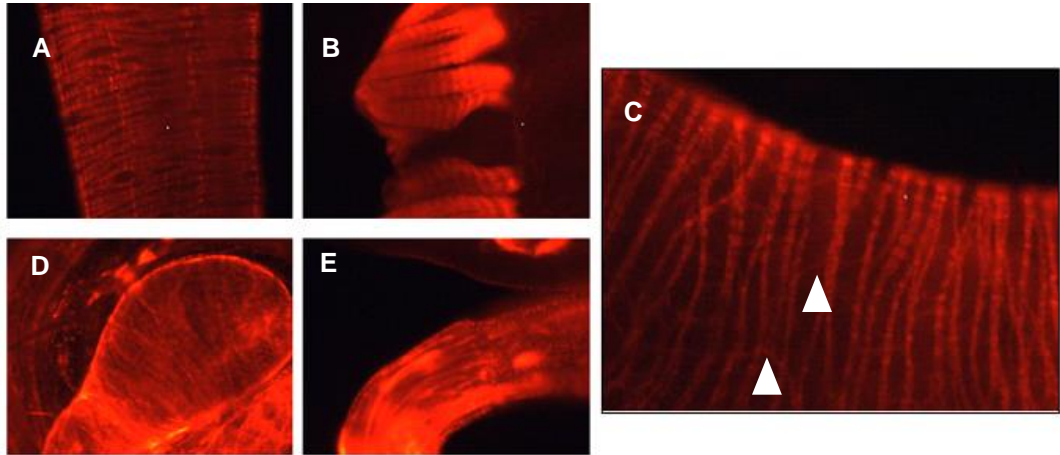


Figure 3 Striated and smooth muscles surround *D. melanogaster* male reproductive tissues. F-actin projected with phalloidin for muscle sheaths. (A) F-actin distributed throughout the whole muscle layer of ED, (B) EB, (C) MAG, (D) SV shows striated muscle layer compare to (E) actin detection at testis tissue shows smooth muscle projection. (C) The muscle fibres of the MAG connected by thin muscle fibres (arrowheads). (20x magnification).

Chapter 2

Materials and Methods

2.1 Source of materials

High-performance liquid chromatography (HPLC) and matrix-assisted laser desorption ionization time of flight mass spectrometry (MALDI-TOF-MS) solvents were purchased from Sigma-Aldrich (Dorset, U.K.). Immunohistochemistry (IHC) rabbit anti-RFa and rat anti-serotonin primary antibodies were obtained from Peninsula (California, U.S.A.) and Serotec (Kidlington, U.K.) respectively. All other primary and secondary antibodies were purchased either from Life Technologies Ltd. (Paisley, U.K.) or were a gift from collaborators as stated in Table 4. The phosphate buffer saline (PBS) tablets and Vectashield® Mounting Medium was purchased from MP Biomedicals (U.K.) and Vector Laboratories Incorporation (Burlingame, U.K.) respectively. Fosinopril was purchased from Generon Ltd., Maidenhead, Berkshire, U.K. TMOF and BPP-12b was purchased from Biomatik USA, LLC, Wilmington, Delaware, U.S.A. The ACE substrate Abz-Phe-Arg-Lys(Dnp)-Pro-OH (Abz-FRK(Dnp)-P) was from Enzo Life Sciences (U.K.) Ltd, Exeter, U.K. All other ACE inhibitors and chemicals were purchased from Sigma-Aldrich (Dorset, U.K.) and were of molecular biology grade.

2.2 Mosquito culture

Aedes aegypti and *Anopheles gambiae* were maintained in a room kept at $27 \pm 2^\circ\text{C}$ with 70 - 85% relative humidity (RH) under 12:12, light:dark photoperiod. Larvae were reared in white trays containing distilled water. Pupae were transferred from the trays into a small beaker containing distilled water and placed in a screened cage (30 cm x 30 cm x 30 cm) where adults emerged and were maintained. Adults were continuously provided with sucrose solution (10% (w/v)). On day 5 post-emergence, the adult females were deprived of sucrose overnight, then provided with a tube of human blood for blood-feeding for egg production. Eggs were collected on wet filter paper and stored at $27 \pm 2^\circ\text{C}$ with 70 - 85% RH.

2.3 Fly culture

D. melanogaster strains were maintained in bottles on a standard *Drosophila* diet (7.38% (w/v) fine oatmeal, 0.84% (w/v) fly agar, 0.84% (w/v) yeast, 5.00% (w/v) molasses, 3.40% (w/v) 10% (w/v) methyl 4-hydroxy benzoate) at 25°C with a 12:12; light: dark photoperiod. The newly eclosed male and female adults were collected at least 3 days before dissection after light anaesthesia under CO_2 and maintained separately in food vials at 25°C .

2.4 Fly strains

All *Drosophila* strains and crosses were maintained as described above. Wild-type *D. melanogaster* Oregon-R, *D. yakuba*, *D. erecta*, and *D. simulans* laboratory strains were obtained from Department of Genetics, University of Cambridge, U.K. *D. suzukii* (Italian strain) was from Food and Environment Research Agency (FERA), York, U.K. The *D. melanogaster* transformed line stocks used in this study were from the Bloomington Stock Centre (<http://bdsc.indiana.edu/>) (Table 1) and the Vienna Drosophila Resource Centre (VDRC) via Gwangju Institute of Science and Technology, Republic of Korea (Professor Young-Joon Kim) (Table 2). The flies from the Bloomington Stock Centre were produced under The FlyLight Project by Rubin Lab in Janelia Research Campus, Ashburn, Virginia, U.S.A. Constructs were inserted by site-specific recombination into the attP2 site at 68A4 on 3L. The GAL4 lines were crossed to *UAS-IVS-Syn21-GFP-p10* (pJFRC81) to observe the expression of green fluorescent protein (GFP). The myosin-active GFP strain was a gift from Professor Dr. Christopher J. H. Elliott (Department of Biology, University of York, U.K.) and *sNPF-GAL4* strain was a gift from Prof. Dr. Christian Wegener (University of Würzburg, Würzburg, Germany).

2.5 High-performance liquid chromatography (HPLC) and matrix-assisted laser desorption ionization time of flight mass spectrometry (MALDI-TOF-MS)

75 MAGs were dissected from *D. melanogaster* Oregon-R wild-type (age 7 to 10 days old) and placed into one 1.5 ml polypropylene tube containing ice-cold 80% methanol/5% acetic acid (750 μ l). The sample was sent to our collaborator, Dr. Neil Audsley (FERA, York, U.K.) for HPLC analysis (Audsley *et al.*, 2011). In FERA, sample preparation for HPLC fractions was carried out as described previously (Audsley *et al.*, 2011). In short, 1 μ l of sample solution (concentrated HPLC fractions) was diluted 1:1 with matrix solution (saturated solution of α -cyano-4-hydroxynamic acid in 50% acetonitrile/0.05% TFA) and were transferred onto the MALDI target plate and air-dried at room temperature.

Mass and sequence analysis was performed by using a Bruker ultraflex mass spectrometer (Bruker Daltonic GmbH, Germany) set in positive ion reflectron mode over the mass range m/z 800-2500. Fragmentation of selected peptides for sequence analysis was performed using LIFTTM technology and data was examined by FlexAnalysis software. Peptide sequences were determined manually and/or by comparing the known peptides by using Protein Prospector (University of California, San Francisco, U.S.A).

Table 1 Details of *DMS-GAL4* and *DMS-R-GAL4* fly stocks from the Bloomington Stock Centre in Janelia Research Campus, Ashburn, Virginia, U.S.A.

| Stock number | Insertion | Associated gene |
|---------------------|-----------------------|------------------------|
| 39278 | P[GMR61H01-GAL4]attP2 | <i>DMS</i> |
| 39262 | P[GMR60H02-GAL4]attP2 | <i>DMS-R1</i> |
| 39297 | P[GMR64C06-GAL4]attP2 | <i>DMS-R1</i> |
| 48230 | P[GMR64E01-GAL4]attP2 | <i>DMS-R1</i> |
| 47703 | P[GMR64E04-GAL4]attP2 | <i>DMS-R1</i> |
| 39310 | P[GMR64F06-GAL4]attP2 | <i>DMS-R1</i> |
| 39312 | P[GMR64F08-GAL4]attP2 | <i>DMS-R1</i> |
| 46546 | P[GMR64G11-GAL4]attP2 | <i>DMS-R1</i> |
| 46548 | P[GMR64H11-GAL4]attP2 | <i>DMS-R1</i> |
| 39353 | P[GMR65D07-GAL4]attP2 | <i>DMS-R1</i> |
| 39355 | P[GMR65E01-GAL4]attP2 | <i>DMS-R1</i> |
| 39378 | P[GMR65H03-GAL4]attP2 | <i>DMS-R1</i> |
| 48292 | P[GMR66B08-GAL4]attP2 | <i>DMS-R1</i> |
| 39391 | P[GMR66B09-GAL4]attP2 | <i>DMS-R1</i> |
| 46575 | P[GMR67A05-GAL4]attP2 | <i>DMS-R1</i> |
| 39437 | P[GMR67D11-GAL4]attP2 | <i>DMS-R1</i> |
| 39445 | P[GMR67E08-GAL4]attP2 | <i>DMS-R1</i> |
| 49600 | P[GMR64C05-GAL4]attP2 | <i>DMS-R1</i> |
| 39247 | P[GMR60D05-GAL4]attP2 | <i>DMS-R2</i> |

| | | |
|-------|-----------------------|---------------|
| 41284 | P[GMR60D10-GAL4]attP2 | <i>DMS-R2</i> |
| 47699 | P[GMR64A08-GAL4]attP2 | <i>DMS-R2</i> |
| 39314 | P[GMR64F10-GAL4]attP2 | <i>DMS-R2</i> |
| 39339 | P[GMR65B08-GAL4]attP2 | <i>DMS-R2</i> |
| 39341 | P[GMR65B11-GAL4]attP2 | <i>DMS-R2</i> |
| 46556 | P[GMR65C09-GAL4]attP2 | <i>DMS-R2</i> |
| 39399 | P[GMR67A10-GAL4]attP2 | <i>DMS-R2</i> |
| 39402 | P[GMR67B02-GAL4]attP2 | <i>DMS-R2</i> |
| 39404 | P[GMR67B08-GAL4]attP2 | <i>DMS-R2</i> |
| 39432 | P[GMR67D04-GAL4]attP2 | <i>DMS-R2</i> |

2.6 Immunohistochemistry

Samples were dissected in fly saline (Table 3) and fixed in 4% (v/v) paraformaldehyde overnight at 4°C. Samples were then washed five times for 2 minutes in 0.3% (v/v) Triton X-100 in PBS (TX-PBS) at room temperature. Then, the blocking procedure was performed in 10% (v/v) goat serum in TX-PBS (GTX-PBS) for 1 hour at room temperature. Fixed samples were transferred into a 1.5 ml polypropylene tube with the primary antibody containing 1 µl of primary antibody in 5% GTX-PBS (1:1000) before incubation for two days at 4°C. Excess reagent was washed away at room temperature with TX-PBS before incubating samples overnight at 4°C with secondary antibody in 10% GTX-PBS (1:500). Throughout the procedure, 1.5 ml polypropylene tubes containing samples were subjected to a gentle rotation on an orbital shaker. Antibodies used for this test are listed in Table 4. Excess reagent was removed by washing five times with TX-PBS (2 minutes each) before the samples were mounted onto microscope slides using Vectashield® Mounting Medium. Slides were stored in the dark at 4°C until examined using a Zeiss Axioplan fluorescence microscope, a Leica fluorescence stereo microscope, and a Zen Light confocal microscope.

Table 2 Stock numbers and associated genes of fly stocks that were obtained from Bloomington Stock Centre and Vienna Drosophila Resource Centre (VDRC) via Gwangju Institute of Science and Technology, Republic of Korea.

| Stock number/reference | Associated gene |
|----------------------------|-----------------------------|
| Bloomington Stock Centre | <i>hid,rpr (1), Sco/Smb</i> |
| IR-37, VDRC 108760 CG 6440 | <i>DMS- RNAi</i> |
| IR-38, VDRC 12975 CG 6440 | <i>DMS- RNAi</i> |
| VDRC 9370 CG 8985 | <i>DMS-R1-RNAi</i> |
| VDRC 9369 CG 8985 | <i>DMS-R1-RNAi</i> |
| VDRC 101845 | <i>DMS-R1-RNAi</i> |
| IR-1-128, VDRC GD 42304 | <i>DMS-R2-RNAi-1(II)</i> |
| IR-1-129, VDRC GD 49952 | <i>DMS-R2-RNAi-2(II)</i> |
| IR-1-130, VDRC GD 49953 | <i>DMS-R2-RNAi-2(III)</i> |
| Bloomington Stock Centre | <i>ETH-1(II)</i> |
| Bloomington Stock Centre | <i>ETH-2(II)</i> |
| Bloomington Stock Centre | <i>nSyb-Gal4/UAS-dicr2</i> |
| Bloomington Stock Centre | <i>Actin 5C-GAL4</i> |

Table 3 Fly saline composition for dissection of *Drosophila* tissues. NaOH and HCl were used to adjust the fly saline to pH 7.2.

| Stock solutions | Final concentration (mM) | Amount of stock solution that are needed |
|---------------------------------------|-----------------------------|---|
| 2M NaCl (58 g/500 ml) | 140 | 70 ml |
| 1M KCl (3.7 g/50 ml) | 5 | 5 ml |
| 1M MgCl ₂ (10 g/50 ml) | 1 | 1 ml |
| 0.5M CaCl ₂ (2.7 g/50 ml) | 5 | 10 ml |
| 0.5M NaHCO ₃ (2.1 g/50 ml) | 4 | 8 ml |
| HEPES (free acid) | 5 | 1.5 g |
| Water (H ₂ O) | | Until 1 liter |

Table 4 Antibodies that were used for immunohistochemistry. The tissues were dissected in fly saline. All antibodies were diluted in blocking solution (5% (v/v) goat serum in triton-phosphate buffer saline (TX-PBS) for primary antibody; 10% (v/v) goat serum in TX-PBS for secondary antibody). (1⁰= primary antibody; 2⁰= secondary antibody).

| | Antibody | Specificity | Host | Manufacturer |
|----------------|------------------------------|--|-------------|-----------------------------------|
| 1 ⁰ | RFa | rabbit anti-H-Phe-M- et-Arg-Phe-NH ₂ , polyclonal | rabbit | Peninsula, California |
| 2 ⁰ | Alexa Fluor [®] 594 | goat anti-rabbit IgG [H+L], 2mg/ml pH 7.2 | goat | Life Technologies Ltd, U.K. |
| 1 ⁰ | ETH | rabbit anti-ETH | rabbit | Gift from FERA, U.K. |
| 2 ⁰ | Alexa Fluor [®] 594 | goat anti-rabbit IgG [H+L], 2mg/ml pH 7.2 | goat | Life Technologies Ltd, U.K. |
| 1 ⁰ | Serotonin | Synthesized from L- tryptophan, monoclonal | rat | Serotec, U.K. |
| 2 ⁰ | Alexa Fluor [®] 488 | goat anti-rat IgG [H+L], 2mg/ml pH 8.0 | goat | Life Technologies Ltd, U.K. |

| | | | | |
|----------------|------------------------------|--|--------|-------------------------------|
| 1 ⁰ | Green fluorescent protein | mouse IgG2a, monoclonal 3E6 (anti-GFP, MaB 3e6) | mouse | Life Technologies Ltd, U.K. |
| 2 ⁰ | Alexa Fluor [®] 488 | goat anti-mouse IgG (H+L), 2 mg/mL | goat | Life Technologies Ltd, U.K. |
| 1 ⁰ | Red fluorescent protein | rabbit IgG2a, monoclonal 3E6 (anti-GFP, MaB 3e6) | rabbit | Life Technologies Ltd, U.K. |
| 2 ⁰ | Alexa Fluor [®] 594 | goat anti-rabbit IgG [H+L], 2mg/ml pH 7.2 | goat | Life Technologies Ltd, U.K. |
| 1 ⁰ | Proctolin | rabbit anti-proctolin | rabbit | Gift from Dr. Susanne Neupert |
| 2 ⁰ | Alexa Fluor [®] 594 | goat anti-rabbit IgG [H+L], 2mg/ml pH 7.2 | goat | Life Technologies Ltd, U.K. |

2.7 Phalloidin staining

Phalloidin F-actin dye was used to observe muscle structure associated with the reproductive tissue. Tissues were dissected in fly saline and fixed in 4% (v/v) paraformaldehyde at room temperature for 20 minutes. After 20 minutes, excess reagent was washed away at room temperature with TX-PBS five times (2 minutes each) before incubating samples in phalloidin (1:100 dilution in TX-PBS) for 20 minutes on a shaker at room temperature. The samples were then mounted on slides and viewed under a Zeiss Axioplan fluorescence microscope.

2.8 *In-situ* hybridization

The protocol used was provided by Dr. Dusan Zitnan and some of the test was performed by Dr. Ivana Daubnerová (Institute of Zoology, Slovak Academy of Sciences, Bratislava, Slovakia) as stated in the result section. Tracheal tissues from wandering 3rd instar larvae of *D. melanogaster* were dissected in fly saline and rapidly transferred into a 1.5 ml polypropylene tube containing 4% paraformaldehyde and incubated overnight at 4⁰C. Tissues were then washed three times with PBS 0.2% Tween 20 (PBST20) for 5 minutes each.

The tissues were incubated with Proteinase K (50 µg PK/1 ml PBST20) for 10 minutes at room temperature. The protease activity was stopped by washing the tissues with glycine (2 mg glycine/ 1 ml PBST20) for 5 minutes at room temperature followed by two further washes with PBST20 before incubation with 4% paraformaldehyde for 1 hour. After an hour, the tissues were washed with PBST20

for 5 minutes each. The tissues were then washed once in PBST20 and hybridization solution (HS) (1:1) followed by washing with HS for 5 minutes each at room temperature before placing the tissues in HS for 1 hour in an incubator at 48°C.

During this 1 hour incubation, the preparation of the cDNA probe was made. The cDNA probe was boiled for 45 minutes for the first time use probe (2 minutes for re-used probe). After 1 hour, the excess HS was removed from the 1.5 ml microcentrifuge tube containing the tissues. The appropriate cDNA probe was added into the tube, and the tissues were left to hybridize for 20-30 hours at 48°C. The probe was removed and stored at -20°C for future use. The tissues were washed with HS followed by incubation in HS overnight at 48°C.

The tissues were then washed once in HS and PBST20 (1:1) and two times with PBST20 for 5 minutes each at room temperature. Then, the blocking procedure was performed with 1% BSA (Albumin/Bovine) in PBST20 for 20-30 minutes at room temperature. The blocking solution was pipetted out, and the tissues were then incubated with a 1:1000 dilution of sheep anti-digoxigenin in PBST20 overnight at 4°C.

Excess antibody was removed by washing three times with alkaline phosphatase buffer (AP) for 5 minutes each. The cDNA probe was detected by incubating the tissues with Nitroblue tetrazolium salt/5-bromo-4-chloro-3-indolyl-phosphate (NBT-BCIP) solution diluted in AP (1:50). Staining was observed under a dissecting microscope, and the reaction of developing colour was stopped by washing the samples five times with PBS (without Tween 20) once staining was considered to be

complete. The tissues were then washed with 50% glycerol in PBS before being mounted in 100% glycerol.

2.9 Contraction assays

The effect of myosuppressin (Biomatik, U.S.A) and sNPF (Gift from Dr. Neil Audsley, FERA, U.K.) on spontaneous contractions of adult *D. melanogaster* Oregon-R males' ejaculatory duct (ED) and male accessory gland (MAG) was investigated. The reproductive tissue was maintained in 80 μ l of fly saline. The peptide was applied to the tissue by removing 40 μ l of fly saline and adding 40 μ l of peptide at various concentrations (one concentration on an individual tissue). The initial 3 minutes of base-line contractions were measured followed by another 3 minutes period of observation after 2 minutes the peptide was applied. These contractions were recorded using a video microscope at 5 frames/second (resolution 1280x1024 pixels, uncompressed RGB format). The video was analysed by using Image J. A vector crossing the ED is selected and analysed with avi_line (http://biolpc22.york.ac.uk/avianal/avi_line/) custom software. The intensity change along this line between frames is determined by changing in brightness between frames at each pixel. The average of this intensity is recorded by the software and the mean square value exported to an Excel format file.

2.10 Development study

Twenty progeny (1st instar larvae) of flies per replicate were collected from egg plates and placed on standard fly food and kept at 26°C in a 12:12; light: dark photoperiod. Mortality was assessed at late pupa and adult. Combinations of parental flies for this development study were listed in Table 5.

Table 5 Combinations of parental flies for development study.

| Genetic combinations and parental lines |
|---|
| <i>nSyb-GAL4/UAS-dicr2>DMS-RNAi</i> (108760) |
| <i>D. melanogaster</i> Or-R wild-type |
| <i>DMS-R2/TM6B</i> (deletion knockout) |
| <i>DMS-RNAi</i> (108760) |
| <i>nSyb-GAL4/UAS-dicr2</i> |
| <i>nSyb-GAL4/UAS-dicr2</i> + |
| <i>DMS-RNAi</i> (108760) + |
| <i>nSyb-GAL4/UAS-dicr2>DMS-RNAi</i> (12975) |

2.11 Effect of ACE inhibitors on *Ae. aegypti* and *An. gambiae* enzymes

2.11.1 Preparation of mosquito enzyme

Larvae (15, 3rd instar) were washed in distilled water 5 times for 10 minutes and final wash for 1 hour at room temperature before storage at -20°C until required. Homogenate was prepared using a glass homogeniser (Jencons, East Grinstead, U.K.), containing 0.5 ml of 100 mM HEPES buffer pH 7.5, 50 mM NaCl and 10 µM ZnCl₂, and 20 up and down strokes of the pestle. A soluble fraction was prepared from the homogenate using a Beckman Optima™ MAX bench-top ultracentrifuge and TLA110 rotor (Beckman Instruments Inc, Palo Alto, California, USA) operating at 55,000 g (4°C) for 1 h. Aliquots of the homogenate were taken prior to centrifugation to determine the relative distribution of the peptidase activity before and after centrifugation.

2.11.2 Assay of peptidyl dipeptidase activity

Rates of hydrolysis of the quenched fluorogenic substrate Abz-FRK(Dnp)-P by *Ae. aegypti* and *An. gambiae* enzymes were performed at 20°C in 96-well black plastic plates (Corning Life Sciences, High Wycombe, U.K.) using a FLUOstar Omega (BMG LABTECH GmbH, Offenburg, Germany) with λ_{ex} at 340nm and λ_{em} set at 430 nm. The reaction was started by adding 1 µl of 5 mM Abz-FRK(Dnp)-P in dimethyl sulfoxide to the enzyme in 200 µl of 100 mM HEPES buffer pH 7.5, 50

mM NaCl and 10 μ M ZnCl₂. For studying the effect of ACE inhibitors, enzyme was pre-incubated with inhibitor for 10 min prior to the addition of substrate.

2.11.3 Behavioural and mortality effect of ACE inhibitors on *Ae. aegypti* and *An. gambiae* larvae

Larvicidal testing was performed in 24-well plastic plates (Becton Dickinson Labware, New Jersey, USA) using 20 *Ae. aegypti* and *An. gambiae* larvae of 1st, 2nd, and 3rd instars in distilled water. Inhibitors dissolved in distilled water were added separately to each well containing larvae to give a final concentration of 5 mM. Control tests were carried out in parallel with the same volume of water and number of larvae. Mortality in each well was recorded after 24, 48, and 72 hours of exposure. Any behavioural and morphological changes of larvae from treated and control wells were recorded during treatment with inhibitors using a stereo microscope.

Chapter 3

Signalling Pathways of *Drosophila* spp. : RFa peptides and Serotonin

3.1 Introduction

Insects use a plethora of neuropeptides as neurotransmitters, neuromodulators, and neurohormones to control a broad range of physiological, developmental, and behavioural events (Nässel, 1993; Nässel, 2000; Nässel and Winther, 2010b). The sequencing of insect genomes with bioinformatics analysis has led to the identification of a vast number of neuropeptide sequences from a variety of species (Gäde and Kellner, 1992; Veenstra and Hagedorn, 1995; Broeck, 2001; Winther and Nassel, 2001; Nässel, 2002; Claeys *et al.*, 2005). However, the physiological role of many of the neuropeptides remains unclear. Our understanding of insect peptidergic signalling mechanisms can be resolved by studying their action on specific tissues and cells and the use of powerful genetic approaches, such as RNAi and targeted gene deletion and editing. These and other genetic tools are available especially for *D. melanogaster*, which makes it an ideal model insect (Dietzl *et al.*, 2007; Huang *et al.*, 2016; Reid and O'Brochta, 2016). This powerful experimental system will allow us to observe the expression of targeted neuropeptides and their receptors to investigate the role they play in insect physiology and development.

3.1.1 Peptides and protein signaling molecules of the male seminal fluid

Within a broad range of insect species from different orders, mating initiates both behavioural and physiological changes in females (Chapman *et al.*, 1995; Ram and Wolfner, 2007; Avila *et al.*, 2011; Boes *et al.*, 2014; Avila *et al.*, 2015). The transfer of sperm and seminal fluid triggers responses in several processes relating to fertility. Proteins and peptides (SFPs) found in the seminal fluid are responsible for many of these changes within females (Avila *et al.*, 2011). SFPs are the products of the male reproductive tract tissues that include the MAGs, SV, ED, EB, and testes and are transferred to females in the seminal fluid with sperm during mating. The involvement of the SFPs in post-mated female behaviour has been reported in several dipteran insects, for example *Ae. aegypti* (Fuchs and Hiss, 1970), *Musca domestica* (Leopold *et al.*, 1971), and *D. melanogaster* (Burnet *et al.*, 1973). The SFPs have been identified by either proteomic analysis or the sequencing of MAG cDNAs and often represent numerous protein classes, including proteases, protease inhibitors, lectins, protein and peptide hormones, and protective proteins, such as antioxidants (Lung *et al.*, 2002; Sirot *et al.*, 2008; Avila *et al.*, 2011; Xu *et al.*, 2013; Boes *et al.*, 2014). Many of these protein classes are present in the ejaculate of organisms from arthropods to mammals (Poiani, 2006). To date, the main reference of information referring to the structure and function of insect SFPs comes from work on the MAGs of the fruit fly *D. melanogaster* (Chen, 1984; Carmel *et al.*, 2016). These proteins are major effectors of a broad range of post-mating responses in female *Drosophila*, including stimulation of egg production, increasing ovulation

and egg laying rates, changing the female preference for re-mating, feeding, sleep, and locomotor activity (Avila *et al.*, 2011).

MAG products received by the female during copulation are also important in the reproductive biology of the mosquito *Ae. aegypti* (Klowden, 1999; Lee and Klowden, 1999). Naccarati *et al.* (2012) reported that MAGs of *Ae. aegypti* are a source of the head peptide Aea-HP-1, pERPhPSLKTRFa, (pE, pyroglutamic acid, hP, 4-hydroxyproline; a, amidated C-terminus) by using immunoassays in conjunction with mass spectrometry (Naccarati *et al.*, 2012). In addition to this finding, they showed that the peptide was transferred to the female reproductive tract during copulation. Aea-HP-1 was first isolated from 620,000 mosquito heads using an antibody that recognised the RFa epitope to monitor purification (Matsumoto *et al.*, 1989; Brown *et al.*, 1994; Veenstra, 1999). The presence of the MAG peptide in head extracts is best explained by contamination of the heads with bodies during the sieving procedure employed to process such large numbers of insects. Aea-HP-1, when injected into adult female mosquitoes, inhibited host-seeking behaviour suggesting that males can alter the behaviour of the female from searching for blood meal to looking for an egg laying site (males congregate around blood-feeding females and inseminate the blood-gorged insect) (Brown *et al.*, 1994). Aea-HP-1 belongs to a large family of RFa peptides found in insects and many other invertebrate groups.

3.1.2 Sex peptide

Probably the best-known dipteran insect SFP is the sex peptide (SP) made by the MAGs and secreted into the seminal fluid. It is transferred with the sperm to the female reproductive tract and is responsible for dramatic changes in behaviour and physiology of the post-mated female (Wolfner, 1997; Kubli, 2003; Liu and Kubli, 2003; Isaac *et al.*, 2010). It is primarily responsible for inducing rejection behaviour in post-mated females towards male advances. This change of behaviour is long lasting for 7-10 days. It also has a major role in elevating egg production and expression of anti-microbial peptides. Recently, it has been shown to increase appetite and food intake of females post-copulation (Carvalho *et al.*, 2006; Domanitskaya *et al.*, 2007). The peptide possesses 36 amino acids and comprises a tryptophan (Trp)-rich region, a proline-rich domain as well as a C-terminal region containing a disulfide bridge (Figure 4) (Kubli, 2003). The Trp-rich N-terminal domain is required for adhering the peptide to the surface of sperm. This results in the SP being carried and stored with sperm in the females' sperm storage organs. The SP is then slowly released from the sperm's tail by a peptidase that cleaves the hydrophobic Trp region (Domanitskaya *et al.*, 2007). The C-terminal half of the peptide is important for receptor activation and the central hydroxyproline-rich section is thought to be involved in eliciting female immune response (Kubli, 2003).

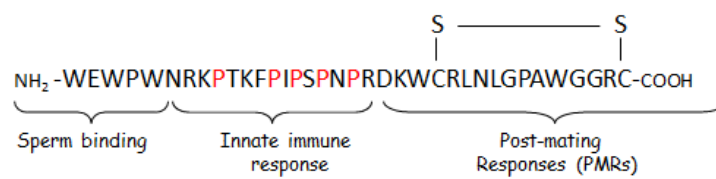


Figure 4 The structure of *D. melanogaster* sex peptide. 4-Hydroxyproline residues are in red (Adapted from Domanitskaya *et al.*, 2007).

3.1.3 RFa peptides

Neuropeptides can be grouped together according to a common structural feature. The RFa family of invertebrate peptides shares the C-terminal sequence of Arg-Pheamide, but can have various N-terminal extensions. The first member of this large peptide family is the molluscan tetrapeptide, FMRFa (Phe-Met-Arg-Phe-NH₂), a cardio excitatory peptide isolated from a ganglion of the clam, *Macrocallista nimbosa*, which led to the commonly used name of FMRFamide- related peptides or FaRPs (Price and Greenberg, 1977). In *Drosophila*, FaRPs include three groups of neuropeptides, which are *Drosophila* FMRFa (dFMRFa), *Drosophila* sulfakinin (DSK), and *Drosophila* myosuppressin (DMS). In addition to the FaRP peptides, *Drosophila* has several other neuropeptides with the RFa C-terminus (see Table 6).

There are antibodies available commercially that recognize the RFa epitope of the peptide FMRFa and they also cross-react with other members of the RFa family. They have been used to reveal relevant immunoreactive peptides in the nervous system and endocrine cells of a host of insect species (White *et al.*, 2004; Nichols *et al.*, 2006). Immunoreactivity is present throughout the insect CNS including cells and processes in the brain lobes, optic lobes, and the ventral ganglion, as well as in endocrine cells of the gastrointestinal tract and the reproductive system in a bilaterally symmetric pattern. This expression is consistent with the role of FaRPs in a diversity of physiological processes. The FMRFa peptide is widely present at an early stage of development, as shown in *D. melanogaster* larval brain. Similarly, the distribution of the RFa immunoreactive material is widespread in other animal species (Kingan *et al.*, 1996). As mentioned, the antibody that recognises only the

common C-terminus RFa does not distinguish between FaRPs with different N-terminal extensions. It might however be possible to make a more selective antibody that recognises the N-terminal sequence of individual members of the family; thus overcoming the problem of lack of specificity of the commonly used RFa antibody.

Table 6 Peptides with C-terminal Arg-Pheamide (RFa) identified in *Drosophila melanogaster*. Adapted from Nässel and Winther, 2010a.

| Gene | | Peptide |
|------------------|-------------------------------|----------------------------|
| dFMRFa | <i>dFMRFa-2</i> | DPKQDFMRFa |
| | <i>dFMRFa-3</i> | TPAEDFMRFa |
| | <i>dFMRFa-4</i> | SDNFMRFa |
| | <i>dFMRFa-5</i> | SPKQDFMRFa |
| | <i>dFMRFa-6</i> | PDNFMRFa |
| | <i>dFMRFa-8</i> | MDSNFIRFa |
| Drosulfakinin | <i>DSK-1</i> | FDDYGHMRFa |
| | <i>DSK-2</i> | GGDDQFDDYGHMRFa |
| Dromyosuppressin | <i>DMS</i> | TDVDHVFLRFa |
| Neuropeptide F | <i>NPF</i> | SNSRPPRKNDVNTMADAYKFLQDLDT |
| | | YYGDRARVRFa |
| short NPF | <i>sNPF-1</i> | AQRSPSLRLRFa |
| | <i>sNPF-1⁴⁻¹¹</i> | SPSLRLRFa |
| | <i>sNPF-2</i> | WFGDVNQKPIRSPSLRLRFa |
| | <i>sNPF-2¹²⁻¹⁹</i> | SPSLRLRFa |

3.1.4 Dromyosuppressin

Dromyosuppressin (DMS, TDVDHVFLRFa) is a FaRP of particular interest since transcriptomic data indicates a high level of expression in the MAG as well as the brain and heart of *D. melanogaster* (Chintapalli *et al.*, 2007). As the name suggests, myosuppressin suppresses muscle contractibility of insect tissues such as the heart, gastrointestinal tract, and oviduct (Holman *et al.*, 1986; Robb and Evans, 1994; Richer *et al.*, 2000). This peptide shares some structure identity with other insect myosuppressins with the general structure XDVDHVFLRFa, where X is pE, P, or T (Holman *et al.*, 1986; Robb *et al.*, 1989; Nichols, 1992b; Peeff *et al.*, 1994).

3.1.5 Serotonin

Serotonin or 5-HT (Figure 5) is an evolutionarily conserved indolealkylamine that has wide-ranging signalling roles as a neurotransmitter, neuromodulator, and a circulating hormone. In insects, it is important for regulating locomotion, sleep, heart contractions, adult crop function, olfaction, water balance, feeding, learning, and memory (Yuan *et al.*, 2006; Johnson *et al.*, 2009; Neckameyer, 2010; Johnson *et al.*, 2011; Luo *et al.*, 2012; Röser *et al.*, 2012; Wu and Cooper, 2012; Gasque *et al.*, 2013; French *et al.*, 2014; Silva *et al.*, 2014; Pooryasin and Fiala, 2015). 5-HT also has an important role in the control of ejaculation and determining the length of copulation in *D. melanogaster*. Interference with 5-HT signalling from neurons in the abdominal ganglion results in a defective transfer of sperm and SFPs to the female and in extended copulation periods (Lee *et al.*, 2001; Tayler *et al.*, 2012). The

abdominal 5-HT neurons innervate the male reproductive tissues (SV, MAGs, and ED) and 5-HT applied exogenously to the ED of male *D. melanogaster* increased the frequency of spontaneous peristaltic contractions (Norville *et al.*, 2010).

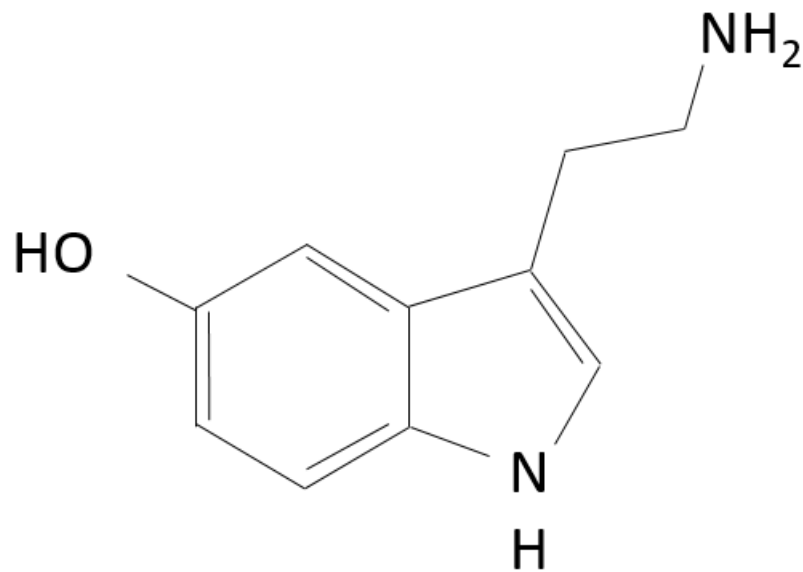


Figure 5 The structure of serotonin or 5-hydroxytryptamine (5-HT).

3.1.6 Chapter aims

The primary aim of the work described in this chapter was to provide chemical evidence for the presence of DMS (TDVDHVFLRFa) in the MAGs of *D. melanogaster* using HPLC and MALDI-TOF-MS, supported by IHC methods using antibodies recognising the RFa epitope. Contrary to expectations, DMS was not detected in extracts of the *D. melanogaster* MAGs using HPLC-MS, but strong IHC staining of neuronal processes were observed on the surfaces of the MAG, ED, and SV. These results suggested that DMS is neuronal and is not synthesised by MAG cells for secretion in the seminal fluid. Since serotonergic neurons are known to control muscle activity of reproductive tissues and ejaculation in male *D. melanogaster*, it was of interest to investigate any co-localisation of RFa peptide with the biogenic amine. If DMS serves as an inhibitory transmitter then the expectation is that the DMS and serotonergic neurons are distinct. The neuronal expression of a DMS-like peptide in the male reproductive system was also studied in other drosophilids (*D. erecta*, *D. yakuba*, *D. virilis*, *D. simulans*, and *D. sukuii*).

3.2 Results

3.2.1 High-performance liquid chromatography-mass spectrometry (HPLC-MS) of peptides extracted from *D. melanogaster* MAGs

In the search for DMS in *D. melanogaster* MAGs 75 glands were extracted with methanol/acid and the extract was fractionated by reverse-phase HPLC (Figure 6A). Synthetic DMS (1 nmole) was used to determine the elution time (32 min) of synthesised DMS (TDVDHVFLRFa, Figure 6B). HPLC fractions from the gland extract were collected every minute covering the expected elution period of any DMS and were subjected to MALDI-TOF-MS analysis. The mass spectrum of fraction 32 (Figure 6C) did not reveal elution of a peptide with a characteristic DMS mass ion of m/z 1247.6.

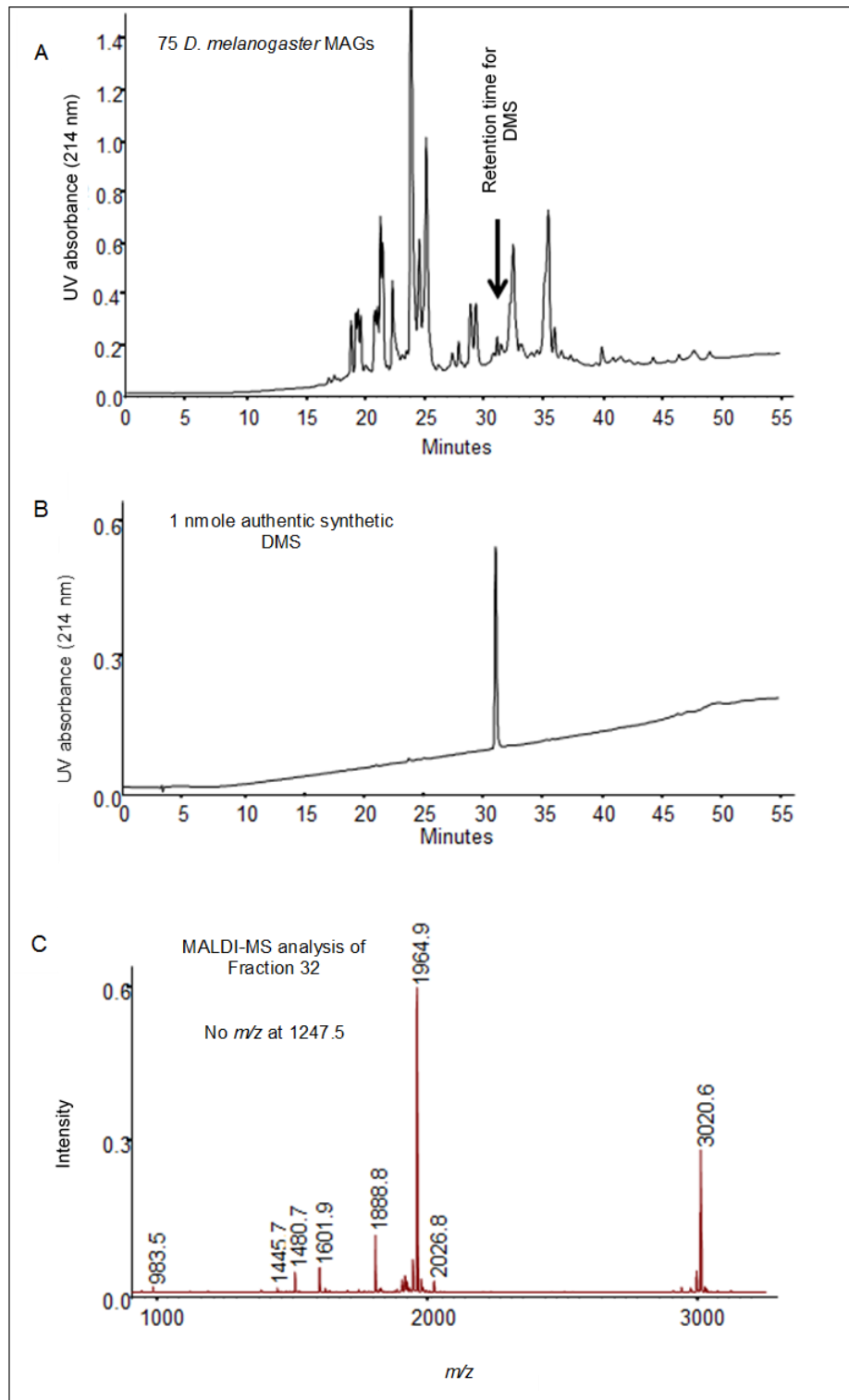


Figure 6 HPLC traces (214 nm) from the reverse-phase chromatography of an extract of 75 *D. melanogaster* MAGs. (A) Separation of UV- absorbing compounds from a methanol/acid extract of 75 *D. melanogaster* MAGs. (B) Synthetic DMS (1 nmole) was used to determine the elution time of DMS. (C) Mass spectrum of fraction 32 and the absence of a molecular ion $[M+H]^+$ at m/z 1247.6.

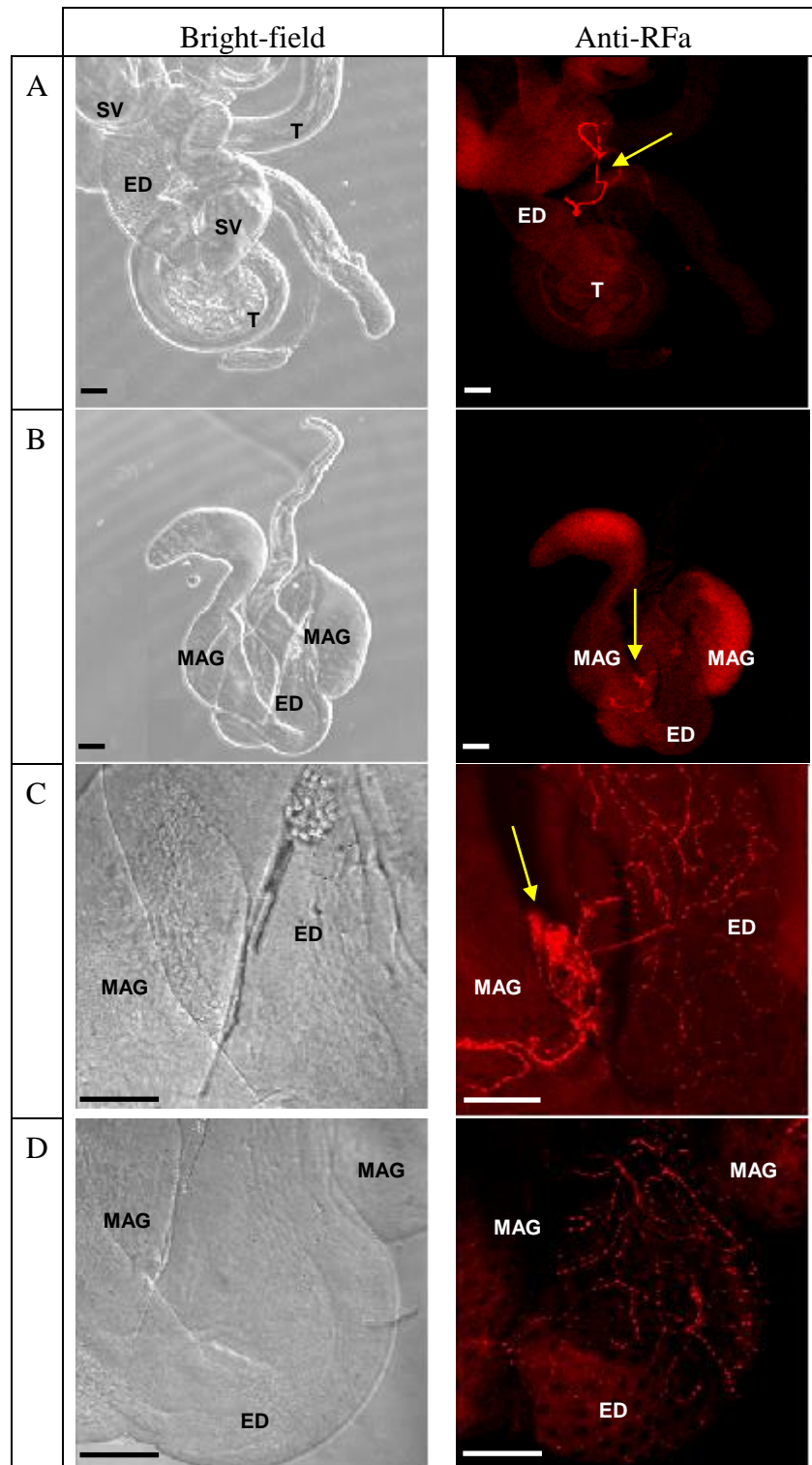
3.2.2 RFa immunoreactivity associated with the reproductive tissues of *Drosophila* spp.

A specific DMS antibody capable of distinguishing between the various RFa peptides of *D. melanogaster* was not available. Instead, antiserum recognising the RFa epitope of DMS was used to visualise DMS-like peptide expression in male *Drosophila* reproductive tissues (MAGs, ED, testes, SV, and EB). A serotonin (5-HT) specific antibody was used to assess whether the RFa co-localised with previously identified serotonergic innervation of the MAG and ED (Lee *et al.*, 2001; Billeter and Goodwin, 2004).

3.2.2.1 RFa neurons innervate the MAG, ED, and SV of *D. melanogaster*

An immunoreactive fibre is seen to project outside the tissue and on to the surface of the ED and MAGs (Figure 7). The fibre is located at the ED area connecting the ED anterior and posterior part (see yellow arrow in Figure 7A). Examination of the reproductive tissue in a different sample revealed RFa immunoreactivity at the base of the MAG and ED (see yellow arrow in Figure 7B). The same sample was also analysed at higher magnification (40x) using an oil immersion objective (Figure 7C and Figure 7D). A bundle of neurites was observed at the base of the MAG; it connects the ED and MAG (see yellow arrow in Figure 7C). An abundance of intense net-like distribution of neurites were observed over the surface of the ED (Figure 7D). No neuronal staining was observed when the primary antibody was blocked by pre-incubation of the antibody with 1 μ M myosuppressin peptide

(negative sample). However, the background staining was observed in the negative sample, when the image capture was set at the same setting as the test sample to shows clearer RFa expression.



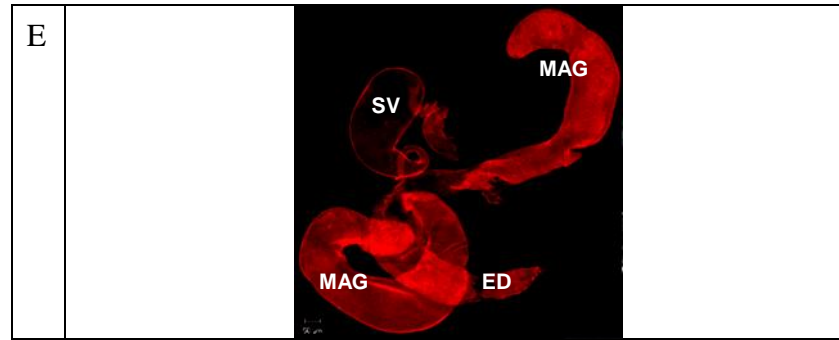


Figure 7 Distribution of RFa immunoreactivity on the surface of *D. melanogaster* MAGs and ED. (A) Fluorescence signal was observed outside the ED (see yellow arrow) connecting the anterior and posterior part of the ED. (B) Staining of neuronal fibres (yellow arrow) at the base of the MAG and adjacent to the ED, and on the surface of the ED. (C) The yellow arrow indicates the bundle of neurites at the base of the MAG; it connects the ED and MAG. (D) RFa-containing neurites ramify over the ED. (E) Negative control shows background staining. Images were captured by using the confocal microscopy. T-testis. The scale bars represent 50 μm .

The cross-section images determine the precise location of the staining. Based on the vertical and horizontal optical cross sections of the tissue (Figure 8), the RFa neurite expression is clearly on the surface of the ED and appears to be absent from the lumen.

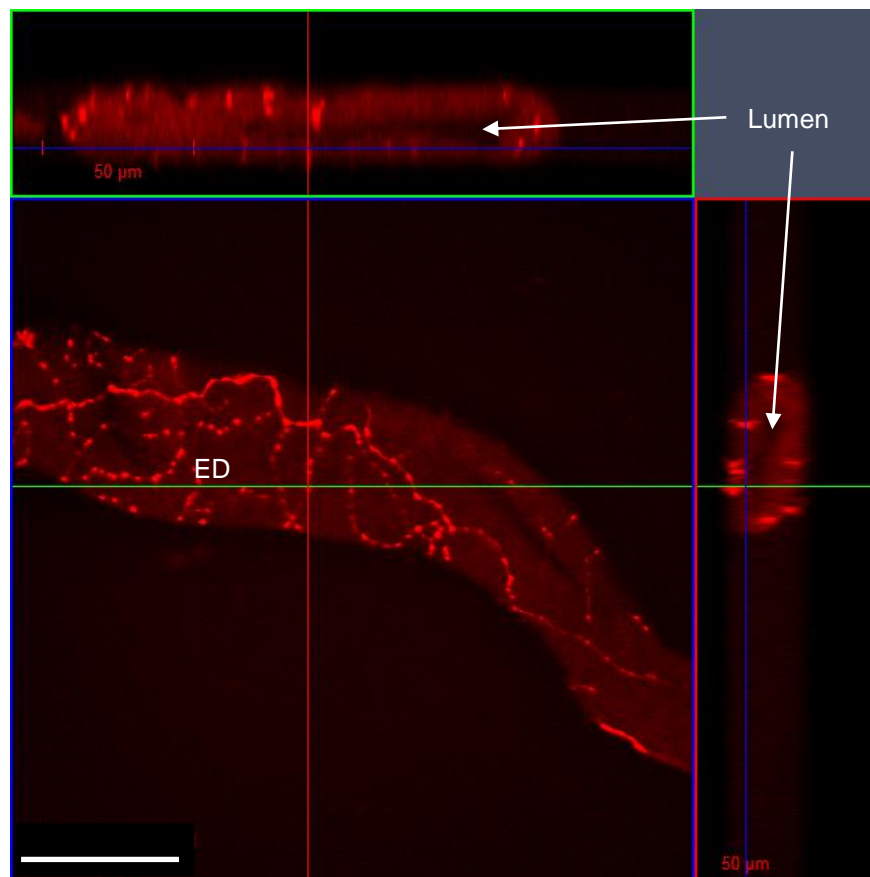


Figure 8 RFa expression in a cross-section of the *D. melanogaster* ED using a confocal microscope. A strong signal was observed in the outer layer of the ED, but not in the lumen. This image was focused on the lumen of the sample to confirmed that the RFa is absent in the lumen. The scale bar represents 50 μm.

This experiment was conducted simultaneously with positive and negative control samples. Brains from *D. melanogaster* (wandering 3rd instar) larvae were used as a positive control and treated with anti-RFa antiserum. Whole-mounted larvae brain shows RFa expression within protocerebra, subesophageal ganglion, and ventral nerve cord (VNC) (Figure 9). Both images show RFa expression at ventral-medial, lateral-medial, and dorsal-medial chains of cells. Furthermore, three pairs of cells in the subesophageal ganglion stained with the RFa antiserum as well as axons projecting the ventral cord. Images were compared with those published previously by Nichols *et al.*, (1999) and the outcome concluded that the staining pattern is similar. As for the negative control, no neuronal staining was observed when the primary antibody was blocked by pre-incubation of the antibody with 1 μ M myosuppressin peptide (negative sample). However, the background staining was observed in the negative sample, when the image capture was set at the same setting as the test sample to shows clearer RFa expression.

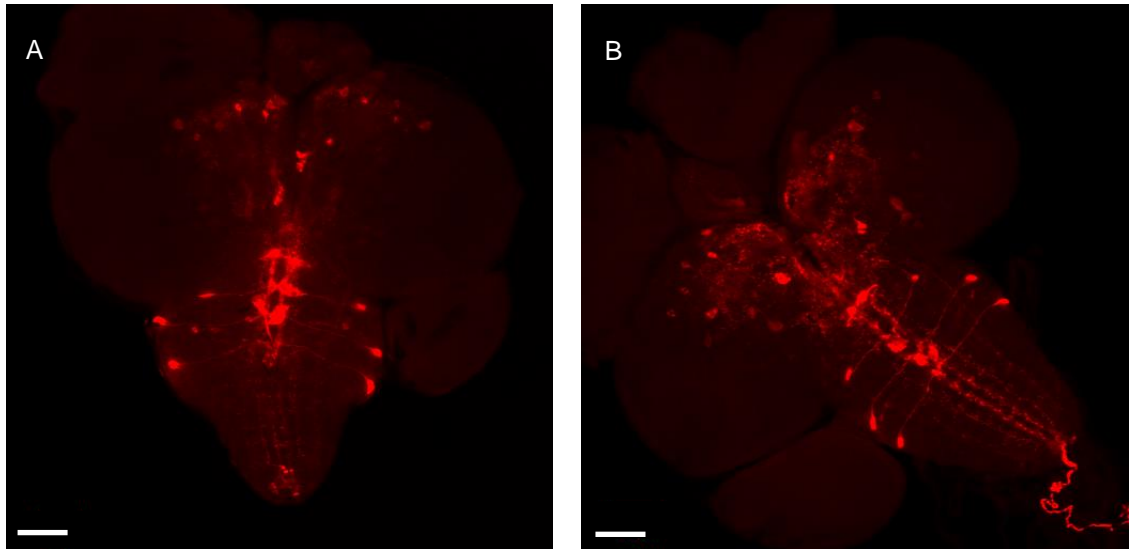


Figure 9 RFa immunoreactivity in the CNS of *D. melanogaster* wandering larvae. Antibodies were visualised with the Alexa Fluor[®] 594 goat anti-rabbit secondary antibody. Image A and B show RFa expression in neurons of the CNS, and the signal was observed in axons descending from the ventral cord (Image B). The scale bars represent 50 μ m.

Studies on the RFa innervation of the male reproductive tissue was extended to other *Drosophila* species. In *D. erecta*, the RFa fibres can be seen outside the tissue connecting the ED and the MAG (see yellow arrows in Figure 10). A similar pattern of RFa expression was found in *D. yakuba* male reproductive tissues (Figure 11) with the RFa fibres (see yellow arrows) present outside the ED (Figure 11A), connecting the ED and the MAG (Figure 11B). The intense and compact RFa neurite expression was observed at the ED (Figure 11A). No neuronal staining was observed when the primary antibody was blocked by pre-incubation of the antibody with 1 μ M myosuppressin peptide (negative sample). However, the background staining was observed in the negative sample, when the image capture was set at the same setting as the test sample to shows clearer RFa expression.

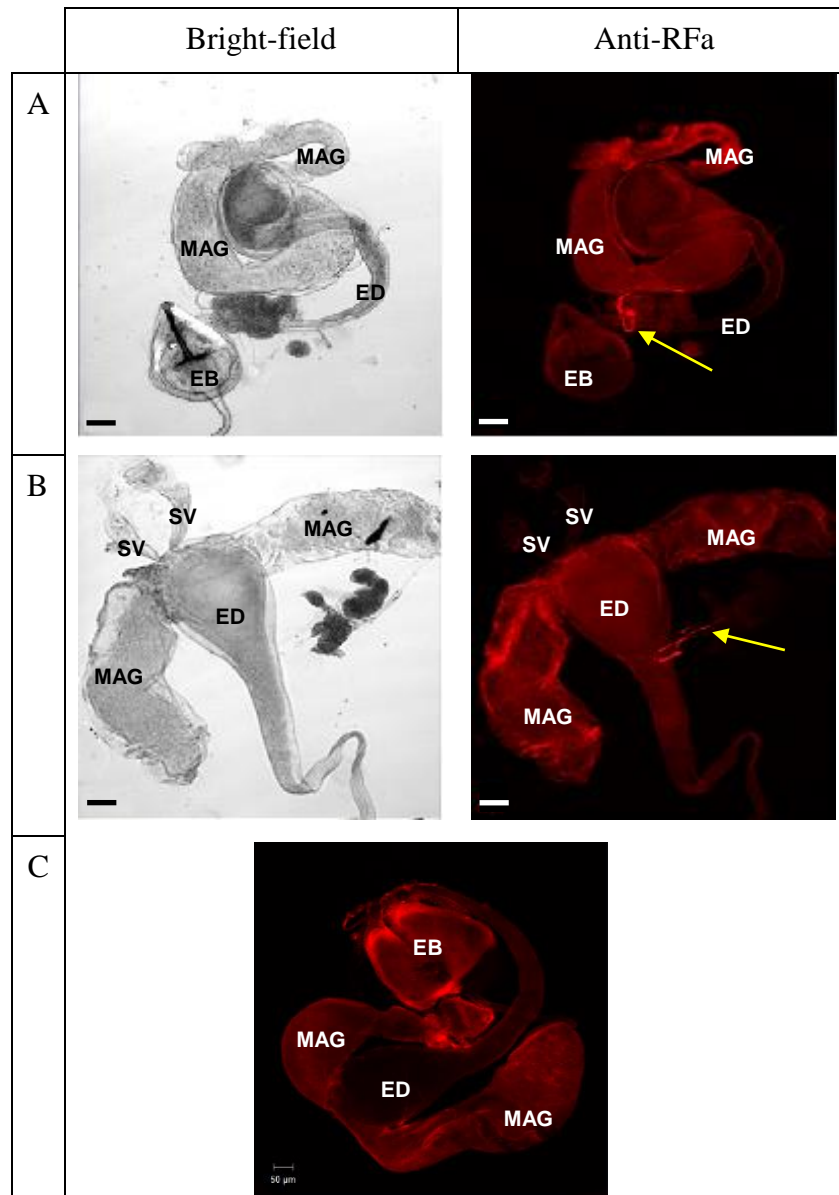


Figure 10 RFa expression in *D. erecta* reproductive tissues. Panel A and B show RFa expression (see yellow arrows) connecting the ED and MAG. (C) Negative control shows background staining. The scale bars represent 50 μm .

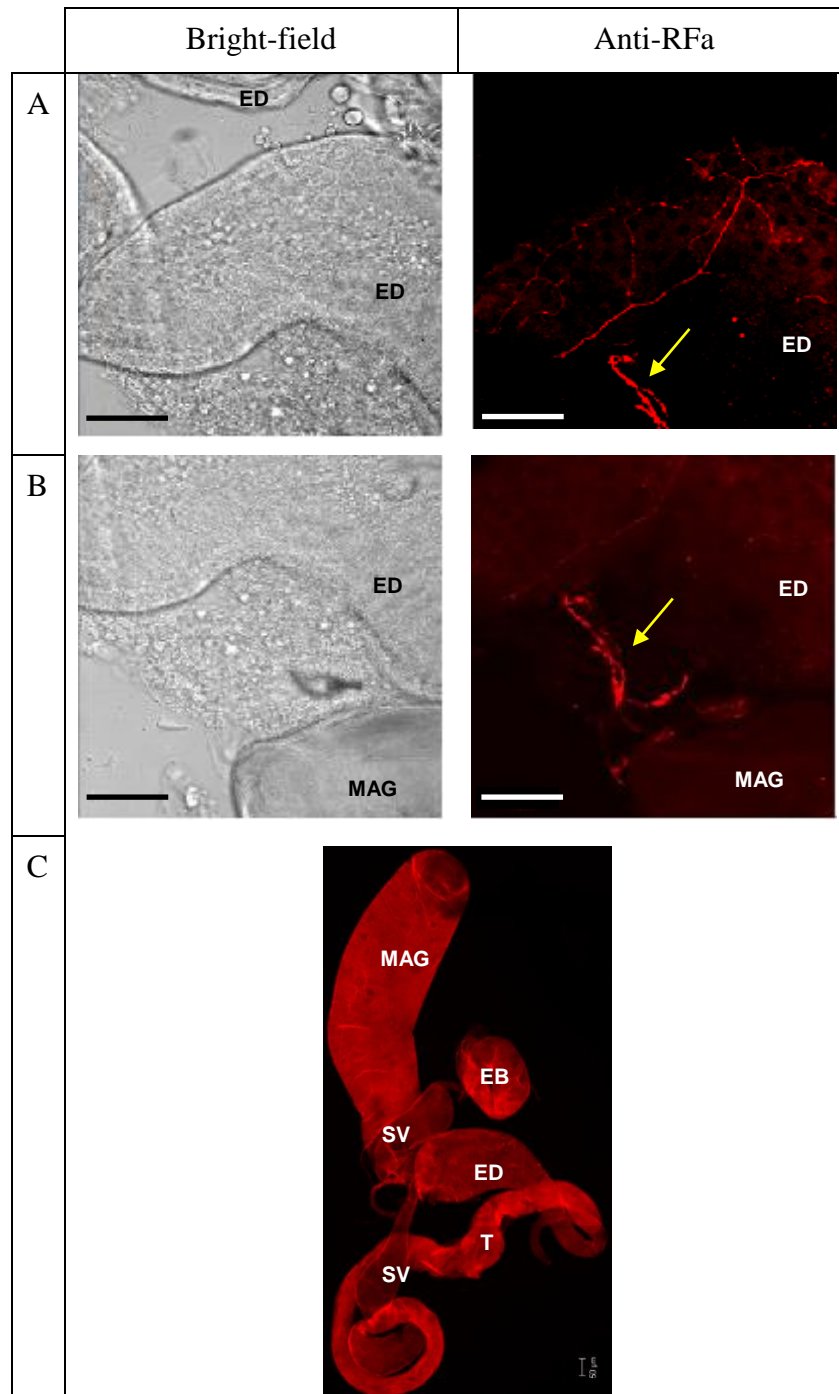


Figure 11 RFa expression in *D. yakuba* tissues. (A) Intense RFa expression at the ED and outside the tissue (yellow arrow). (B) RFa expression at ED and immunoreactivity fibres (yellow arrow) connecting ED and MAG. (C) Negative control shows background staining. The scale bars represent 50 μ m.

In *D. virilis* (Figure 12) and *D. simulans* (Figure 13), similar RFa immuno-fibres (white arrows) can be seen outside the MAG and ED. In conclusion, there is no difference in RFa expression between these *Drosophila* species (*D. melanogaster*, *D. erecta*, *D. yakuba*, *D. virilis*, and *D. simulans*). The RFa immunoreactivity description in *D. suzukii* will be reported in section 3.2.4.

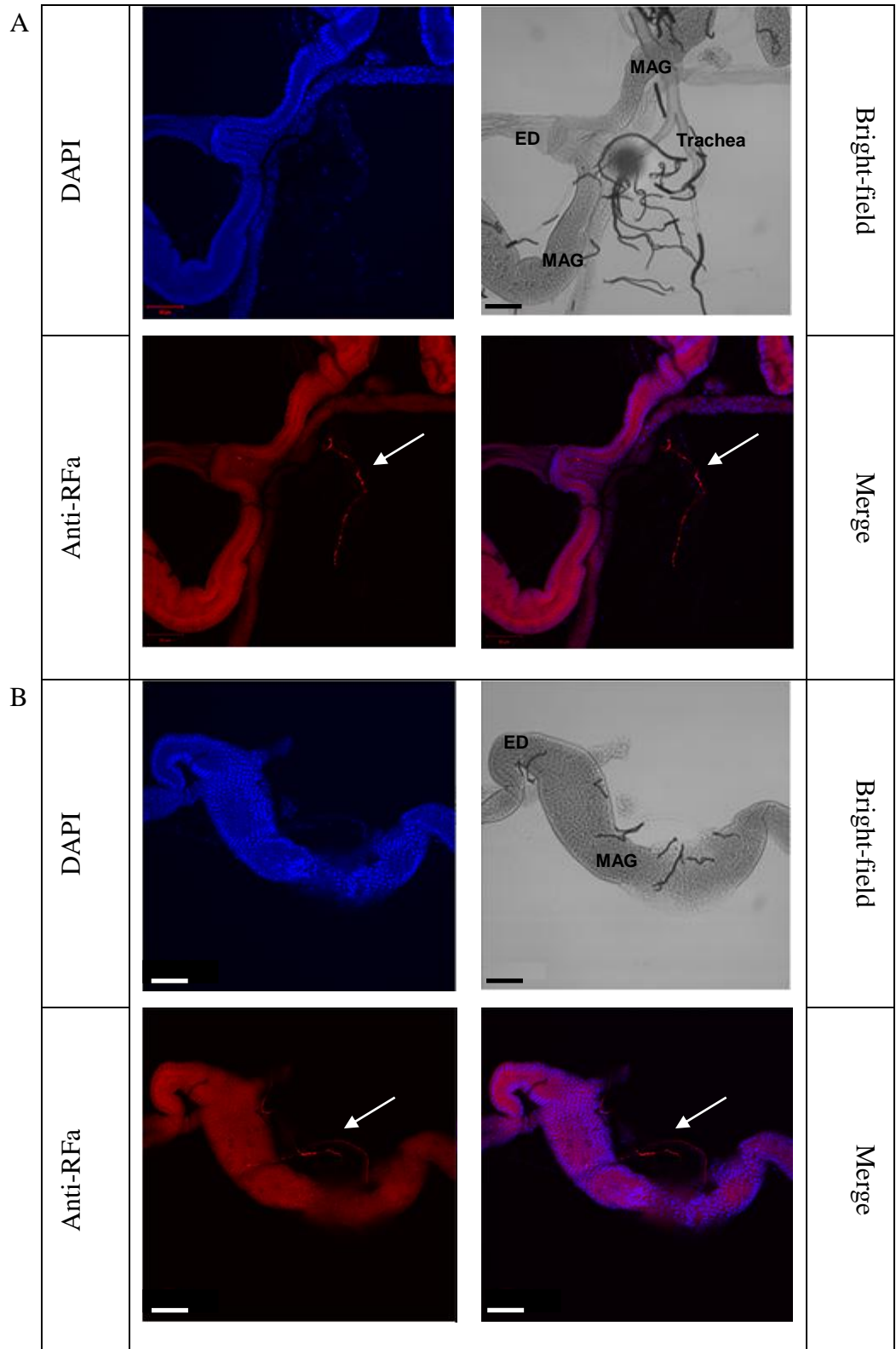


Figure 12 RFa expression (white arrows) in *D. virilis* reproductive tissue detected with RFa antiserum. (A) RFa expression outside the tissue. (B) RFa expression outside the MAG. The scale bars represent 50 μm .

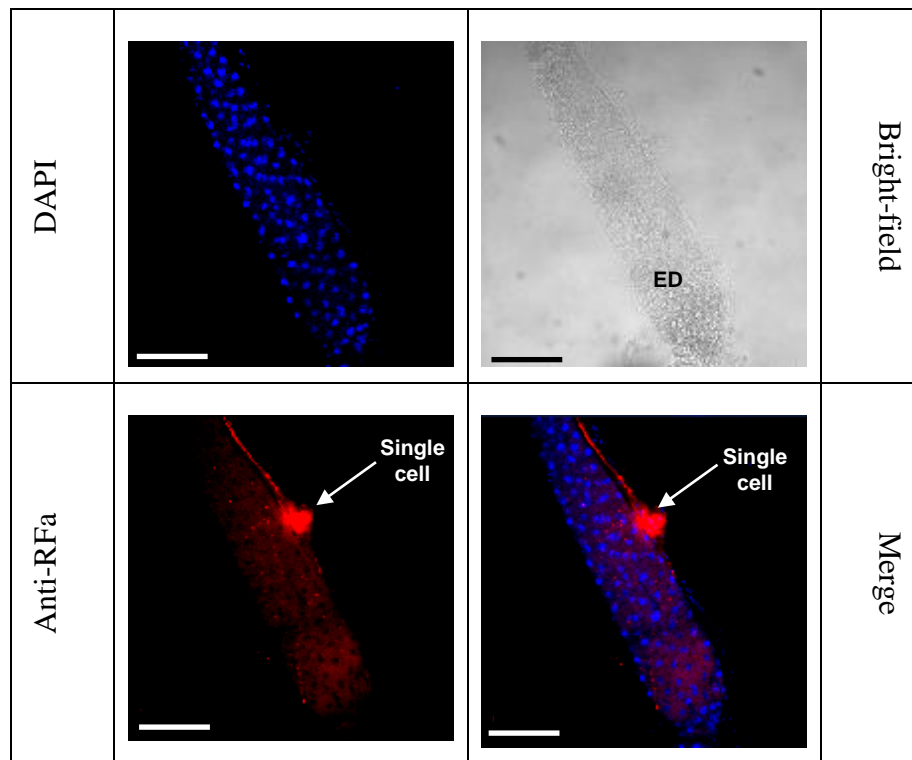


Figure 13 RFa expression in *D. simulans* reproductive tissue detected with RFa antiserum. The RFa-containing neurites present over the ED and a single cell (white arrows) was observed outside the tissue. The scale bars represent 50 μm . Tissues were counterstained with DAPI to reveal cell nuclei.

3.2.2.2 Single cells associated with male reproductive tissue and the rectum

During the careful viewing of *D. melanogaster* reproductive tissues stained using RFa antiserum; a bright single cell was detected attached to the ED (see white arrow, Figure 14). Several immunoreactive fibres can be seen extending from the cell and connecting to the ED.

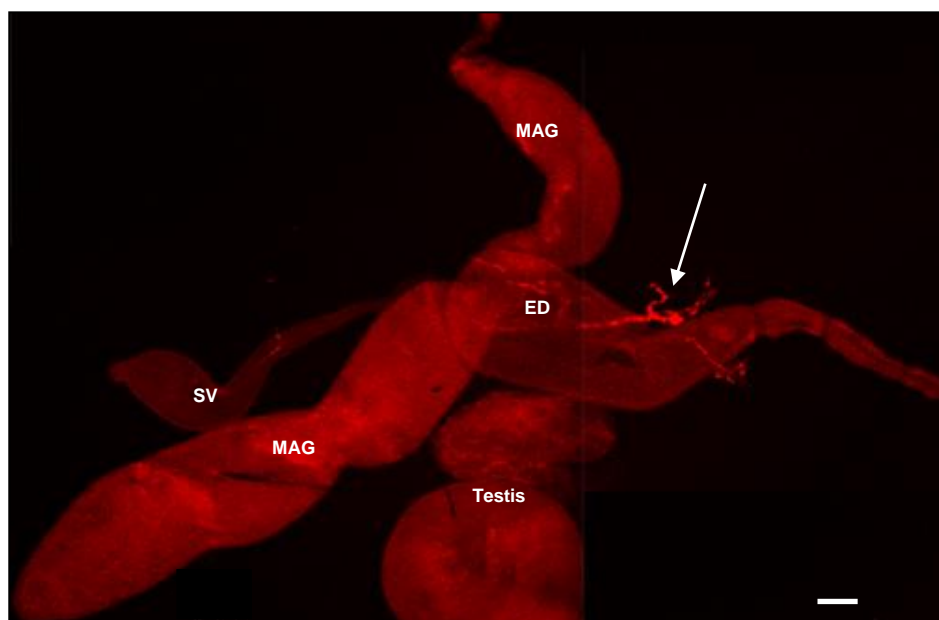


Figure 14 Single bright cell detected with RFa antiserum close to the *D. melanogaster* ED (see white arrow). Whole MAGs including testis, ED, and SV were fixed and then treated with primary RFa antiserum and detected using the fluorescent secondary antibody, as described in Chapter 2. The scale bar represents 50 μm .

The single cell was also found in *D. erecta* (Figure 15), *D. yakuba* (Figure 15), and *D. simulans* (Figure 13), but was not found in *D. virilis*. All single cells show strong immunoreactive processes emanating from the cells.

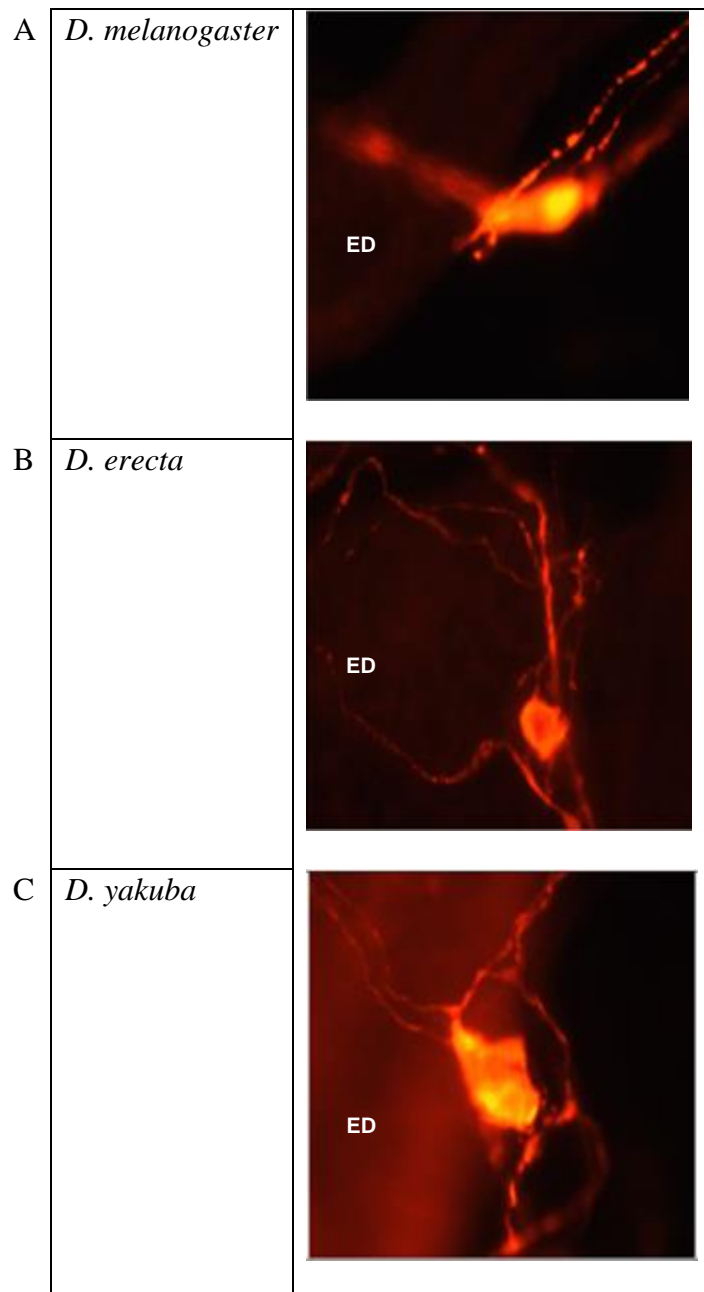


Figure 15 The single ED cell of (A) *D. melanogaster* (B) *D. erecta*, and (C) *D. yakuba* detected with RFa antiserum. Images A-C were captured by using Zeiss Axioplan fluorescence microscope (200x magnification).

More extensive dissection of *D. simulans* abdominal tissues revealed strong RFa staining of two large cells associated with the hindgut (HG) and rectum (Figure 16). Confocal microscopy and serial optical section was carried out to get a precise representation of the cells seen close to the rectum tissue. From the cross-section, the two cells can be seen on two sides of the rectum (see yellow arrows with asterisk). These cells are located on a different plane in the field of view. The cells are connected to each other, and several immunoreactive fibres arise from each cell.

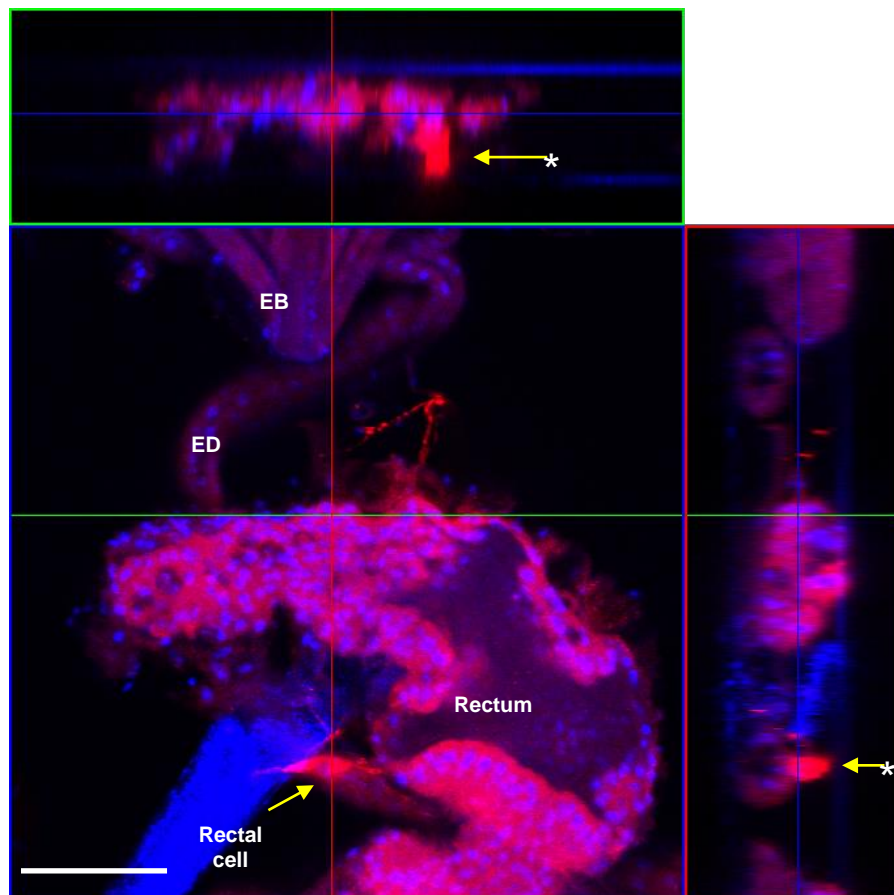


Figure 16 Bright cells detected with RFa antiserum at different plane of the *D. simulans* rectum tissue. The upper plane represents the horizontal cross section of the main plane and right plane represents the vertical cross section. Nuclei are stained with DAPI. The scale bar represents 50 μm .

3.2.3 Serotonin immunoreactivity associated with the reproductive tissue of *Drosophila* spp.

The IHC localisation of 5-HT reveals extensive arborisation around the MAGs, ED, and SVs of *D. melanogaster* (Figure 17). IHC was also performed on *D. erecta* reproductive tissue to reveal 5-HT neurons (Figure 18). The 5-HT neurotransmitter expression was observed to ramify over the MAG, ED, and SV in this species as well. No neuronal staining was observed in the negative sample.

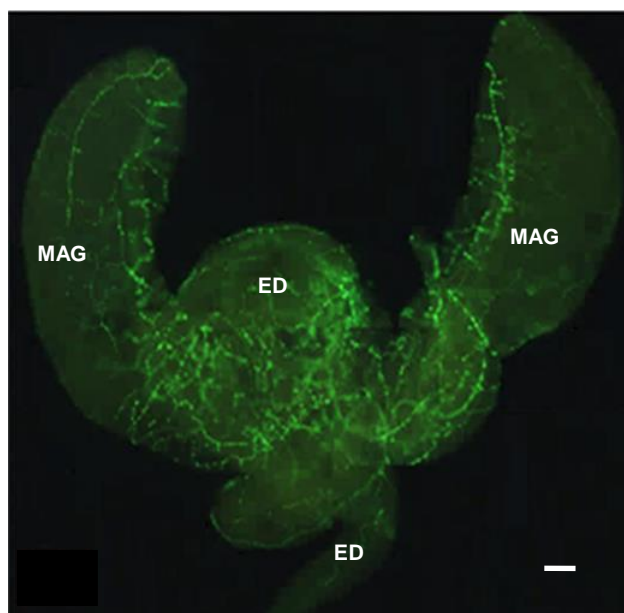


Figure 17 Serotonergic processes at *D. melanogaster* MAGs, SV, and ED detected with 5-HT antibody. Whole MAGs including ED and SV were fixed and then treated with primary 5-HT antibody and detected using the fluorescent secondary antibody, as described in the Chapter 2. No neuronal staining was observed in the negative sample. The scale bar represents 50 μ m.

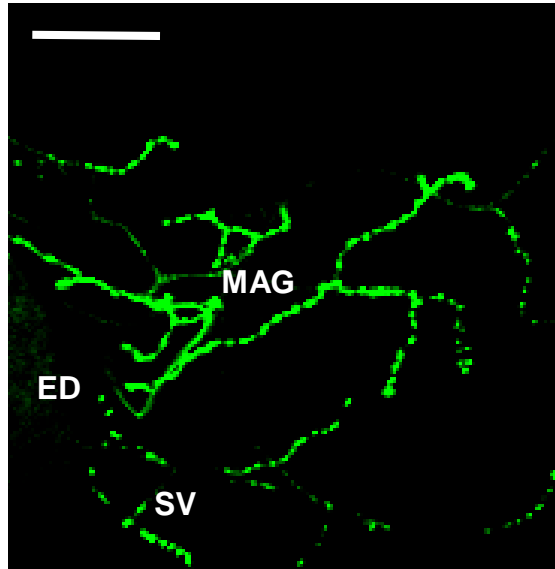


Figure 18 Serotonergic processes in *D. erecta* MAG detected with 5-HT antibody. The immunoreactive projections were observed on MAG, ED, and SV. No neuronal staining was observed in the negative sample. The scale bar represents 50 μm .

A confocal microscope serial optical section images was compiled for the serotonergic expression of the *D. erecta* MAG and SV from 16 images taken every 2.6 μm (Figure 19). The images revealed that this particular expression is on the surface of the MAGs and SV and absent from the lumen. The 5-HT immunoreactivity also stained the same male reproductive tissues of *D. yakuba* (Figure 20). The serotonergic neuronal patterns between these three *Drosophila* species (*D. melanogaster*, *D. erecta*, and *D. yakuba*) appear to be very similar.

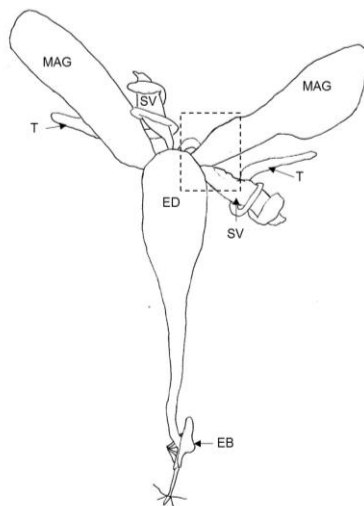
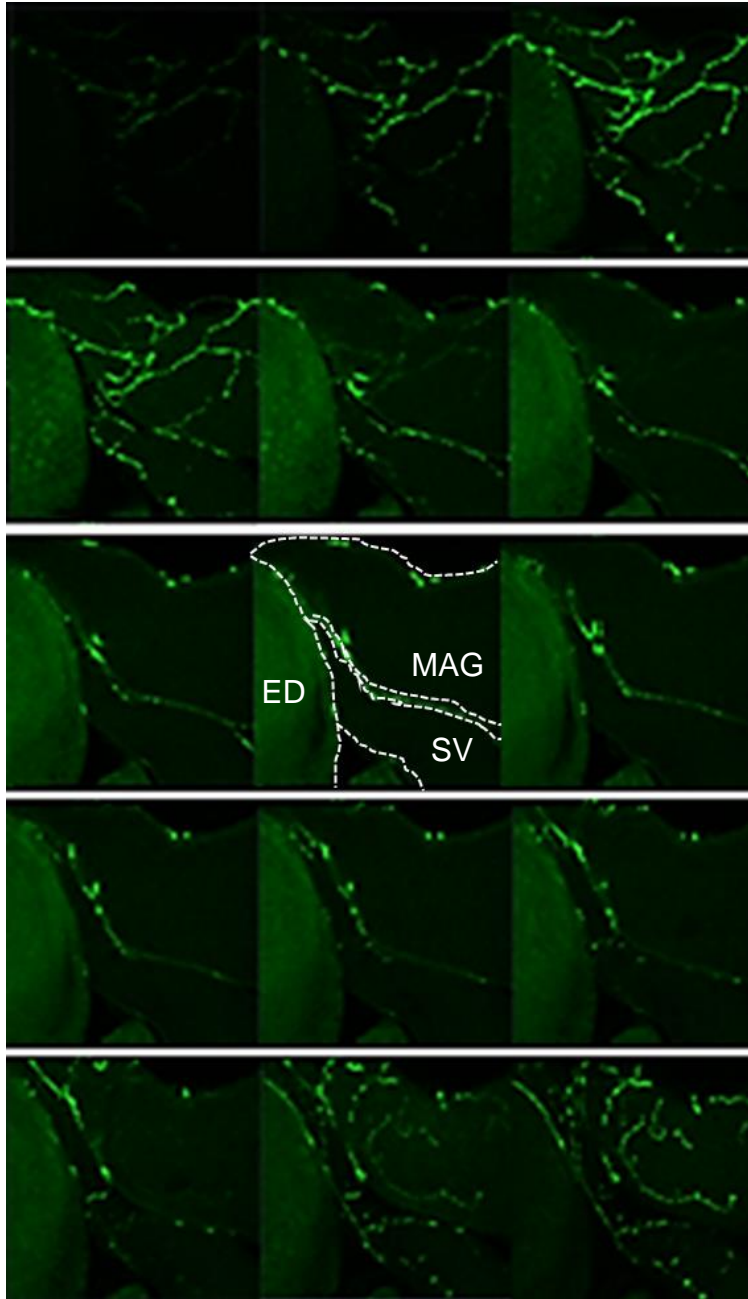


Figure 19 The serial optical section images of *D. erecta* serotonergic processes on MAG, ED, and SV from 16 images taken every 2.6 μm (40x magnification). Immunoreactive projections begin from the ED to cover the MAG and SV. A cartoon describing the tissue area of the serial optical section images of *D. erecta* serotonergic processes (box). T-testis.

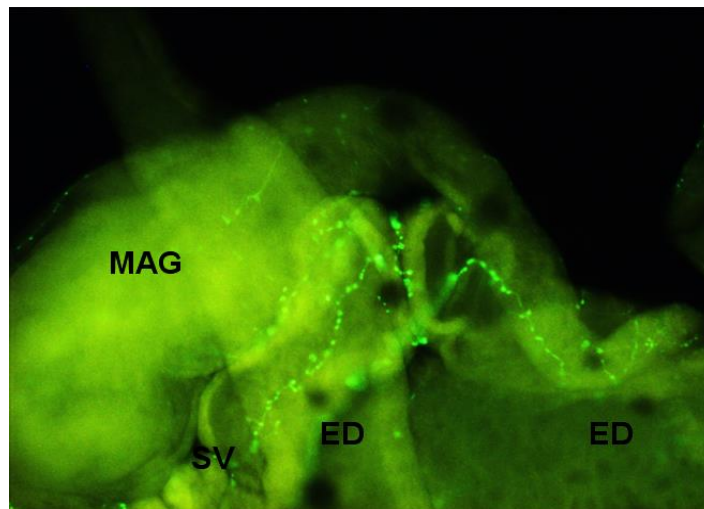


Figure 20 Expression of serotonergic processes in *D. yakuba* MAGs and SV detected with 5-HT antibody (40x magnification). No neuronal staining was observed in the negative sample. However, the background staining was observed when the negative sample image was captured at the same setting as the test sample.

3.2.4 RFa-like peptide is not co-localised with serotonin in the male reproductive tissues of *D. melanogaster* and *D. suzukii*

Double-labelling IHC was performed using anti-RFa antiserum (raised in rabbit) and anti-5-HT monoclonal antibody (raised in rat), which were combined and applied to the tissue. This combination was done to reveal any correlation of RFa and 5-HT in the neuronal processes associated with the reproductive tissues. The primary antibodies were paired with the conjugated secondary antibody with different excitation/emission wavelengths. The RFa and 5-HT expression patterns of *D. melanogaster* ED and MAG were distinct and did not overlap (Figure 21C). The saturation colour of these two fluorescent reporters has been reduced for a fair comparison.

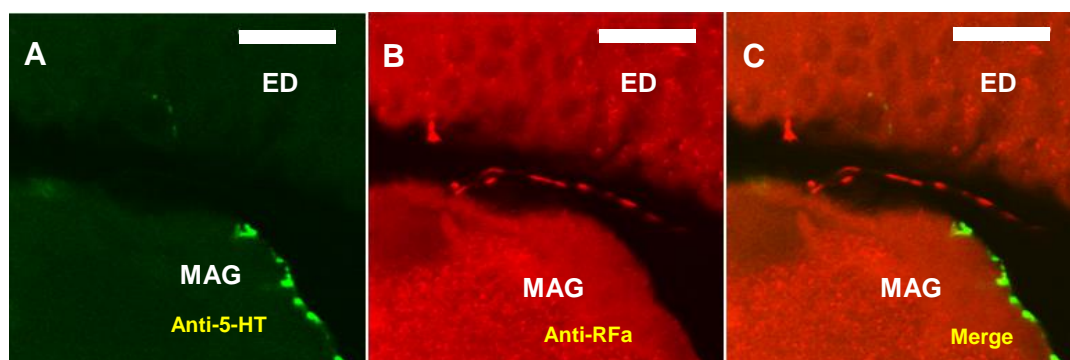


Figure 21 Confocal microscopy of the double-labelling staining of RFa and 5-HT of *D. melanogaster* ED and MAG (40x magnification). (A) 5-HT expression at the MAG (B) RFa expression between the ED and MAG (C) Merge. The respective expressions are situated at different tissues (MAG and ED) and are not co-localised. The scale bars represent 50 μm .

The serial optical section images show layer by layer the RFa (red) and 5-HT (green) expression patterns in the area of the *D. melanogaster* male reproductive tissue (Figure 22). These images confirm that these two neurotransmitter were not co-localised (Figure 23).

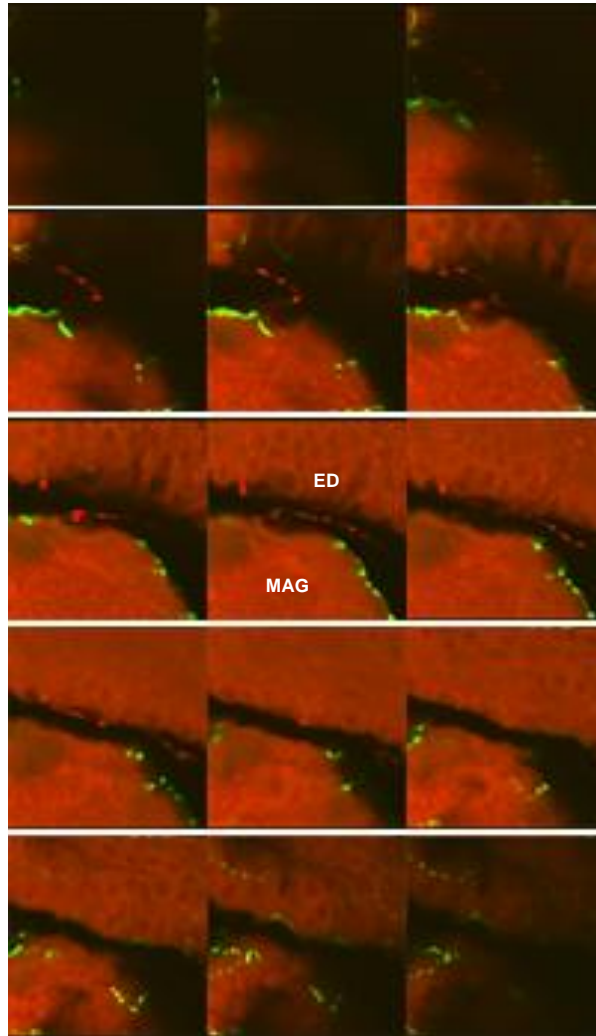


Figure 22 The serial optical section images of RFa (red) and 5-HT (green) IHC (40x magnification) confirm the absence of co-localisation of these neurotransmitters in neurites on the surface of the ED and MAG.

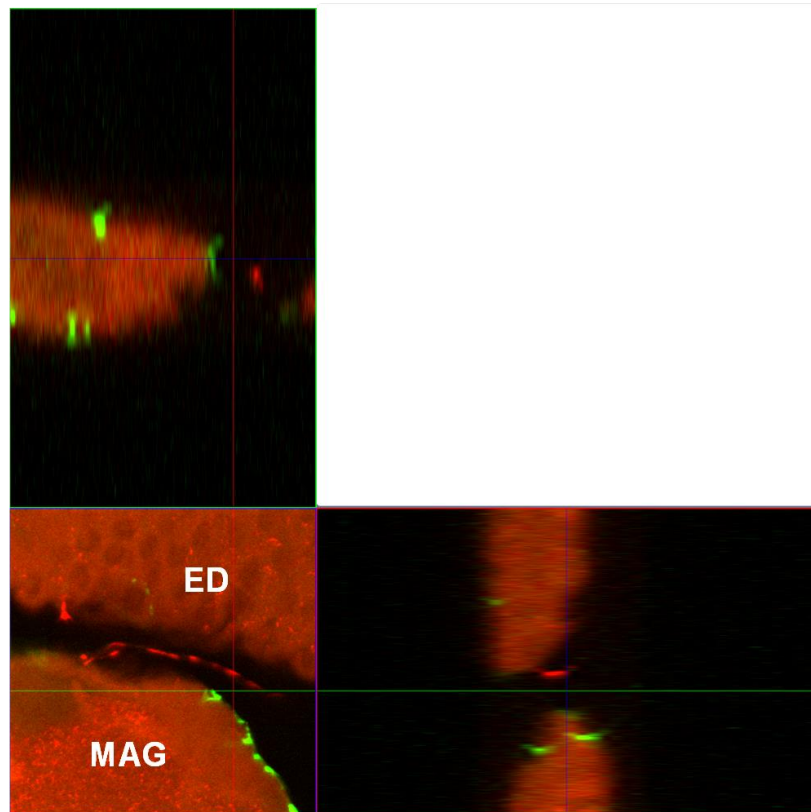


Figure 23 Cross section of *D. melanogaster* RFa (red) and 5-HT (green) staining (40x magnification). The respective stainings are observed to be outside the ED and MAG and are not co-localised. This image was focused on the two expressions of the sample to confirm that the RFa and 5-HT are not present in the same neurons.

Concurrently, the brain of *D. melanogaster* wandering larvae was used as a positive control for the RFa and 5-HT antisera (Figure 24). The patterns of RFa and 5-HT neurons are distinct and non-overlapping. No RFa staining was observed when the primary antibody was blocked with 1 μ M myosuppressin peptide. The non-intense background staining was observed when the image was captured at the same setting as the test sample.

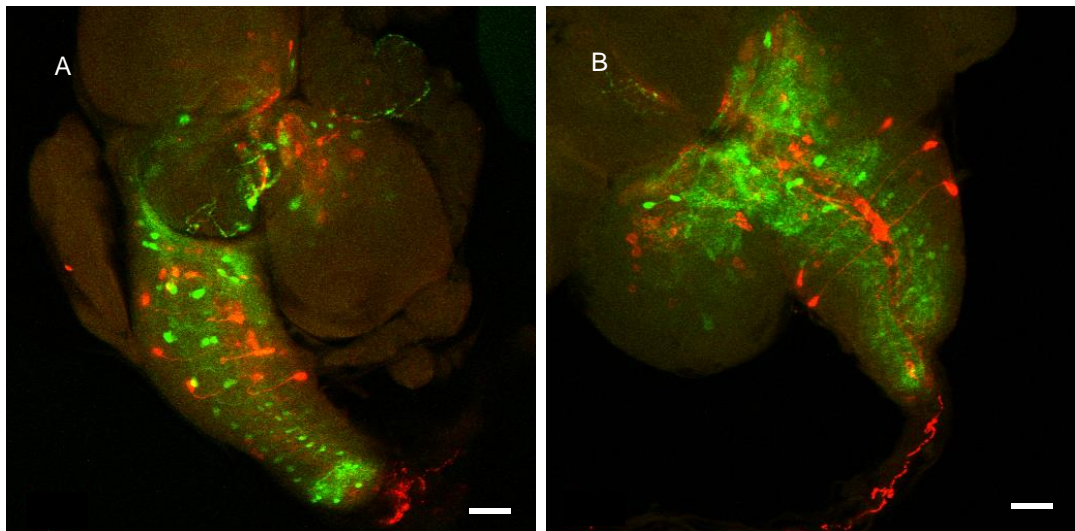


Figure 24 RFa and 5-HT expression in the CNS of wandering larvae of *D. melanogaster*. Brains dissected from wandering larvae were subjected to IHC to determine expression pattern for RFa peptides and 5-HT. Anti-RFa antisera visualised with the Alexa Fluor[®] 594 goat anti-rabbit secondary antibody (red) and anti-5-HT antibody visualised with the Alexa Fluor[®] 488 goat anti-rat secondary antibody (green). Images A and B show RFa and 5-HT expression are distinct and non-overlapping. The scale bars represent 50 μ m.

The double-labelling IHC was also carried out on the reproductive tissues of the important crop pest, *D. suzukii*. Figure 25A shows that RFa and 5-HT neurons are distinct and non-overlapping at the MAG and ED. By using higher magnification, these expression patterns are clearly distinct. The RFa expression is seen outside the tissue, and the 5-HT dominantly covers the MAG. In another tissue sample from *D. suzukii*, both RFa and 5-HT expression are non-overlapping (Figure 26).

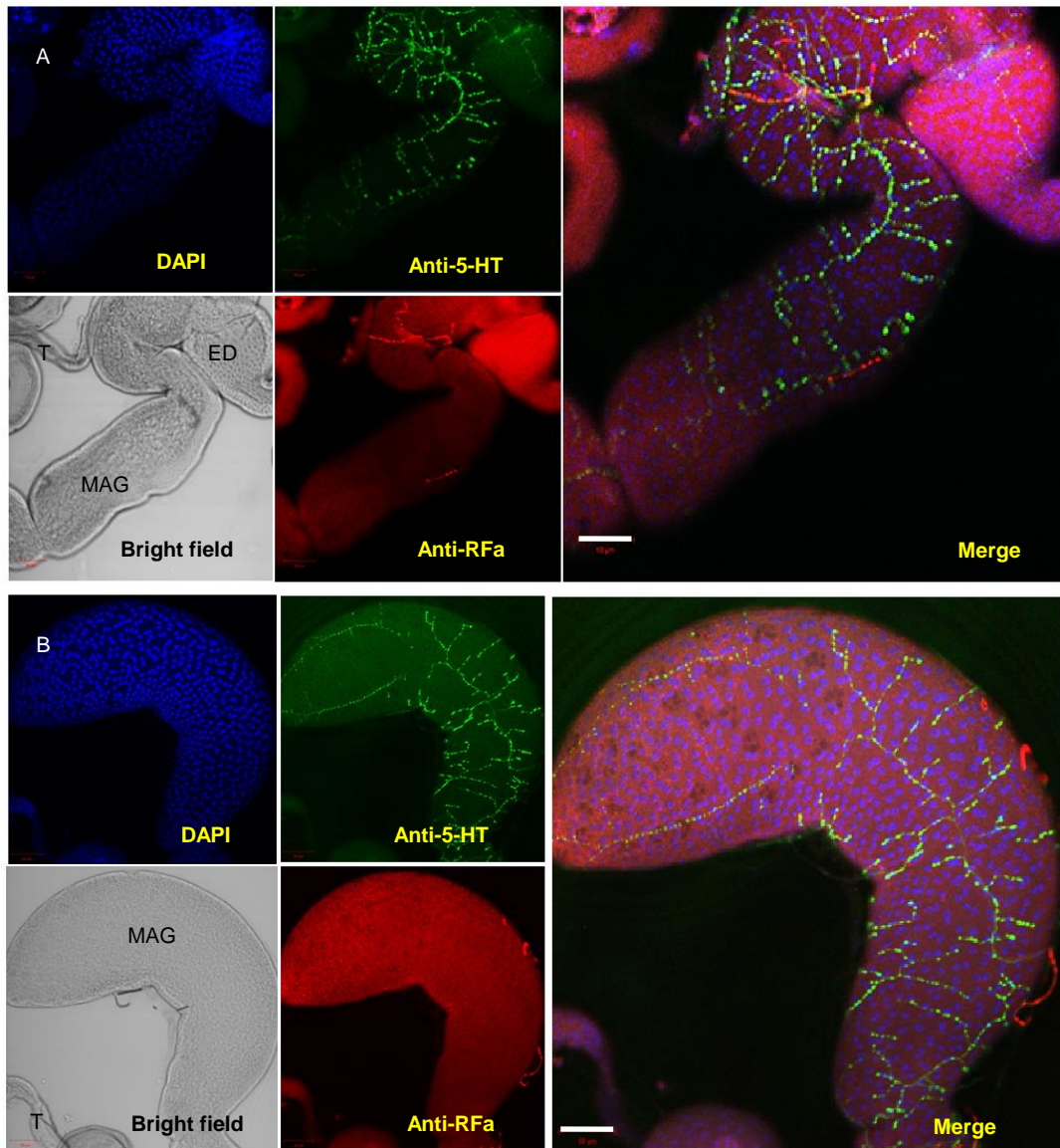


Figure 25 RFa and 5-HT expressions at *D. sukuzii* MAG detected with RFa and 5-HT antisera. (A) expressions of RFa (red) and 5-HT (green) neurons are distinct and non-overlapping at the MAG and ED. (B) The RFa expression is seen outside the tissue, and the 5-HT dominantly cover the MAG. The scale bars represent 50 μm .

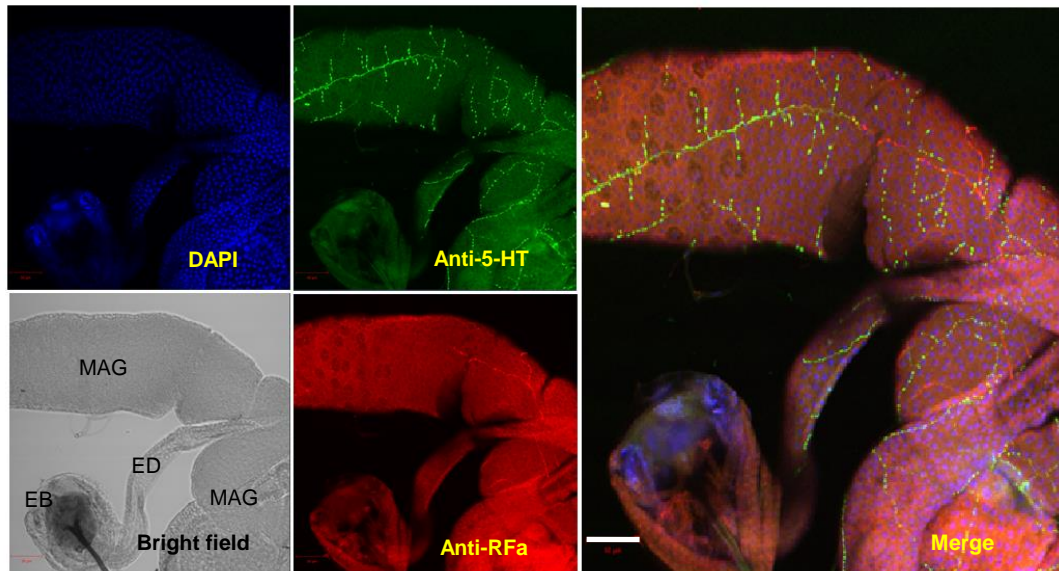


Figure 26 RFa (red) and 5-HT (green) neurons in *D. sukukii* MAG and ED.

Both RFa and 5-HT staining are non-overlapping (Merge). The scale bars represent 50 μm .

3.3 Discussion

Male seminal fluid components are known to alter the behaviour of the post-mated female of *D. melanogaster* (Avila *et al.*, 2011). The best known is the 36 amino acid SP, but other proteins and peptides have also been identified in the MAGs of the *D. melanogaster* which may also act as elicitors of behavioural changes in the post-mated female. Based on the FlyAtlas, it has been shown the DMS is highly expressed in *D. melanogaster* MAG (Chintapalli *et al.*, 2007) suggesting that this peptide might act as another behaviour modifying ‘sex’ peptide. Using a combination of RP-HPLC and MALDI-TOF-MS, a peptide extract from *D. melanogaster* MAGs was analysed for evidence of the presence of DMS stored in the lumen of the glands. No molecular ion corresponding to mature DMS (m/z 1247.6) was detected. This finding appeared to be at odds with the finding reported in FlyAtlas. To confirm this finding, IHC was done by using RFa antiserum to visualise any DMS (TDVDHVFLRFa) in the reproductive tissue of the *D. melanogaster*.

RFa immunoreactivity was shown to present outside the tissue and on the surface of the MAG and ED. No RFa expression was found on the testes (Figure 7). These immunoreactive fibres connected the anterior and posterior part of the ED (Figure 7A), and connected the MAG with the ED (Figure 7B) and ramified over the surface of the ED. We also found a bundle of neurites at the base of the MAG connecting to the ED (Figure 7C). A similar neurite bundle has been described by Billeter and Goodwin (2004). In *fru(16)-GAL4>GFP* flies, the GFP neurite bundle is co-localised with 5-HT (Billeter and Goodwin, 2004). The *fruitless (fru)* gene functions in *Drosophila* courtship specifically in the male CNS (Ryner *et al.*, 1996). Silencing

fru will disturb the development of male-specific muscle of Lawrence (MOL), initiating courtship process in sex determination, courtship songs, and copulation (reviewed by (Goodwin, 1999)). We suggest the *fru(16)-GAL4>GFP* and 5-HT neurons are located adjacent to the RFa neurons, as shown in the double-stained images of 5-HT and RFa expressions.

Using confocal microscopy software, z-stack images were captured to obtain 3-dimensional pictures and cross sections. From the cross section, RFa expression is outside the tissue and not in the lumen (Figure 8). Hence, suggesting that the RFa peptide is not part of the seminal fluid that is transferred into the female reproductive tract during copulation. Based on the FlyAtlas and FlyBase, DMS is the only RFa peptide expressed in the MAGs. Hence, the RFa expression detected with antibodies in the reproductive tissue is most likely referring to DMS. However, further study will be reported in the next chapter to confirm the identity of this RFa. From the outcome of the expression pattern presented here, the function of the DMS is probably as a neurotransmitter/modulator. In addition, a positive control study was done simultaneously using *D. melanogaster* 3rd instar larvae brain treated with anti-RFa antiserum. The immunoreactive expression in Figure 9 is similar to the finding reported previously (Nichols *et al.*, 1999). The similar expression in the positive control is important to ensure the reliability of the RFa antiserum and the IHC method used.

The study described in this chapter was extended to several additional *Drosophila* species (*D. erecta*, *D. yakuba*, *D. simulans*, *D. virilis*, and *D. suzukii*) for species comparison. *D. suzukii* is of special interest as it is the only important pest crop amongst these species. It was first identified in Japan (Matsumura, 1931), but is now a major problem across Europe and the U.S.A. (Adrion *et al.*, 2014; Asplen *et al.*, 2015). Adult *D. suzukii* oviposit in fresh fruit and cause damage to the crop due to the larvae developing inside the fruit. It is becoming an economic problem in Europe and other countries worldwide (Calabria *et al.*, 2012). Based on the RFa expression shown in each species, the location and expression pattern is similar (Figure 10, Figure 11, Figure 12, and Figure 13). We suggest that the neuronal function of DMS in the male reproductive tract is evolutionarily conserved amongst the drosophilid fruit fly species and this role might also extend to other dipteran pests, such as mosquitoes. During slide viewing, a single bright cell associated with the ED was consistently observed in all studied *Drosophila* species, except in *D. virilis* and *D. suzukii* (Figure 14 and Figure 15). The RFa (DMS)-containing single cell associated with the ED is difficult to retain during dissection. Thus, the lack of staining in *D. virilis* and *D. suzukii* may be due to the removal of this single cell, not to the absence of RFa (DMS) immunoreactivity. The function and identity of this cell is unknown and will be discussed in the next chapter.

Several steps in IHC were optimised to maximise the sensitivity of the antibody staining and keeping the sample in excellent condition. In the first phase for the IHC, samples were exposed to the fixing agent (4% paraformaldehyde) by opening the cuticle rather than performing clean dissection of the tissue. This method of dissection protected the fragile reproductive tissue and kept it intact during each step

of the IHC. The targeted tissue should be entirely exposed to the solution to ensure it is properly treated during each phase of the IHC. During incubation of the fixing agent, it is advisable to leave the tissue overnight in 4°C on the shaker instead of an hour incubation time at room temperature. Also, several methods of dissection were tried and the incubation time for each solution as well as the concentration of the antibodies were optimised for the final method. For the last process of the IHC, mounting was done using a fluorescence microscope. The dissection was guided by the fluorescence emitted from the binding of the secondary antibody to the primary antibody. This method helped to keep the reproductive tissues and associated nervous system intact. The final method is described in the methods chapter and was used in subsequent studies described in later chapters.

To learn more about the single cell associated with the ED, tissues were mounted carefully onto slides to keep the reproductive tissues intact. *D. simulans* is a *Drosophila* species that is closely related to *D. melanogaster* (Sturtevant, 1920; Capy *et al.*, 1993). Careful dissection of *D. simulans* abdominal tissues revealed strong RFa staining of cells associated with the HG (Figure 16). The cells are located in a different plane of the rectum. The description is similar to the finding reported by McCormick and Nichols (2004) of DMS-containing cells in the HG region of *D. melanogaster*. These cells were called ‘rectal cells’ and were detected by using an antibody that recognised the N-terminal region (TDVDHV) of DMS, providing strong evidence in support of the identification of the RFa peptide as DMS. The question of whether the single cell associated with ED is one of the rectal cells is important from the identity and regulatory aspects.

DMS is known to inhibit muscle contraction of the heart, gastrointestinal tract, and oviduct (Holman *et al.*, 1986; Robb and Evans, 1994; Richer *et al.*, 2000) and therefore it is a reasonable hypothesis that DMS has a role in controlling the muscles of the male reproductive system. The 5-HT neurons are known to be involved in the control of copulation and seminal fluid transfer from the male to the female probably by increasing the frequency of ED peristalsis (Norville *et al.*, 2010).

Double immunostaining experiments for 5-HT and RFa (DMS) were done to investigate the relationship between the two neuronal signalling pathways. The RFa peptide (DMS) and 5-HT signals are not co-localised but are present in the same tissue and located close to each other in *D. melanogaster* (Figure 21). This is consistent with the RFa peptide (DMS) and 5-HT having different regulatory roles in these tissues. In addition, a distinct non-overlapping of RFa (DMS) and 5-HT was shown in the pest insect, *D. sukuzii* (Figure 25 and Figure 26). Referring to the expression of both RFa (DMS) and 5-HT in the reproductive tissue, we propose that the serotonergic neurons stimulate spontaneous peristalsis muscle contractions of the reproductive tissues while DMS innervation will be myoinhibitory.

Chapter 4

Spatial Expression and Function of the *Dromyosuppressin* gene (*DMS*) in Male Reproductive Structures of *Drosophila melanogaster*

4.1 Introduction

The expression pattern of a gene of interest at a specific restricted area in transgenic *Drosophila* has significantly contributed to biological sciences research alongside gene mutations and suppressing gene expression with RNA interference. Genes that have been targeted and engineered enable the visualisation of where and when a gene is expressed. Thus, especially for nervous system studies, it is valuable to use such genetic tools to identify and map cells, and to understand the function of genes in a particular signaling pathway. These tools can also be used to interfere with the functioning of a neuronal pathway by either inhibition or stimulation of a targeted neuron or even by ablation of the entire cell (Pfeiffer *et al.*, 2008; Pfeiffer *et al.*, 2010; Venken *et al.*, 2011; Griffith, 2012; Garbutt *et al.*, 2013).

One of the elements that has revolutionised the field of insect neurobiology is GAL4, a protein from the yeast *Saccharomyces cerevisiae* that binds to and activates a transcriptional activator (upstream activator sequence or UAS) under the control of the regulatory components that drive expression of the GAL4 protein. It is now routine to use the GAL4-UAS system in a binary fashion to express proteins or RNA (e.g. green fluorescent protein or GFP; hairpin RNA for RNA interference; cell death proteins; light activated ion channels) to map cells or to manipulate the functioning of neuronal pathways. Expression pattern information can be generated by expressing GAL4 under the control of enhancer regions for a gene of interest. Flies homozygous for the GAL4 gene can be crossed with flies transgenic for genes with UAS domains up-stream of reporter genes encoding, for example, GFP. GFP will only be detected in cells that express the GAL4 protein (Pfeiffer *et al.*, 2008; Pfeiffer

et al., 2010; Pfeiffer *et al.*, 2012; Jenett *et al.*, 2012). Many *D. melanogaster* lines are also available from stock centres (e.g. the Bloomington Drosophila Stock Center at Indiana University (<http://bdsc.indiana.edu/>)) that express GAL4 in specific tissues or sub-sets of cells. These lines are valuable for functional studies by expressing effector proteins or hairpin RNA in a cell or tissue specific manner (Dietzl *et al.*, 2007). RNAi lines are publicly available from Vienna Drosophila Research Center (<http://www.vdrc.at>).

FlyAtlas records high *DMS* transcript levels in the MAG of *D. melanogaster*, but HPLC/mass spectrometry failed to detect DMS in extracts of the MAGs, suggesting that the DMS is not a seminal fluid component (Chapter 3). It was also shown in Chapter 3 that antibodies raised against RFa which also recognised the RFa epitope of DMS, stained neurites on the surface of the MAG, ED, and SV, in paired rectal cells and a single ED cell of males of *D. melanogaster* as well as several other *Drosophila* species. The most likely explanation for the relatively high level of *DMS* transcript reported in FlyAtlas (Chintapalli *et al.*, 2007) for the MAGs is the strong expression in the three cells closely associated with the male reproductive structures, the ED and MAGs.

RFa is a C-terminal dipeptide sequence common to 19 *Drosophila* neuropeptides (Table 6) and therefore IHC on its own cannot identify unequivocally DMS-containing cells. An antibody specific for DMS was not available, and therefore an alternative approach was taken to provide evidence that the aforementioned neuronal RFa staining matched the expression of *DMS*. A GAL4 fly line (61H01) generated as part of the FlyLight Project at the Janelia Research Campus, Ashburn, Virginia,

U.S.A. (see Figure 27) was obtained to drive expression of GFP using the bipartite GAL4-UAS expression system. 61H01 uses a 1413bp intergenic promoter region that extends into the first exon of *DMS* to drive expression of the yeast transcriptional activator GAL4.

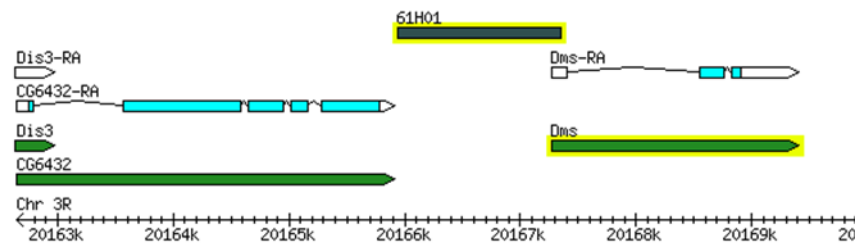


Figure 27 The GAL4 fly line (61H01) uses a 1413bp intergenic promoter region that extends into the first exon of *DMS* to drive expression of the yeast transcriptional activator GAL4.

This chapter reports the outcome of experiments using the 61H01 *DMS-GAL4* line to drive expression of GFP using the *10XUAS-IVS-Syn21-GFP-p10* (pJFRC81) GFP reporter line (henceforth *DMS>GFP*). In addition, the *DMS-GAL4* was crossed with flies carrying the cell death gene (*UAS-hid/rpr*) as one of the control experiments.

4.1.1 Chapter aims

The aim of the work described in this chapter was firstly to provide evidence to support the contention made in Chapter 3 that the RFa neurons of the male reproductive tissues contain myosuppressin (DMS, TDVDHVFLRFa). This was achieved by matching the expression pattern of GFP and RFa staining in *DMS>GFP* flies and by using single cell MALDI-MS to unequivocally identify DMS in the GFP-expressing ED cell of these flies. Mass spectrometry also identified sNPF⁴⁻¹¹ in the ED cells. Both peptides were tested for inhibitory effects on the spontaneous contractions of the MAG and ED tissues. Evidence was also sought for the expression of *Dromyosuppressin receptors (DMS-R)* in the reproductive tissue using GAL4 lines from Janelia Research Campus.

4.2 Results

4.2.1 *Dromyosuppressin* neurons of the male reproductive tract in

DMS>GFP flies

The spatial distribution of GFP in male reproductive tissues from *DMS>GFP* flies was compared with the staining pattern obtained using RFa antiserum. Reproductive tissues were dissected from adult male *DMS>GFP* flies, fixed in paraformaldehyde and double stained using antisera to RFa and GFP in order to determine whether RFa and GFP (*DMS*) co-localised in the same neurons.

The *DMS-GAL4* drove GFP expression in neurites of the reproductive tissues and these co-localised with RFa immunoreactivity as shown for the ED, indicating that the C-terminal dipeptide amide of DMS was cross-reacting with the RFa antibody (Figure 28A) and that the IHC was faithfully reporting DMS expression. Because of an issue with low intensity staining with RFa antiserum, a high magnification image was needed to scrutinize in detail the co-localisation of peptide and GFP staining (Figure 28B). The homozygous parental *UAS-pJFRC81* line did not show any detectable GFP expression (Figure 29). This parental line works as a negative control to show no leakage of GFP in the studied tissues. McCormick and Nichols (2004) have previously shown using N-terminal specific DMS antibody that DMS neurons innervate the adult crop. The GFP-reporter expressed under the control of *DMS-GAL4* generated GFP fibres extending from the CNS observed from the brain onto the proventriculus towards and onto the crop (Figure 30). This concurrence with the work from the Nichols laboratory provided supporting evidence that the

61H01 GAL4 line could be used to provide valuable information on the identity and pattern of DMS neurons.

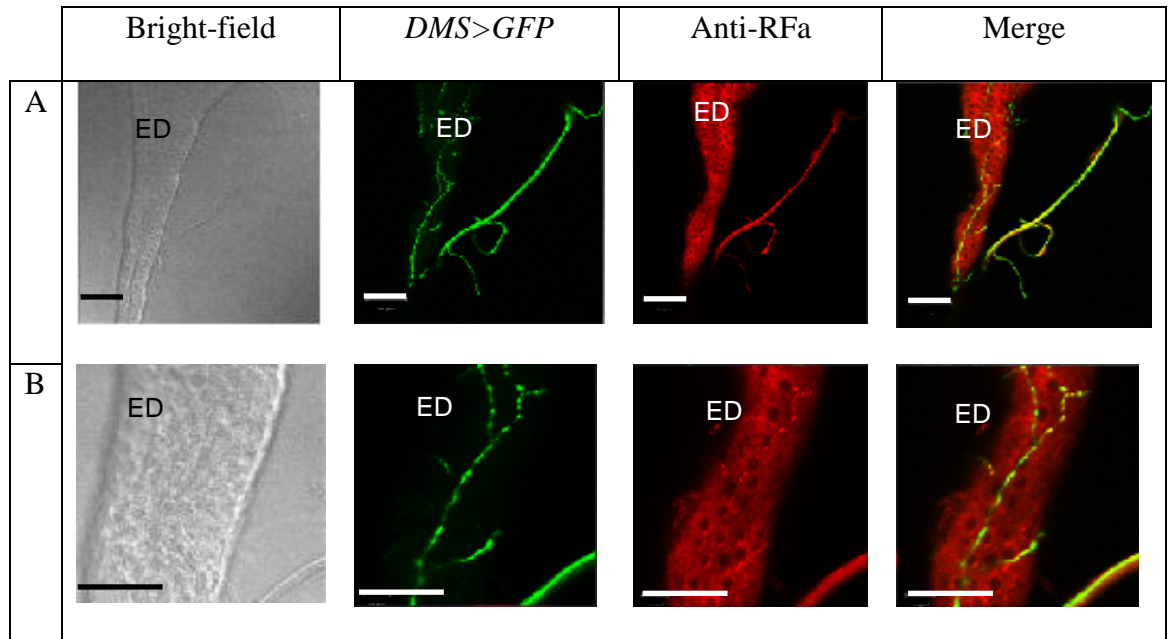


Figure 28 Characterisation of RFa immunoreactivity on the surface of the ED in *DMS>GFP* male flies.

- (A) Confocal images of the overall DMS neurons on the surface of the ED expressing *DMS>GFP* co-stained with anti-GFP (green) and anti-RFa (red) antisera. Note comprehensive co-localisation of GFP and anti-RFa (Merge). The scale bars represent 50 μ m.
- (B) Confocal images of DMS neurons at higher magnification on the surface of the ED expressing *DMS>GFP* co-stained with anti-GFP (green) and anti-RFa (red) antisera. Note comprehensive co-localisation of GFP and anti-RFa antisera (yellow). The scale bars represent 50 μ m.

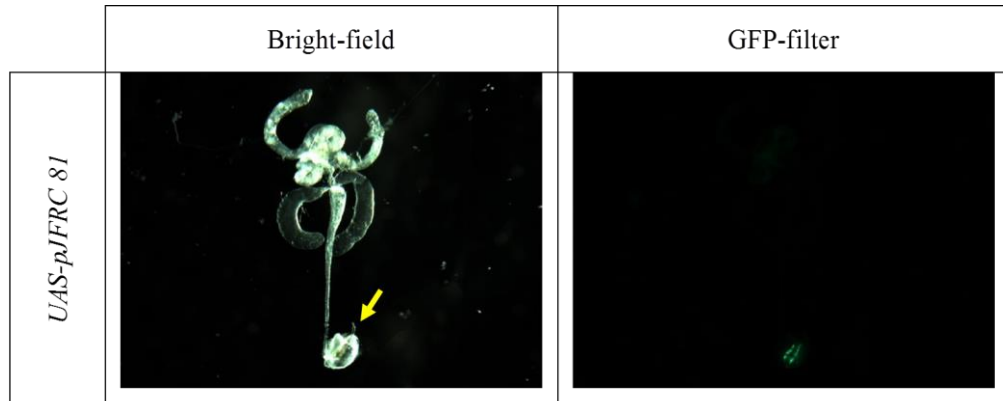


Figure 29 Ejaculatory bulb (EB) auto-fluorescent expression in *UAS-pJFRC81* male flies (4x magnification). Image was taken by using Leica fluorescence stereo microscope.

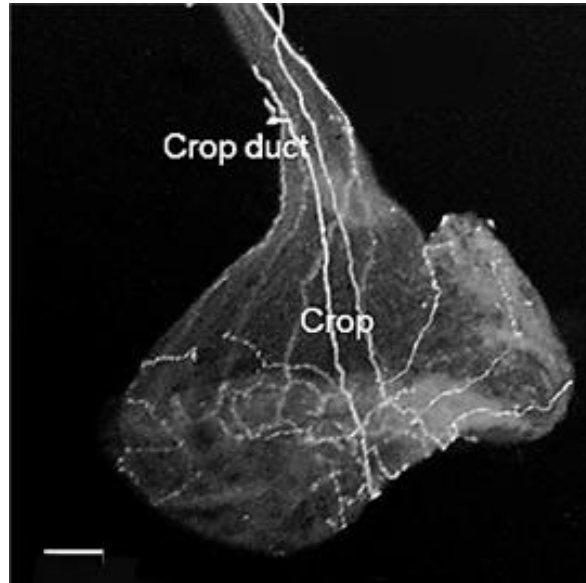


Figure 30 *DMS* neurons in the adult male *DMS>GFP* in crop. The GFP expression is projecting from the brain heading to the proventriculus and finally to the crop. Images were captured by confocal microscopy. The scale bar represents 50 μm .

4.2.2 No co-localisation of GFP and 5-HT in *DMS >GFP* male flies

This study was carried out to determine whether *DMS-GAL4* generates expression present in different neurons to serotonergic neurons. Male internal reproductive organs were dissected from adult males expressing GFP under the control of *DMS-GAL4* and incubated with anti-GFP and anti-5-HT antisera (Figure 31). *DMS-GAL4* neurites innervate the MAG (Figure 31A), ED (Figure 31B), and SV (Figure 15C). In general, serotonergic processes are more widely distributed compared to *DMS >GFP* expressing neurons. 5-HT and DMS neurites were abundant in the ED (Figure 31B) and SV (Figure 31C), but there was no co-localisation of these two neurotransmitters, establishing that 5-HT and DMS have different control functions. This finding supports the conclusion in Chapter 3 that the RFa-like peptide (DMS) and 5-HT are not present in the same neurons innervating the male reproductive tissues of both *D. melanogaster* and *D. suzukii*. However, the merge images in Figure 31 shows yellow colour expression indicating that both expressions may co-localise in some places. The yellow merge colour is due to the high-intensity expression of both DMS and 5-HT that are situated very close to each other and it is not being expressed in the same neurons.

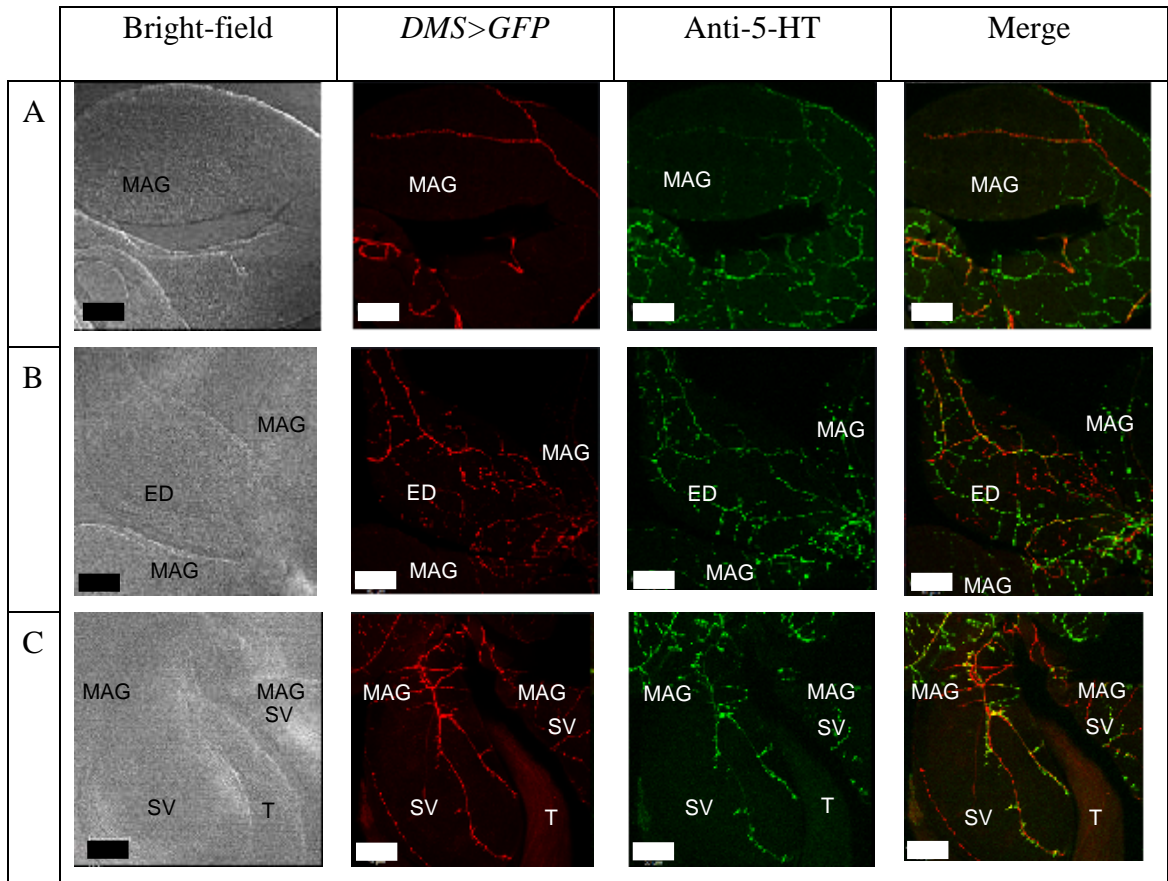


Figure 31 The *DMS-GAL4* transgene generates GFP expression in the MAG, ED, and SV tissues. Whole-mounted internal reproductive tissues from adult males expressing the GFP reporter under the control of the *DMS-GAL4* transgene were double-labelled with anti-GFP (red) and anti-5-HT (green) antisera. Images were captured by confocal microscopy. 5-HT-containing neurites spread over the tissues and show no co-localisation with neurites expressing GAL4-driven GFP on the MAG surface (Figure 31A), ED (Figure 31B), and SV (Figure 31C). The yellow merge colour in some places in the tissues (Figure 31) indicate there may be co-localisation present in the tissue, however, using higher magnification, both expressions are present in different neurons. The scale bars represent 50 μm .

4.2.3 *Dromyosuppressin* expression in the male abdominal ganglion, ejaculatory duct cell, and a pair of rectal cells

The relatively high intensity of RFa (putative DMS) immunoreactivity in the ED cell and a pair of rectal cells in male *Drosophila sp.* (Chapter 3) prompted us to examine the complete projection of these cells. Transgenic males carrying *DMS-GAL4* were crossed to a GAL4-responsive GFP transgene (*UAS-pJFRC81*) to label the neuronal processes. Scrutiny of *DMS>GFP* expression gave GFP expression in the ED cell and the pair of rectal cells (see yellow arrows in Figure 32B) close to and attached to the reproductive tissue and HG. GFP was present in several soma in the posterior part of the abdominal ganglion (AbG) of the ventral nerve cord (VNC) (Figure 32E and Figure 32F). The GFP axons from these AbG cell bodies project into the abdomen and branches (see white arrows in Figure 32C and Figure 32D) innervate the reproductive organs as well as the HG (Figure 32D).

Dissections were performed on unfixed tissue using a Leica fluorescence stereo microscope to maximise the chances of a complete dissection of the neuronal tissue and cells attached to the reproductive tissues. In each dissection, however, this was challenging as the fibres are easily detached, and the dissection needs to be quick to minimise loss of GFP expression. Furthermore, complications can arise since the ED and rectal cells often attach to the abdomen body wall. Hence, a cartoon describing the *DMS* expression in *Drosophila* abdominal organs is shown in Figure 33.

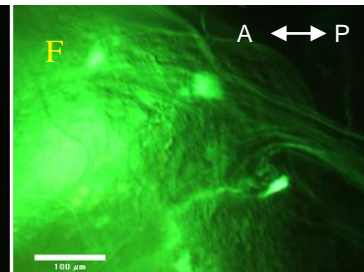
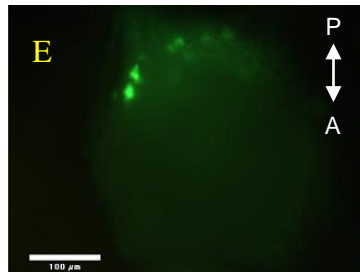
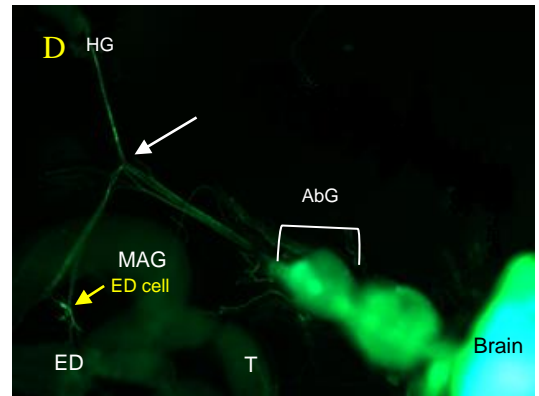
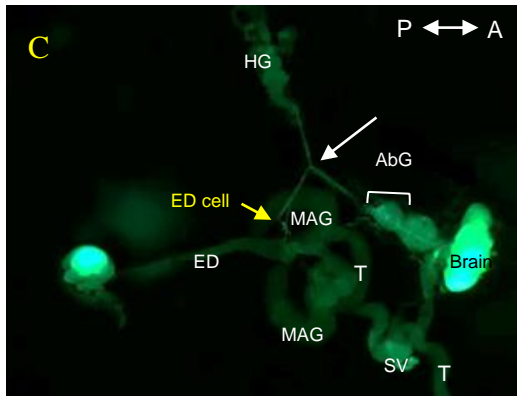
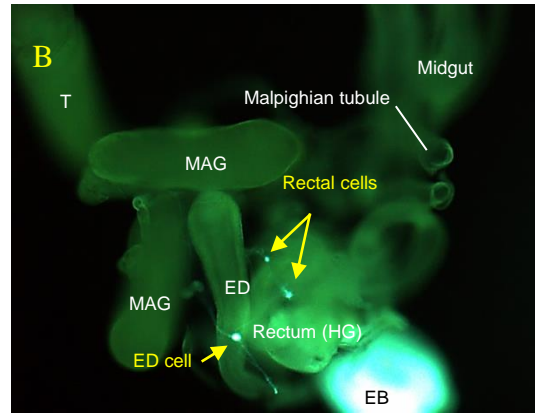
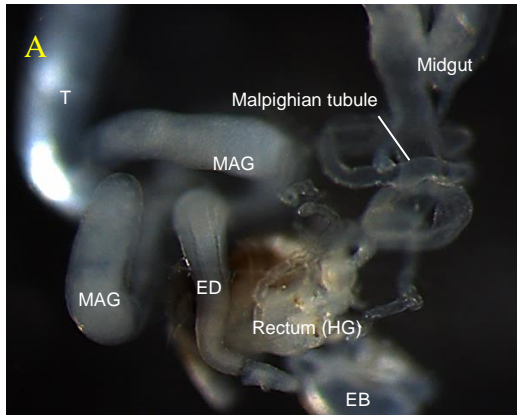


Figure 32 Male *DMS-GAL4* neurons of the AbG that innervate abdominal organs. Tissues were dissected from *DMS>GFP* adult males in fly saline, and the GFP fluorescence was captured using a fluorescence stereo dissecting microscope. (A) Bright-field image of unfixed abdominal organs. (B) The ED and two rectal cells (see yellow arrows) are connected to each other. There is strong auto-fluorescent from the EB. (C-D) GFP neuronal projections emerge from the AbG and project to the male's internal reproductive organs and HG. Neurites branching off (see white arrows) from the AbG ramify the male's internal reproductive organs and rectum (HG). The yellow arrows show the ED cell attached to the neurites near the ED. There is strong auto-fluorescent from the EB. The orientation of the sample is indicated at the top of the image: A, anterior; P, posterior. (E-F) The AbG was observed from dorsal view. (E) Several GFP soma are present at the posterior part of the AbG. (F) Neuronal projections emerge from the AbG and send axons to the posterior part of the body. The orientation of the sample is indicated at the top of the image: A, anterior; P, posterior. T-testis. The scale bars represent 100 μm .

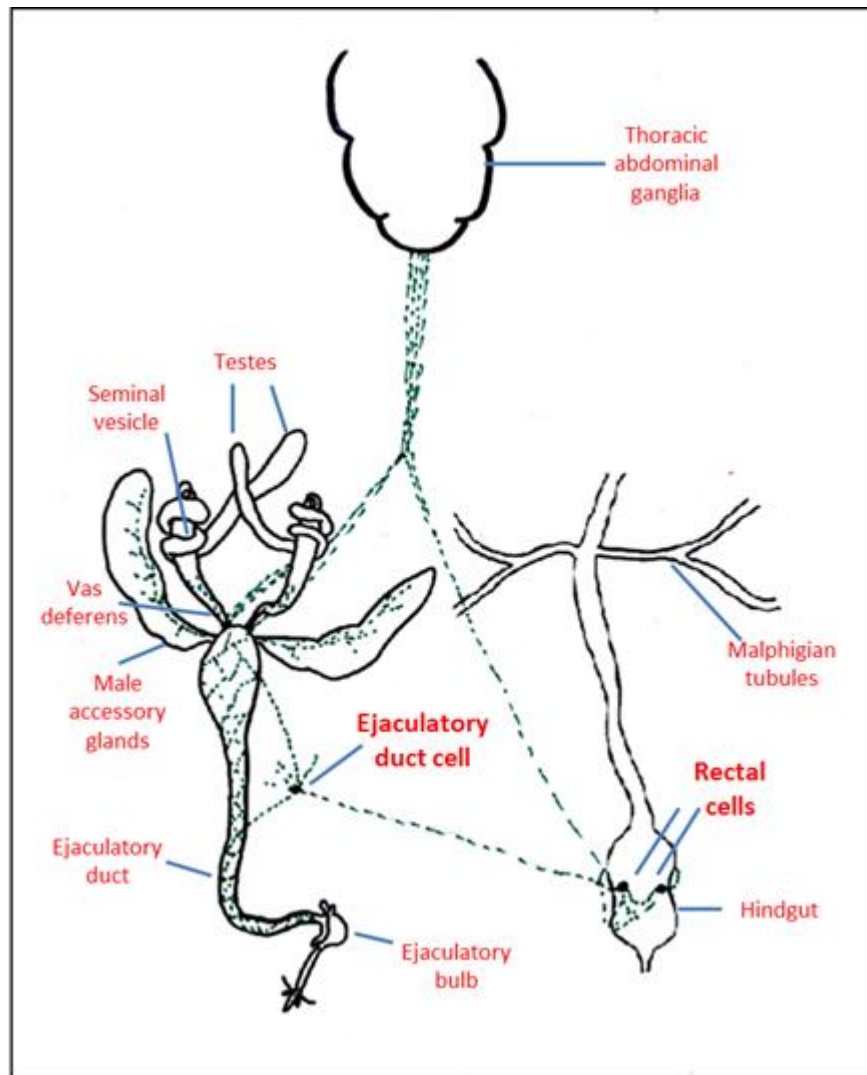


Figure 33 A cartoon describing the innervation of male abdominal organs by *DMS* neurons. The *DMS* axons emerge from the AbG and branch off to ramify over the VD, SV, MAG, ED, and HG. No branches were observed at the testes and EB. The *DMS* axons reach the male's reproductive organs at the base of the VD. The innervations connect the SV and ED to the ED cell and a pair of rectal cells at the HG. The rectal cells are also connected to the axons from the AbG.

4.2.4 Single-cell peptidomics of *Drosophila melanogaster* ejaculatory duct cell

The ED single-cell in *DMS>GFP* adult male flies, was isolated by dissecting the cell under a fluorescence microscope guided by the GFP expression. This neuron was subjected to MALDI-TOF mass spectrometry to identify peptide/s that is present in the cell. The work was performed by our collaborator Dr. Susanne Neupert, University of Cologne, Germany using the single-cell peptidomics analysis method (Neupert *et al.*, 2007).

The representative spectra for the ED cell applied directly onto the MALDI plate shows significant monoisotopic peaks ($[M+H]^+$) over the m/z range of 900-4000 (Figure 34A). The mass ions at m/z 1247.717 and 1269.701 are in agreement with the monoisotopic mass of myosuppressin (TDVDHVFLRFa). The sequence of myosuppressin was confirmed by fragmentation of the parent ion, 1247.717 (Figure 34B). Furthermore, the mass ion 974.597 corresponds to the truncated short neuropeptide F (sNPF⁴⁻¹¹), SPSLRLRFa (Figure 34A).

sNPF-GAL drives expression of GFP in the ED cell using the *10XUAS-IVS-Syn21-GFP-p10* (pJFRC81) GFP reporter line (henceforth *sNPF>GFP*) (Figure 35A). The single ED cell is attached to the ED and rectum without any rectal cells present in the abdominal posterior part area. GFP is absent from the reproductive tract tissue. GFP was not present at the posterior part of the digestive tract of 3rd instar larval stage (see yellow arrows in Figure 35C). The GFP expression in the *sNPF>GFP* 3rd

instar larvae hypocerebral ganglion and anterior endocrine cells acts as a positive control (see yellow arrows in Figure 35B).

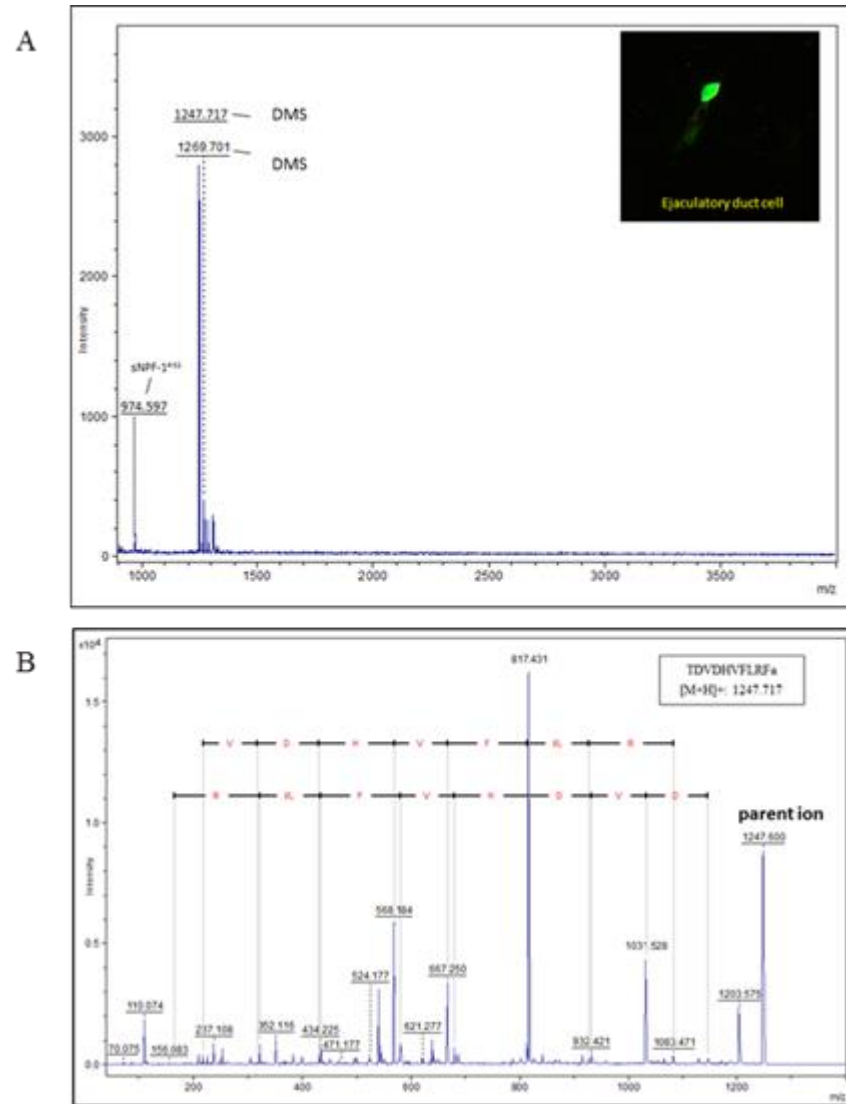


Figure 34 MALDI-TOF mass spectra obtained from a single ED cell of *DMS>GFP* adult male fly. (A) Mass fingerprint, representing dromyosuppressin (DMS) and truncated short neuropeptide F (sNPF⁴⁻¹¹). (B) MALDI-TOF/TOF tandem fragmentation mass spectrum of the parent mass ion [M+H]⁺: 1247.717.

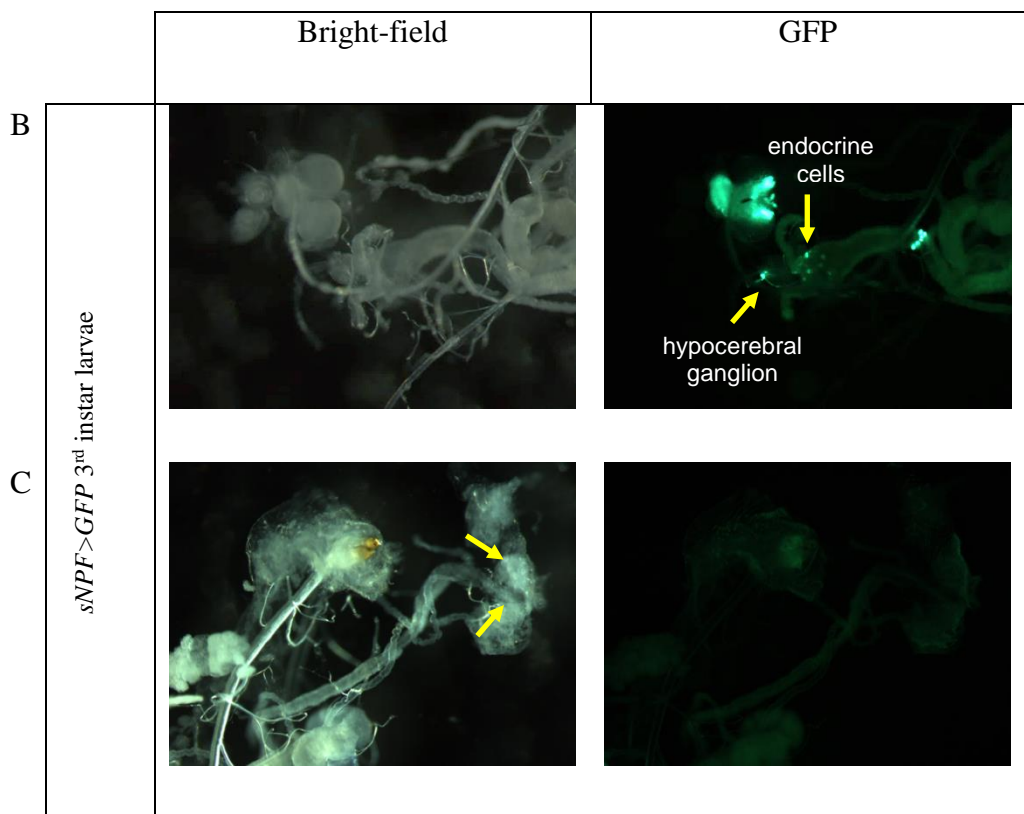
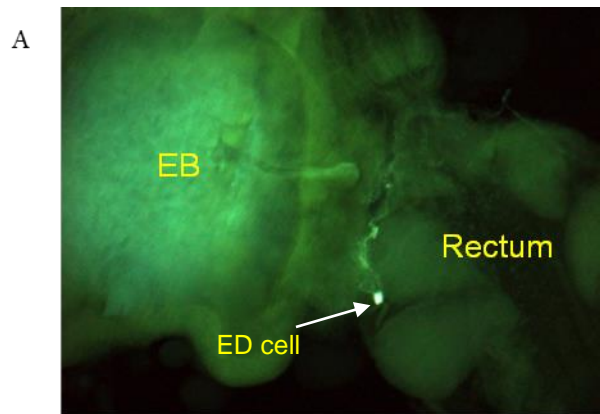


Figure 35 The *sNPF-GAL4* transgene generates GFP expression in the ED cell.

(A) The GFP immunoreactivity in the ED cell (white arrow) connecting ED and rectum. No GFP expression in the rectal cells at the rectum area. (B) The *sNPF-GAL4* transgene generates GFP expression in the hypocerebral ganglion and anterior endocrine cells of 3rd instar larvae (see yellow arrows). (C) No GFP expression in the rectal cells (see yellow arrows) at the rectum area. Images were captured by using a fluorescence stereo microscope (6.3x objective).

4.2.5 **DMS>GFP in rectal cells of the 3rd instar wandering larvae and adult female**

In *DMS>GFP* larvae and adult females, GFP expression was present in rectal cells but no other GFP labelled cells were found in the area of the HG or female reproductive tract (Figure 36). In *DMS>GFP* adult female and larvae, two adjacent GFP immunoreactive cells are connected to each other and to the rectum (Figure 36A and Figure 36C). After careful dissection, the rectal cells can be seen attached to the base of the female reproductive tissue (Figure 36B). Combination of *DMS-GAL4* and *UAS-hid/rpr* (henceforth *DMS>hid/rpr*) shows no RFa (DMS) immunoreactivity in the reproductive tissue of both male and female.

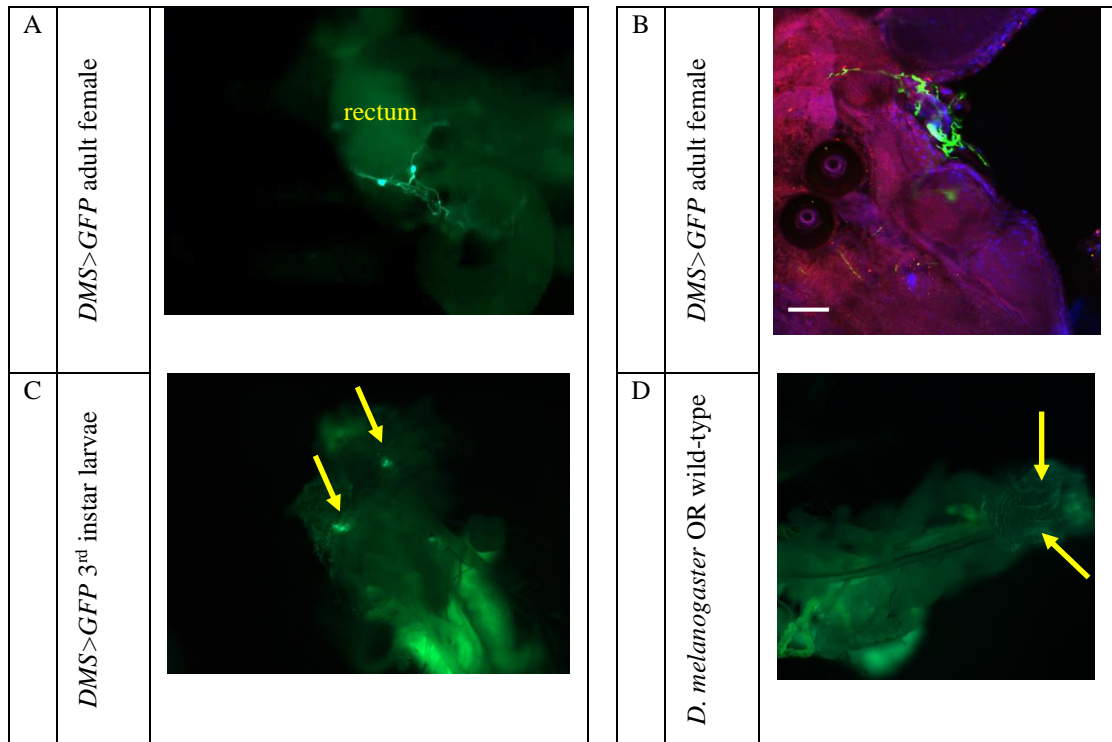


Figure 36 The *DMS-GAL4* transgene generates GFP expression in the rectal cells of adult female and 3rd instar larvae. (A) Rectal cells at the rectum area of the *DMS>GFP* adult female (12x magnification). (B) Rectal cells (green) are connected to the base of the female reproductive tissue. No proctolin (red) expression present in the rectal cell. The scale bar represents 50 μ m. (C) Two immunoreactive cells (yellow arrows) near the posterior part of the larval gut of *DMS>GFP* 3rd instar larvae (8x magnification). (D) No auto-fluorescent expression at the posterior area (yellow arrows) of the *D. melanogaster* OR wild-type 3rd instar larvae (6.3x magnification). Images were captured by using fluorescence stereo microscope (Figure 36A, C, and D) and confocal microscope (Figure 36B).

4.2.6 Dromyosuppressin control of muscular activity of the ejaculatory duct and male accessory glands in *Drosophila melanogaster*

To gain more insight into DMS and sNPF function in the male reproductive tissues, the effect of peptide on the contractions of the respective tissues was done. A basal rate of the tissues' motility was determined as the number of contractions. The contractions were also recorded using a video microscope and analysed by using custom software to detect the frequency changes between frames. The ED contractions are composed of a variable strength of frequency (see fly saline frequency in Figure 37). DMS decreases the amplitude and frequency of spontaneous ED contractions in a dose-dependent manner, with an EC_{50} of 1.5×10^{-8} M (Figure 38). Complete inhibition of the ED contractions was not achieved even with higher DMS concentrations. The effect of DMS was reversible, and spontaneous contractions resumed a few minutes after washing several times with fly saline. In a control experiment, ED contractions in the absence of peptide remained stable for more than 20 minutes.

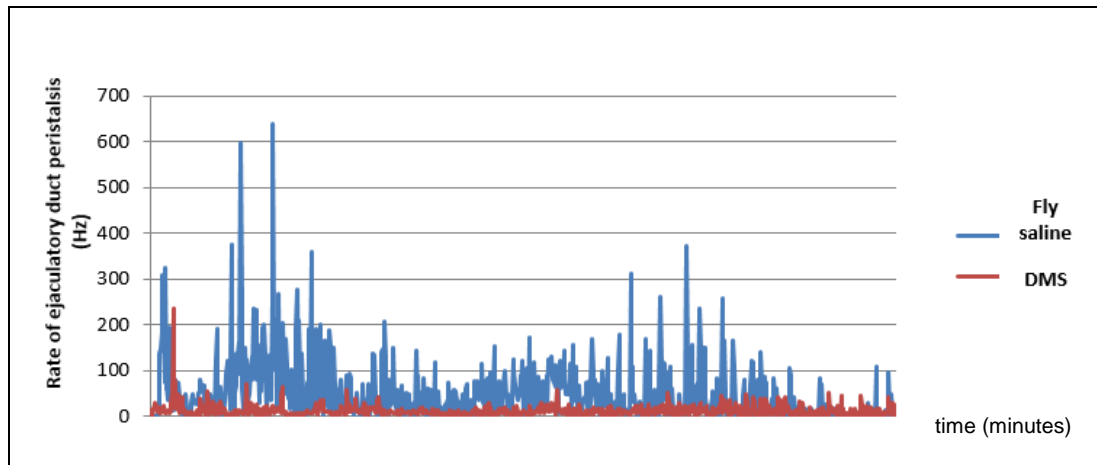


Figure 37 DMS inhibits the frequency of ED contractions. The traces show the fly saline control (blue) peristalsis frequency before adding the peptide followed by the addition of 5 μm DMS (red) 2 minutes after the addition.

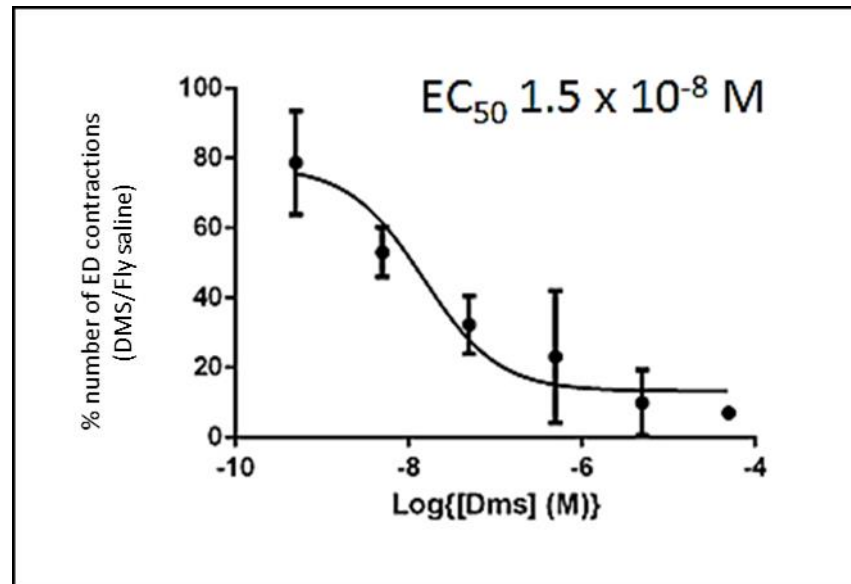


Figure 38 DMS inhibits the number of ED contractions in a dose dependent manner, with EC₅₀ of 1.5x10⁻⁸ M.

sNPF⁴⁻¹¹ also inhibits the frequency of ED contractions (Figure 39). However, the tissue is not as sensitive to sNPF⁴⁻¹¹ compared to DMS. At 50 μ M, the inhibition of the ED contractions is very visibly similar to that of 5 μ M DMS. sNPF⁴⁻¹¹ applied at a concentration of 5.00×10^{-07} M inhibited the ED contractions by 53.13%. The effect of sNPF⁴⁻¹¹ is reversible, and spontaneous contractions resumed a few minutes after washing several times with fly saline (data not shown). The *D. melanogaster* MAG contractions are composed of circular muscle contractions of variable strength and frequencies (Figure 40). Both 50 μ M DMS (Figure 40A) and sNPF⁴⁻¹¹ (Figure 40B) inhibited the MAG contractions respectively. However, only the DMS peptide gave complete inhibition. The effect of DMS and sNPF⁴⁻¹¹ was reversible, and spontaneous contractions resumed a few minutes after washing several times with fly saline.

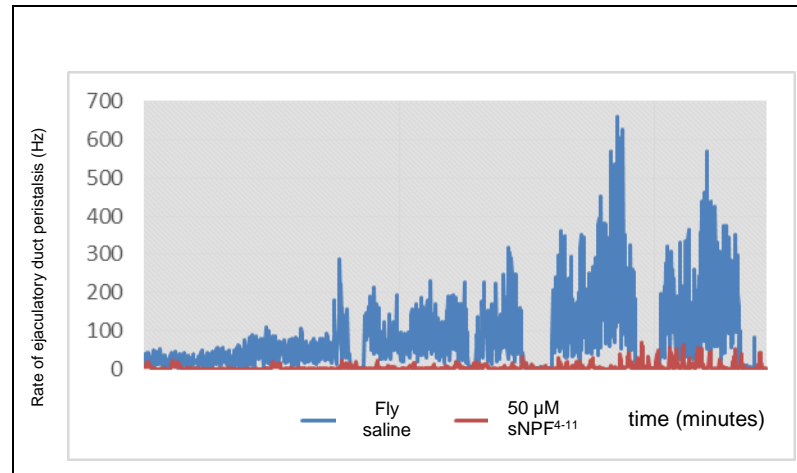


Figure 39 sNPF⁴⁻¹¹ inhibits the frequency of ED contractions. The ED contractions are composed of a variable strength of frequency. The traces show the fly saline control (blue) peristalsis frequency before adding the peptide followed by the addition of 50 μM sNPF⁴⁻¹¹ (red) frequency 2 minutes after the peptide addition. There is inhibition of peristalsis of the ED with a relatively high concentration of sNPF⁴⁻¹¹ (50 μM).

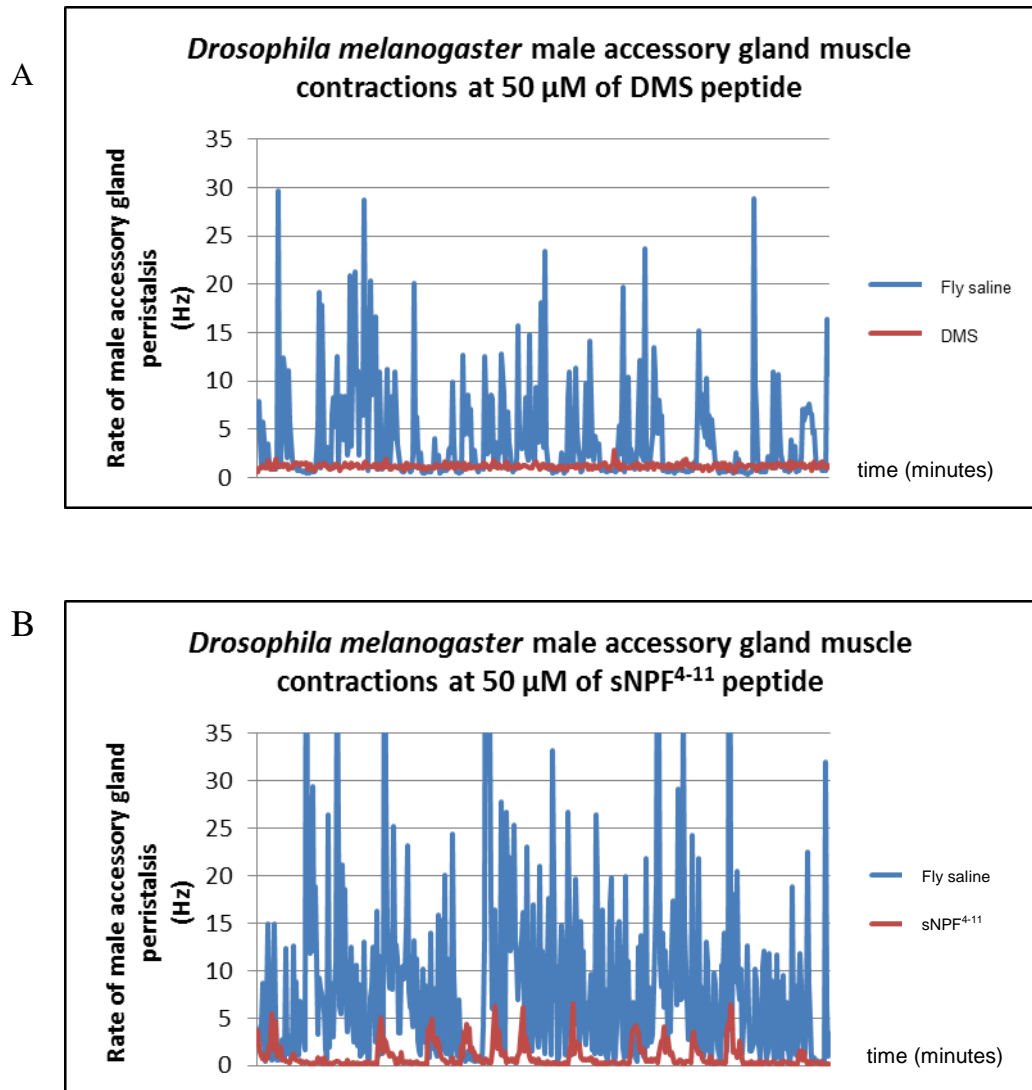


Figure 40 DMS and sNPF⁴⁻¹¹ inhibit the frequency of MAG contractions. The MAG contractions are composed of a variable strength of frequency. The traces show the fly saline control peristalsis frequency (blue) before adding the peptide, followed by the addition of 50 μ M DMS (Figure 40A) and sNPF⁴⁻¹¹ (Figure 40B) frequency (red) 2 minutes after the peptide addition respectively. There is complete inhibition of the MAG with 50 μ M DMS compared to the 50 μ M sNPF⁴⁻¹¹.

4.2.7 **Dromyosuppressin receptor expression in the male reproductive tissue**

We have shown DMS neurons innervate the MAGs, ED, and SV tissues. This peptide also inhibits ED and MAGs muscle contractions. This action requires expression of a DMS receptor in these tissues. 27 GAL4 lines for the *Dromyosuppressin receptor* (*DMS-R1* and *DMS-R2*, FlyLight Project, Janelia Research Campus) were screened for expression of GFP using the *10XUAS-IVS-Syn21-GFP-p10* (pJFRC81) GFP reporter line (henceforth *DMS-R1>GFP* and *DMS-R2>GFP*) in the male reproductive tissues. Each GAL4 line carries part of the upstream promoter region for *DMS-R1* or *DMS-R2*.

Four GAL4 lines from the *DMS-R1* (46546, 46575, and 48230) and *DMS-R2* (47699) showed GFP expression in neuronal fibres and muscle cells of the SV, MAGs, and ED tissues, while the others showed expression in some of the tissues or no expression (Table 7). All the neuronal expression patterns are similar to the expression pattern for *DMS>GFP* (refer to Figure 28 and Figure 31). For two GAL4 lines some GFP was expressed in the cytoplasm of the secondary cells of the MAGs (see Figure 41). *DMS-R1* (48230)*>GFP* is the only line showing both neuronal and muscle-like expression in the MAGs (Figure 42C). In the MAG muscle, a single bright nucleus stains for GFP in between the junctions of the myofibres (Figure 42C-D). The myofibre expression in the MAGs of *DMS-R1* (48230)*>GFP* flies was compared with phalloidin (actin filament) staining of the MAGs from wild type (Figure 42F). A myosin-active GFP line was also used for comparison (Figure 43A).

No muscle-like expression was present in any of the reproductive tissues of DMS-R2>GFP lines.

Table 7 The *DMS-R* expression in male reproductive tissues of *DMS-R1* and *DMS-R2-GAL4* lines from Janelia Research Campus.

| GAL4 | <i>DMS-R</i> | SV | MAG | ED |
|-------------|---------------------|-----------|------------|-----------|
| 39247 | 2 | - | - | - |
| 39262 | 1 | - | - | neuronal |
| 39297 | 1 | - | - | - |
| 39310 | 1 | - | - | - |
| 39312 | 1 | - | neuronal | neuronal |
| 39314 | 2 | - | - | - |
| 39339 | 2 | - | - | - |
| 39341 | 2 | - | - | neuronal |
| 39355 | 1 | - | neuronal | neuronal |
| 39378 | 1 | - | - | - |
| 39391 | 1 | - | - | - |
| 39399 | 2 | - | - | - |
| 39402 | 2 | - | - | - |
| 39404 | 2 | - | neuronal | neuronal |
| 39432 | 2 | - | neuronal | neuronal |
| 39437 | 1 | - | - | - |
| 39445 | 1 | - | - | neuronal |

| | | | | |
|-------|---|----------|--------------|----------|
| 41284 | 2 | - | - | - |
| 46546 | 1 | neuronal | neuronal | neuronal |
| 46548 | 1 | - | - | - |
| 46556 | 2 | - | - | - |
| 46575 | 1 | neuronal | neuronal | neuronal |
| 47699 | 2 | neuronal | neuronal | neuronal |
| 47703 | 1 | - | neuronal | - |
| | | | neuronal and | |
| 48230 | 1 | neuronal | muscle | neuronal |
| 48292 | 1 | - | - | - |
| 49600 | 1 | - | - | - |

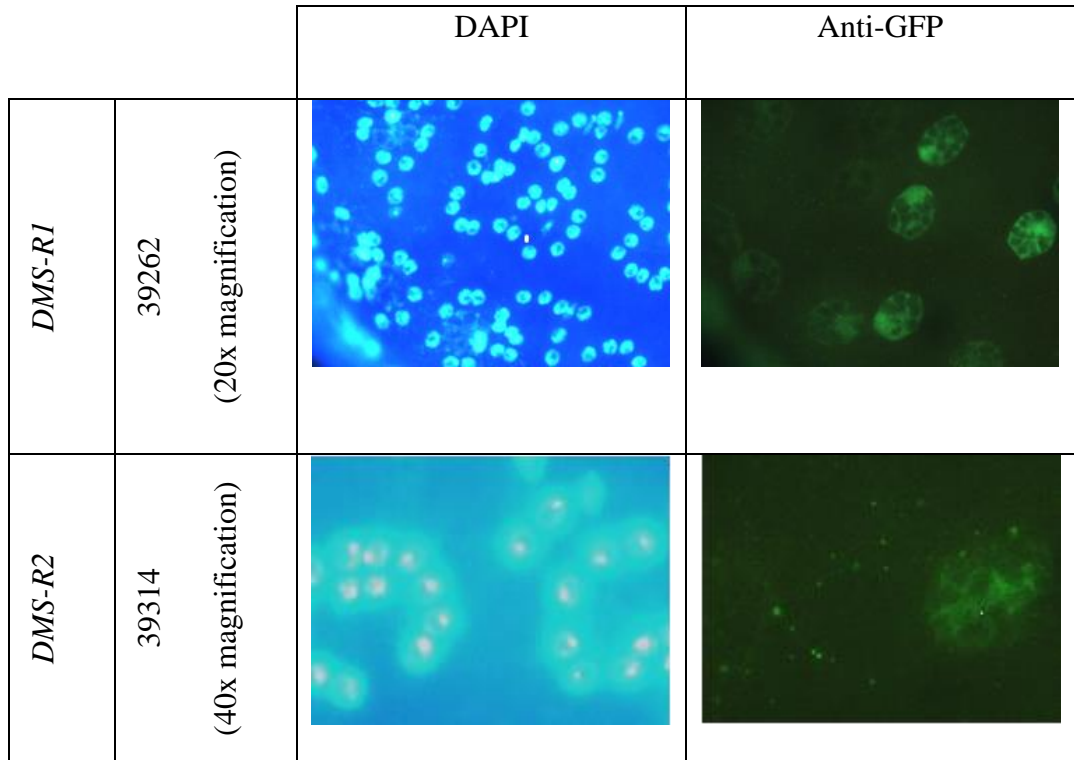


Figure 41 GFP in the secondary cells of *DMS-R1* and *DMS-R2* present in two short fragments of the respective receptors. The reason why these receptors present in this particular area are still unknown.

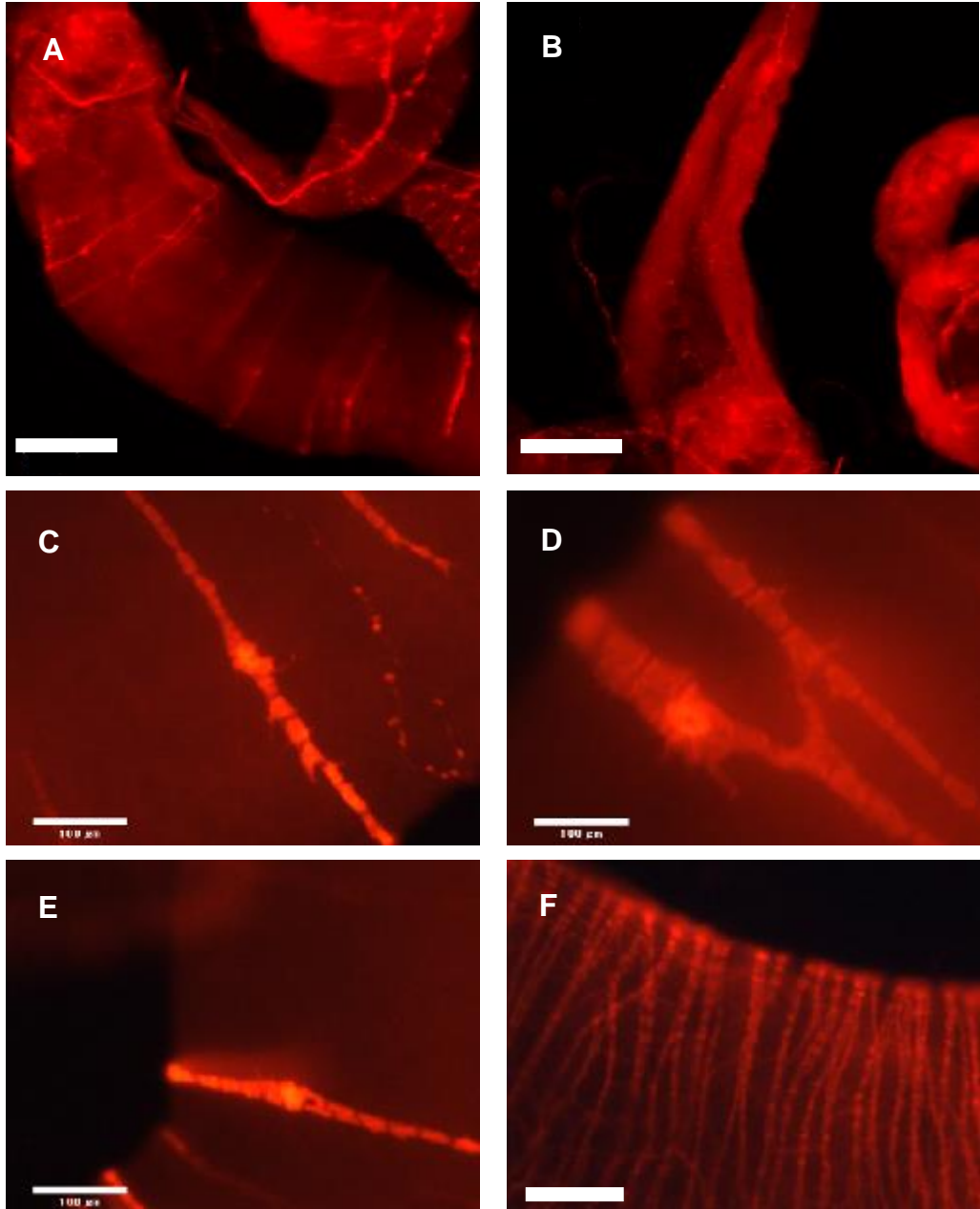


Figure 42 Characterisation of *DMS-R1 (48230)>GFP* on the surface of the male reproductive tissues. (A) Confocal image of the GFP expression in the MAG and SVs consist of neuronal and several myofibres junctions containing single-bright cell. (B) Confocal image of neuronal GFP expression on the ED tissue. (C) Neuronal and muscle GFP expression on the MAG. (D-E) A single-bright cell in between the junctions of the myofibres surrounds the MAGs. (F) Myofibres were visualised with phalloidin staining in *D. melanogaster* OR wild-type. The scale bars represent 100 μm . (C-F) Images were taken by using Zeiss Axioplan fluorescence microscope.

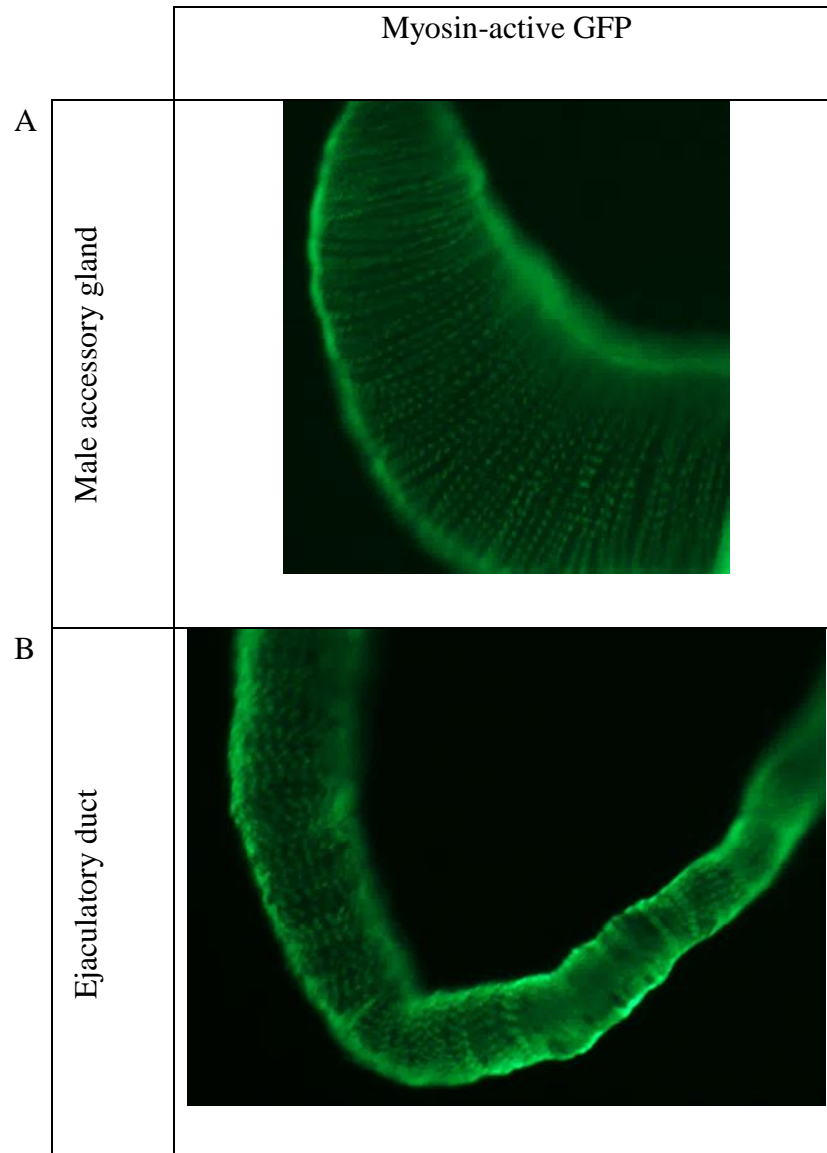


Figure 43 Characterisation of myofibres expression in the MAGs and ED of tagged GFP myosin flies. Myofibres surround the (A) MAGs (24x magnification) and (B) ED (16x magnification). Images were taken by using Leica fluorescence stereo microscope.

4.3 Discussion

We have used the GAL4-UAS bipartite binary system to support the contention made in Chapter 3 that the RFa immunoreactivity reflects the presence of DMS in the male reproductive tissue. In this system, the expression of the gene of interest, the responder, is controlled by the UAS element. However, this responder will remain in a silent state without the GAL4. The responder line is mated to the GAL4 driver line to activate transcription. The resulting progeny will express the responder in a pattern that reflects the respective GAL4 driver expression pattern. There are several responder lines available to express a GFP reporter according to GAL4 driver specific transcription. Besides GFP, there are other reporter gene lines to extend the study, for example *reaper* gene to trigger the cell death programme, and *ricin a* toxin to ablate the cell of interest (Moffat *et al.*, 1992; Zhou *et al.*, 1997; Duffy, 2002; Ito *et al.*, 2003).

We obtained a *DMS-GAL4* (61H01) line that uses a 1413bp intergenic promoter region that extends into the first exon of *DMS* to drive expression of the yeast transcriptional activator GAL4 in DMS cells. We then used this line to express GFP to reveal DMS neurons and pathways. Particular care was taken to choose the GFP reporter. Several available reporters give overexpression that can cause abnormal cellular morphology which sometimes causes lethality (Williams *et al.*, 2000). The membrane-bound proteins *mCD8::GFP* (Lee and Luo, 1999) and *10XUAS-IVS-myr-GFP-p10* (pJFRC29); and cytoplasmic-bound protein *10XUAS-IVS-Syn21-GFP-p10* (pJFRC81), are the safest choices for GFP expression (Ito *et al.*, 2003). The *DMS-GAL4* driven expression of *10XUAS-IVS-Syn21-GFP-p10* (pJFRC81) provided clear

images of the neuronal processes compared to the other two lines. In comparison, *10XUAS-IVS-myr-GFP-p10* (pJFRC29) and *UAS-mCD8::GFP* showed moderate and weak GFP expression respectively. The observations were performed by using high gain fluorescent exposure to reveal any faint expression that might be difficult to record. The use of the cytoplasmic GFP reporter to image the fine neuronal process is the best reporter choice (Pfeiffer *et al.*, 2012; Ito *et al.*, 2003). The reporter background expression can be present even without the GAL4 driver. Hence, this is another important factor to be considered. The UAS-linked reporter gene contains a minimum promoter in its construct. Thus, it can act as an enhancer-trap system expressing endogenous GFP expression (Ito *et al.*, 2003). In UAS-pJFRC81 adult male flies, we have screened for any endogenous GFP expression and the EB is the only tissue that shows this expression. The endogenous GFP expression in the UAS-pJFRC81 reporter is different to the auto-GFP expression of PEB-me peptide in the EB. The *DMS>GFP* flies were kept in a 26°C incubator. This is important as lower temperature storage will result in lower expression of GFP.

The double-labelling IHC staining was done to support the identity of the RFa in the previous chapter. The expression of the *DMS>GFP* and RFa indeed indicated that most if not all neurons at the ED expressed both markers. The co-localisation was not complete however, probably due to either weaker binding of anti-RFa antibody or some ectopic expression of GFP (Figure 28). However, all RFa immunoreactivity co-localised with the GFP consistent with the identity of DMS neurons. The presence of sNPF in the MAG, SV, and ED is unlikely since *sNPF >GFP* males do not express GFP in these tissues. It is concluded that the RFa immunoreactivity in the *Drosophila sp.* reproductive tissues reported in the previous chapter is indeed

due to cross-reactivity with DMS. Fresh samples were routinely dissected under the fluorescence stereo microscope to monitor the pattern of the *DMS>GFP* signal in comparison with the IHC method of staining. Tissues were also incubated without primary GFP antibody to eliminate any false staining resulting from non-specific binding of the secondary antibody.

It was clear from the double-labelling studies that the serotonergic innervation of the MAG, SV, and ED was distinct from that revealed in *DMS>GFP* flies (Figure 31). This separation of the two signalling pathways is to be expected if they have direct antagonist functions in controlling the physiology of these tissues. Furthermore, a previous study has been reported that 5-HT stimulates spontaneous muscle contractions in *D. melanogaster* ED (Norville *et al.*, 2010). Hence, we propose that the male DMS pathway is part of the mechanism together with 5-HT controlling muscle activity of the male reproductive tract and the transfer of sperm and seminal fluid into the female during copulation.

To address the question of the relationship between the ED cell and the paired rectal cells a careful dissection of *DMS>GFP* male adult flies was done under the fluorescence stereo microscope. During dissection, a nerve connection between HG (rectum) and ED could be seen (Figure 32C). A single ED cell is present connecting both tissues and is connected to one of the rectal cells (Figure 32B). The rectal cells are connected to each other and present at opposite sides of the rectum (Figure 32B). The ED single cell (see yellow arrow in Figure 32D) is also connected to the ED which led to or from the VD/SV (Figure 32D and Figure 33). The pathway was scrutinised to know the possible source. The pathway leads to the last AbG (see

white arrow in Figure 32D). Several neuronal fibres emanated from the AbG (Figure 32D and Figure 32F) which might supply DMS to the male reproductive tissues. The fibres from the AbG appeared to pass the reproductive tissues reaching the ED cell (see white arrow in Figure 32D), suggesting that they might coordinate control of the MAG/ED muscle contractions with rectum physiology. The auto-fluorescent expression in the EB is from the PEB-me peptide (Figure 32C).

One of the research gaps that was raised by McCormick and Nichols (2004) is whether DMS and other peptides containing RFa C-terminus are present in the same cell. It is of course important to know the identity of the peptides in the ED cell to fully understand the functions and mechanism involved in the functioning of this cell. From our collaboration with Dr. Susanne Neupert, University of Cologne, Germany, two peptides were present in the ED cell detected using HPLC and MALDI-TOF-MS. These peptides are DMS (TDVDHVFLRFa) and sNPF⁴⁻¹¹ (SPSLRLRFa), both of which contain RFa C-terminus (Figure 34). GFP was detected in the ED cell, but not the rectal cells, of male *sNPF>GFP* flies (Figure 35A). The absence of GFP in the rectal cells of *sNPF>GFP* 3rd instar larvae supports the conclusion that the rectal cells are devoid of sNPF (Figure 35C). Larvae were chosen for this confirmation since the rectal cells were detected with N-terminal DMS specific antibody in a previous publication (McCormick and Nichols, 2004) (Figure 36C). From our personal communication with Dr. Susanne Neupert, DMS is present in both rectal cells for both male and female *Drosophila*. Mass ions for proctolin (in female) and kinin (in male) were also found in the mass spectra for some of the replicates, but we suggest that these may be due to contamination from the external arborisation and attachment to the hindgut. Proctolin IHC using a

specific anti-proctolin antibody did not stain the rectal cells of *DMS>GFP* adult females. In these females there was no GFP- expressing cell associated with the rectal cells, confirming the male specificity of the ED cell (Figure 36A).

From the ED and MAGs muscle bioassay contractions, both DMS and sNPF⁴⁻¹¹ peptides inhibit muscle contractions of these tissues (Figure 37, Figure 39, and Figure 40). DMS was very potent with an EC₅₀ of 1.5×10^{-8} M (Figure 38). sNPF⁴⁻¹¹ inhibited the contractions, but at higher concentrations (Figure 39). In MAGs, DMS shows complete inhibition of the MAGs contractions compared to the sNPF⁴⁻¹¹ by using the same concentration of peptide. *sNPF receptor* has been shown to be expressed in the MAGs (Chintapalli *et al.*, 2007) which is consistent with the observation in the present study that the MAG responds to applied sNPF⁴⁻¹¹ peptide. The lack of sNPF⁴⁻¹¹ expression in the neuronal fibres on the surface of the MAGs of *sNPF>GFP* flies, suggests that the MAG muscle might respond to peptide released from neuroendocrine cells some distance away from the tissue (Chintapalli *et al.*, 2007). All tissues recovered from the inhibition after several washes with fly saline; this is important as it shows that the inhibition is reversible, consistent with a physiologically regulatory role. Several precautions need to be considered for example suitable room temperature, the total timing of the experiments to avoid peptide and fly saline evaporation, and avoiding excessive ice and carbon dioxide usage. The method has been approved by Prof. Dr. Christopher Elliot (Department of Biology, University of York, U.K.) and Prof. Dr. Angela Lange (Department of Biology, University of Toronto Mississauga, Canada) who are the core persons in this field (personal communication).

A total of 27 lines of *DMS-R1>GFP* and *DMS-R2>GFP* carrying short DNA elements from the promoter regions were screened to relate the inhibition of the muscle contraction with the receptors (Table 7). From the screening, the *DMS-R1 (48230)>GFP* shows muscle-like expression on the MAGs (Figure 42C-E). This expression is similar to the myofibres expression from the Phalloidin staining (Figure 42F).

In conclusion, the RFa expression in the reproductive tissues is indeed DMS, and it is not co-expressed in the same neurons as the 5-HT. Both neuropeptide and neurotransmitter give antagonistic signals to the male reproductive tissues. We propose that the ED cell plays a role in this inhibition and connects via the rectal cells to the HG. The finding that MAG myofibres express GFP in the *DMS-R1>GFP* flies suggests the involvement of this receptor, however, FlyAtlas suggests that MAG expression of DMS-R2 is stronger than DMS-R1 and therefore interpretation of the *GAL4>GFP* has to be treated with caution, especially since the *DMS-R-GAL4* lines rely on relatively small sections of the up-stream promoter region.

Chapter 5

RNAi Silencing of Dromyosupressin Expression Generates an Ecdysis Wing Phenotype

5.1 Introduction

The application of powerful genetic tools in combination with state-of-the-art peptidomics technology have established *D. melanogaster* as an excellent model for studying the role of neuropeptides in modulating animal behaviour and development. In particular the binary GAL4-UAS expression system described in Chapter 4 permits the expression of transgenes in a tissue and cell specific manner (Duffy, 2002). This approach is widely used to knock-down gene expression by RNAi (Figure 44), for expression of cell death genes for cell ablation as well as GFP for mapping expression patterns. Importantly, many of these tools in the form of fly lines are available from stock centres or other *Drosophila* laboratories. In this chapter, the GAL4-UAS system was used to obtain information about the physiological role of DMS in *D. melanogaster*.

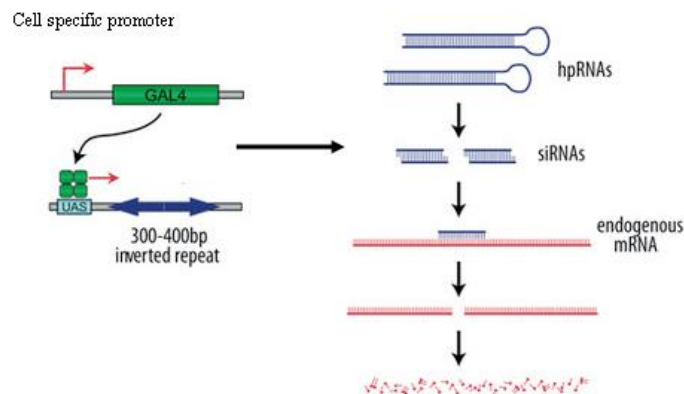


Figure 44 Diagram of transgenic RNAi in *Drosophila* adapted from the VDRC.

The expression of a hairpin RNA (hpRNAs) is driven by using the GAL4-UAS system. A Dicer processes the double-stranded RNAs into siRNA that sequence-specifically directs the degradation of the target mRNA.

Strong abnormal ecdysis phenotype and adult lethality was obtained when one of the *DMS-RNAi* lines was crossed with a pan-neuronal GAL4 driver. This result precluded functional genetic analysis of DMS in male reproduction, but suggested the importance of neuronal DMS signalling in regulating ecdysis behaviour. A screen of available GAL4 lines carrying constructs comprising *DMS-R* enhancer elements (Figure 45) provided evidence for expression of DMS-R2 in Inka cells and DMS-R1 in the second cell of the epitracheal gland. There is substantial evidence that the role of the endocrine Inka cells is the production of the ecdysis triggering hormones (ETH1 and ETH2) for initiating moulting behaviour and that these cells and their endocrine role are conserved across insect orders (Park *et al.*, 1999). These peptides are released from the Inka cells which are attached along the length of the main tracheal trunks (Figure 46) and are essential for shedding of the old cuticle at the end of each developmental stage (Zitnan and Adams, 2000).

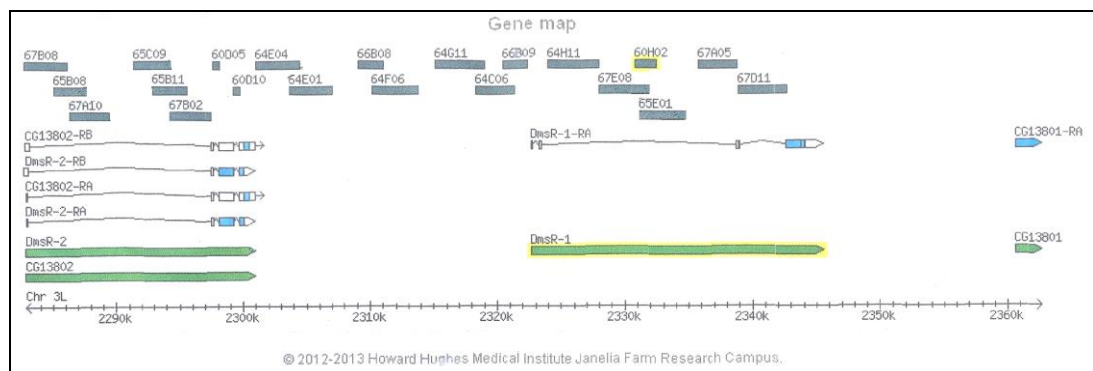


Figure 45 Janelia Research Campus GAL4 lines *DMS-R* gene map.

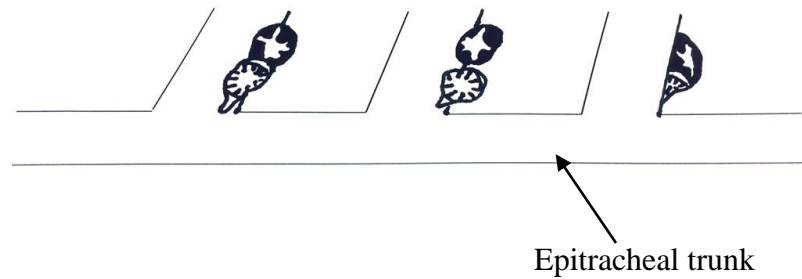


Figure 46 Epitracheal cells in *D. melanogaster* larvae. (Adapted from Žitňan et al., 2003).

Some aspects of the work reported in this chapter were undertaken in collaboration with Dr. Ivana Daubnerova during a visit to the laboratory of Dr. Dušan Žitňan (Institute of Zoology, Slovak Academy of Sciences, Bratislava, Slovakia). At the same time as this work was being carried out a paper was published describing phenotypes of VDRC RNAi flies for several peptide genes of the RFa family, including DMS and DMS receptors (Kiss *et al.*, 2013). The findings reported in this chapter will be compared with the results published by Kiss *et al.* in the discussion section.

5.1.1 Chapter aims

The aim of the work described in this chapter was to observe the effect of silencing DMS by using the RNAi flies. Further study proceeded based on these results.

5.2 Results

5.2.1 Development and phenotypic effects of RNAi silencing of *DMS* expression

Flies carrying the *UAS-RNAi* constructs for *DMS* were crossed with *nSyb-GAL4/UAS-dicer2* flies to generate pan-neuronal expression of *DMS* double stranded RNA. The offspring carrying the hair-pin RNAi (*DMS-RNAi* (108760)) and the *nSyb-GAL4/UAS-dicer2* transgenes showed abnormal wing phenotype (failure to expand wings post-eclosion, Figure 48) and failure to expand the abdomen to the normal shape and dimensions (Figure 47). In addition, adult life is curtailed to no more than five days. The abnormal wing phenotype and lethal effect is absent in the *DMS-RNAi* (12975).

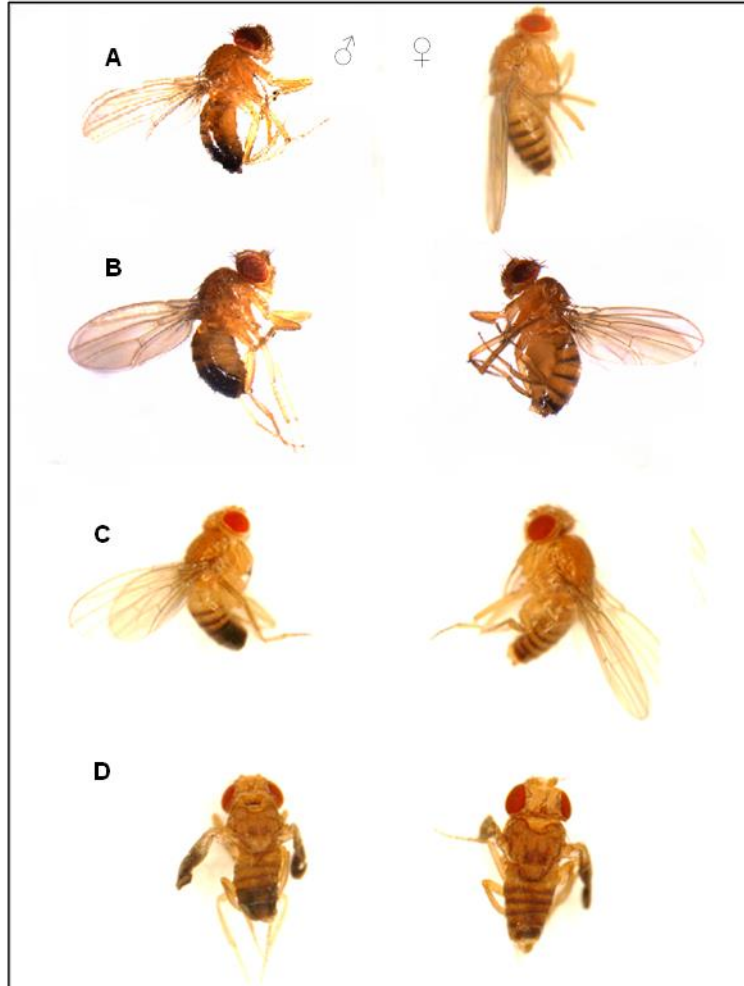


Figure 47 Phenotype of adult *D. melanogaster* Or-R wild-type, adult *nSyb-GAL4/UAS-dicr2*, adult *DMS-RNAi* (108760), and adult *nSyb-GAL4/UAS-dicr2>DMS-RNAi* (108760) flies. (A) Control male and female wild-type *D. melanogaster* Or-R flies showing normal wing expansion and abdomen formation. (B) Control male and female *D. melanogaster nSyb-GAL4/UAS-dicr2* flies showing normal wing expansion and abdomen formation. (C) Control male and female *D. melanogaster DMS-RNAi* (108760) flies showing normal wing expansion and abdomen formation. (D) A male and female *D. melanogaster nSyb-GAL4/UAS-dicr2>DMS-RNAi* (108760) flies showing abnormal wing expansion and malformed abdomen.

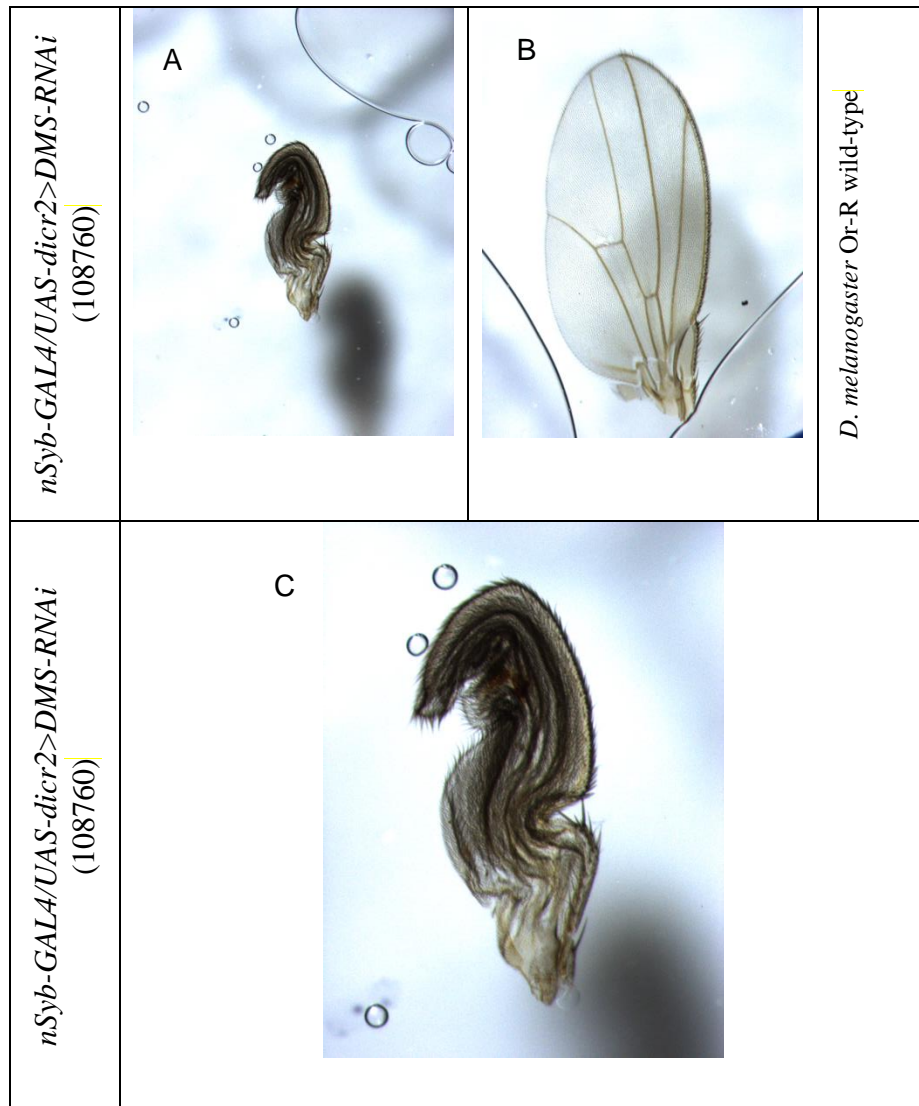


Figure 48 Morphology of the wings in flies lacking *DMS* function. Comparison of (A) *nSyb-GAL4/UAS-dicr2>DMS-RNAi* (108760) mutant flies shows failed inflated wings, and (B) wild-type flies expressed wild-type wings morphology. The size of wild-type wings is bigger compared to the *nSyb-GAL4/UAS-dicr2>DMS-RNAi* (108760) wings due to the abnormality (6.3x objective). (C) The *nSyb-GAL4/UAS-dicr2>DMS-RNAi* (108760) flies shows failed wing expansion (12x objective).

Immunohistochemistry was undertaken to confirm the effectiveness of the RNAi knock-down of DMS expression. Whole-mounts of reproductive tissue and digestive tract from *nSyb-GAL4/UAS-dicer2>DMS-RNAi* (108760) adult male flies were stained with RFa antiserum and scrutinized for RFa expression in the male reproductive tissue and associated ED and rectal cells which are known to contain DMS. No RFa innervations of the accessory gland and ED were observed in *nSyb-GAL4/UAS-dicer2>DMS-RNAi* (108760) male flies nor was there staining of the ejaculatory cell and the rectal cells (Figure 49A), confirming successful interference with DMS expression in the *nSyb-GAL4/UAS-dicer2>DMS-RNAi* (108760) flies. The non-neuronal background staining was observed when the image was captured at the same setting as the test sample. Some endocrine cells of the midgut however did stain with the RFa antibody, but these cells were most likely expressing other RFa peptides (e.g. FMRFa) (Figure 49B).

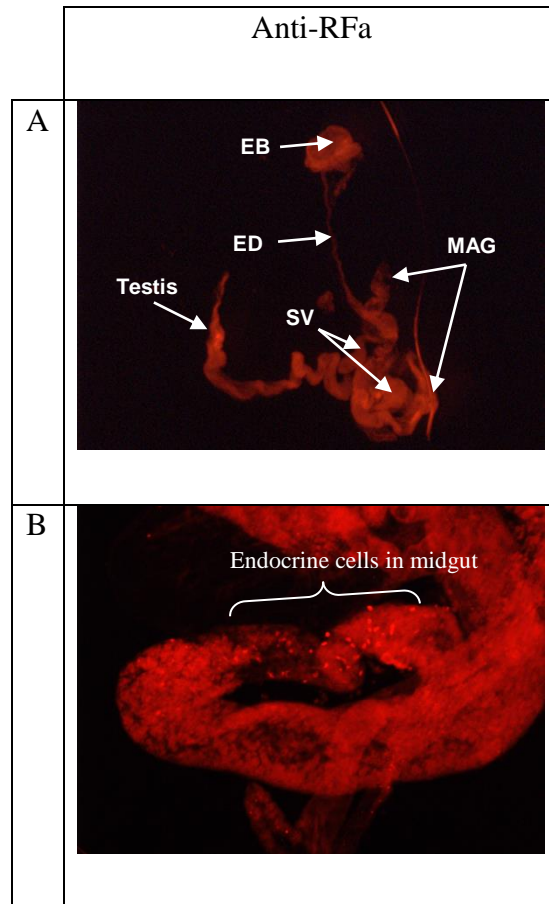


Figure 49 The *nSyb-GAL4/UAS-dicr2>DMS-RNAi* (108760) adult male shows no expression of RFa (DMS) in reproductive tissue. Whole-mounted reproductive tissue from adult male *nSyb-GAL4/UAS-dicr2>DMS-RNAi* (108760) shows (A) No RFa (DMS) expression when stained with anti-RFa antiserum (6.3x objective). (B) Immunoreactivity is present in endocrine cells stained with anti-RFa in the same fly midgut which serves as a positive control (12x objective).

5.2.2 Expression of DMS-R1 and DMS-R2 in the epitracheal gland cells

The abnormal ecdysis phenotype from silencing *DMS* lead us to consider possible interaction of neuronal-derived DMS peptide with epitracheal cells that are responsible for initiating eclosion behaviour by releasing ETH into the circulation. GAL4 lines carrying up-stream enhancer regions of *DMS-R1* and *DMS-R2* were crossed with pJFRC81 (henceforth *DMS-R1*>*GFP* or *DMS-R2*>*GFP*) and the progeny were screened for GFP expression in the epitracheal cells. One *DMS-R2-GAL4* and two *DMS-R1-GAL4* lines were identified from this screen (Table 8).

Table 8 A screen of Janelia Research Campus GAL4 lines for enhancers that drive expression in epitracheal cells.

| Stock number | Insertion | Associated gene | GFP expression in the epitracheal cells |
|--------------|-----------------------|-----------------|---|
| 39262 | P[GMR60H02-GAL4]attP2 | <i>DMS-R1</i> | NIL |
| 39297 | P[GMR64C06-GAL4]attP2 | <i>DMS-R1</i> | NIL |
| 48230 | P[GMR64E01-GAL4]attP2 | <i>DMS-R1</i> | Present in the second epitracheal cells |
| 47703 | P[GMR64E04-GAL4]attP2 | <i>DMS-R1</i> | NIL |
| 39310 | P[GMR64F06-GAL4]attP2 | <i>DMS-R1</i> | NIL |
| 39312 | P[GMR64F08-GAL4]attP2 | <i>DMS-R1</i> | NIL |
| 46546 | P[GMR64G11-GAL4]attP2 | <i>DMS-R1</i> | Present in the second epitracheal cells |
| 46548 | P[GMR64H11-GAL4]attP2 | <i>DMS-R1</i> | NIL |
| 39353 | P[GMR65D07-GAL4]attP2 | <i>DMS-R1</i> | NIL |

| | GAL4]attP2 | | |
|-------|---------------------------|---------------|-----|
| 39355 | P[GMR65E01- GAL4]attP2 | <i>DMS-R1</i> | NIL |
| 39378 | P[GMR65H03- GAL4]attP2 | <i>DMS-R1</i> | NIL |
| 48292 | P[GMR66B08- GAL4]attP2 | <i>DMS-R1</i> | NIL |
| 39391 | P[GMR66B09- GAL4]attP2 | <i>DMS-R1</i> | NIL |
| 46575 | P[GMR67A05- GAL4]attP2 | <i>DMS-R1</i> | NIL |
| 39437 | P[GMR67D11- GAL4]attP2 | <i>DMS-R1</i> | NIL |
| 49600 | P[GMR64C05- GAL4]attP2 | <i>DMS-R1</i> | NIL |
| 39247 | P[GMR60D05- GAL4]attP2 | <i>DMS-R2</i> | NIL |
| 41284 | P[GMR60D10- GAL4]attP2 | <i>DMS-R2</i> | NIL |
| 47699 | P[GMR64A08- GAL4]attP2 | <i>DMS-R2</i> | NIL |
| 39314 | P[GMR64F10- | <i>DMS-R2</i> | NIL |

| | GAL4]attP2 | | |
|-------|---------------------------|---------------|------------------------------|
| 39339 | P[GMR65B08- GAL4]attP2 | <i>DMS-R2</i> | NIL |
| 39341 | P[GMR65B11- GAL4]attP2 | <i>DMS-R2</i> | NIL |
| 46556 | P[GMR65C09- GAL4]attP2 | <i>DMS-R2</i> | NIL |
| 39399 | P[GMR67A10- GAL4]attP2 | <i>DMS-R2</i> | Present in the Inka cells |
| 39402 | P[GMR67B02- GAL4]attP2 | <i>DMS-R2</i> | NIL |
| 39404 | P[GMR67B08- GAL4]attP2 | <i>DMS-R2</i> | NIL |
| 39432 | P[GMR67D04- GAL4]attP2 | <i>DMS-R2</i> | NIL |

The *DMS-R2* (39399)-*GAL4* line gave GFP expression in what looked like ETH-containing Inka cells with their distinctive finger-like cytoplasmic extensions (Figure 50). Double-immunolabelling of GFP and ETH showed that the *DMS-R2*>*GFP* expression was indeed co-localised with ETH in the Inka cells (arrow head in Figure 50C). The identity of the Inka cells was confirmed using an *ETH-GAL4* line to drive expression of GFP (*ETH*>*GFP*) in the epitracheal glands of 3rd instar larvae at the junction of the main trachea trunk and the transverse connectives (Figure 51).

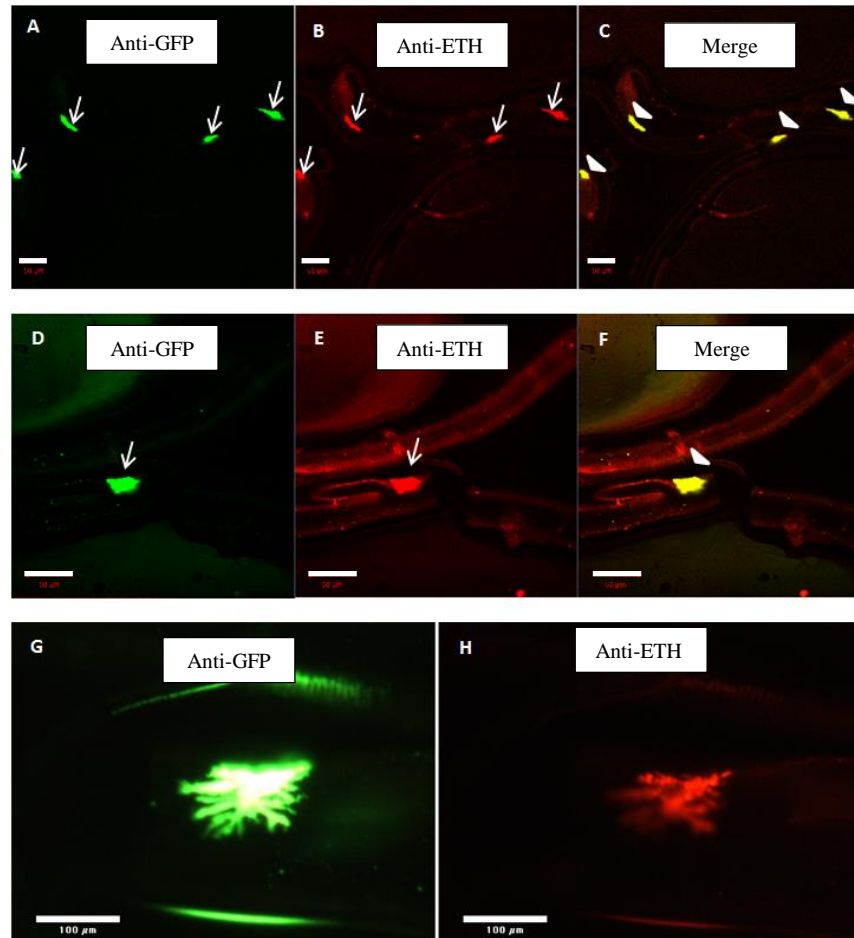


Figure 50 Double-labelling with anti-GFP (green) and anti-ETH (red) antibodies in *DMS-R2 (39399)>GFP* 3rd instar larvae. (A-F) Arrows point to the labelled *DMS-R2 (39399)* detected with anti-GFP and Inka cells detected with anti-ETH. Arrows head denotes the co-localisation of *DMS-R2* and Inka cells. The scale bars represent 50 μm . (G-H) *DMS-R2 (39399)* detected with anti-GFP and Inka cells detected with anti-ETH immunoreactivity in *DMS-R2 (39339)>GFP* 3rd instar larvae. The scale bars represent 100 μm .

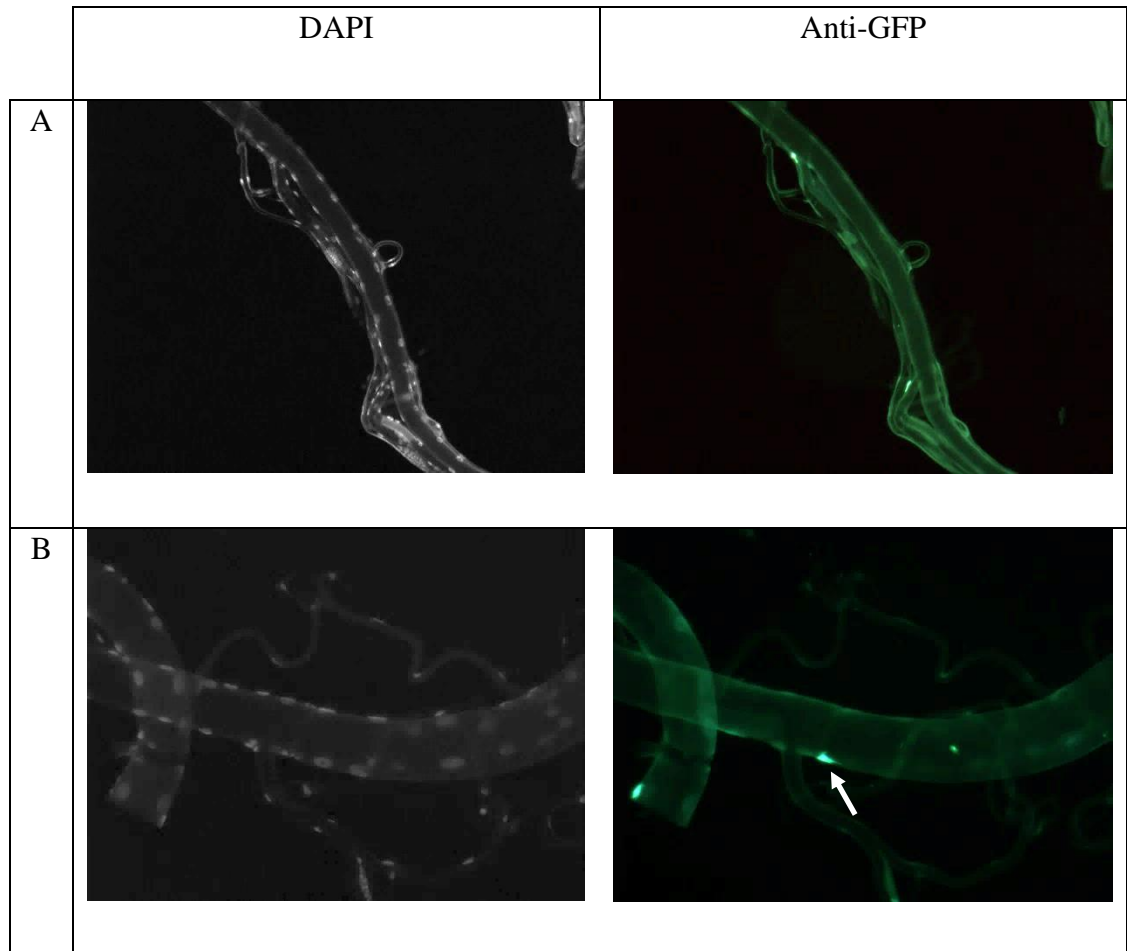


Figure 51 ETH-GFP reporter activity in epitracheal cells (stained green) on 3rd instar *ETH>GFP* larvae. (A) The GFP-cells attached to tracheal junctions (12.6x objective). (B) Note the finger-like (white arrow) cytoplasmic GFP-cell expression resembles the *DMS-R2 (39399)>GFP* and Inka cells detected with anti-ETH in Figure 50 (24x objective).

GFP was also expressed in the epitracheal gland of *DMS-R1 (48230)>GFP* 3rd instar larvae. The expression occurred in the second cell that lies adjacent to the finger-like Inka cell detected with anti-ETH (red) (Figure 52D). DMS-R1 expression in these epitracheal cells was confirmed and done by Dr. Ivana Daubnerová via *in-situ* hybridization (Figure 52E) using cDNA probes by (Figure 52F).

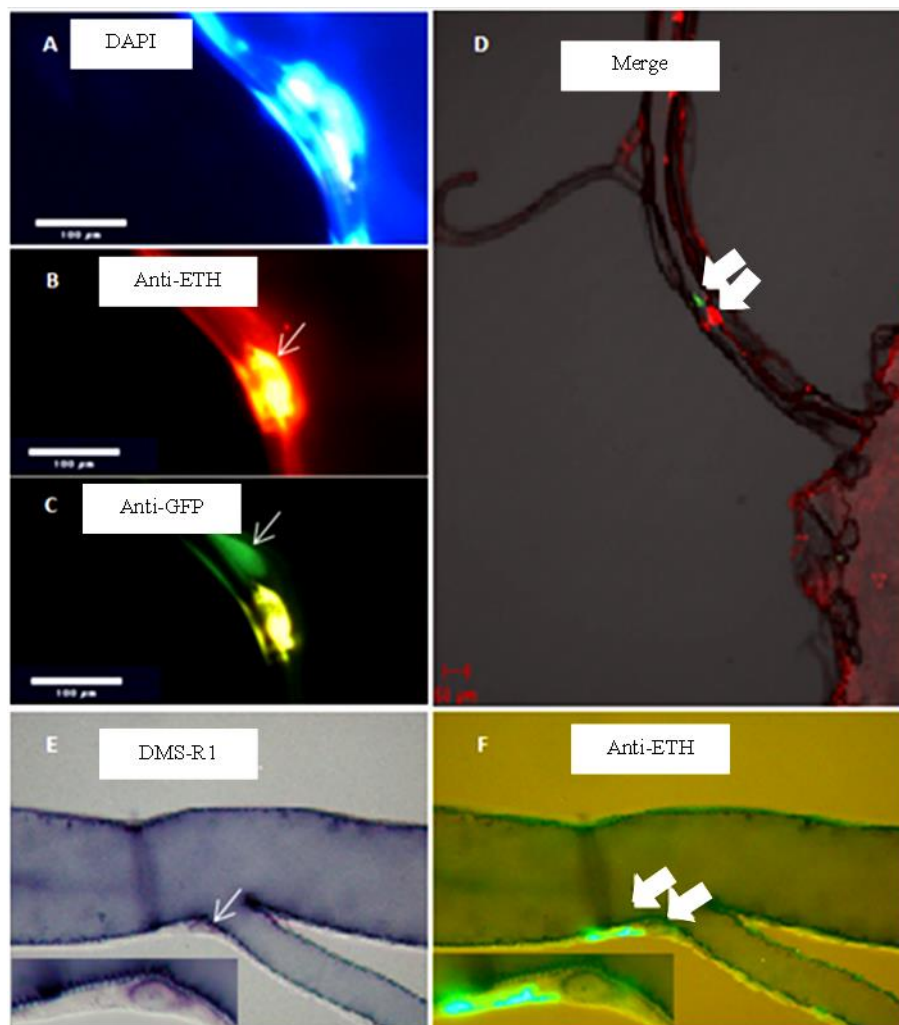
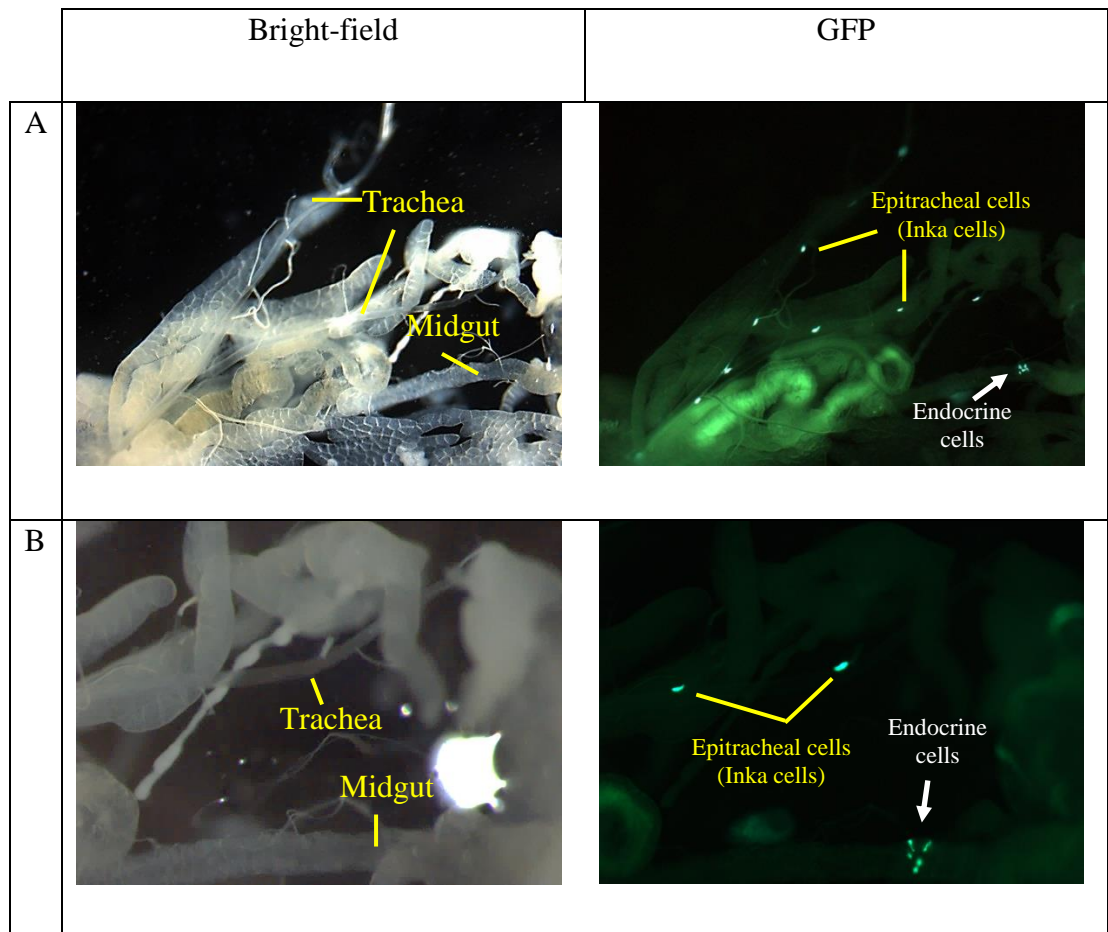


Figure 52 Double-labelling with anti-GFP and anti-ETH antibodies of the trachea from 3rd instar larvae of *D. melanogaster* *DMS-R1 (48230)>GFP*. The expressions were confirmed using the *in-situ* hybridization technique. (A-C) Double-labelling in the larval epitracheal cells of the *DMS-R1 (48230)>GFP*. Arrows point to the labelled *DMS-R1 (48230)* detected with anti-GFP (green) and Inka cells detected with anti-ETH (red). (D) Arrows denotes the non-co-localisation of *DMS-R1* (green) and Inka cells (red). (E-F) *DMS-R1* detected with *DMS-R1* cDNA probe and Inka cells detected with anti-ETH (green) immunoreactivity in wild-type *D. melanogaster* 3rd instar larvae. Arrows show *DMS-R1* (see Figure 52E and F (besides the green staining)) and ETH (see green staining in F) in the same sample.

5.2.3 Expression of DMS-R2 in midgut enteroendocrine cells

In *DMS-R2 (39399)>GFP* 3rd instar larvae, there are a group of five endocrine cells in the midgut that express GFP in addition to the expression in the Inka cells (Figure 53A-B). No GFP fluorescence occurred in any other part of the digestive tract. GFP expression was also present from the brain (Figure 53C).



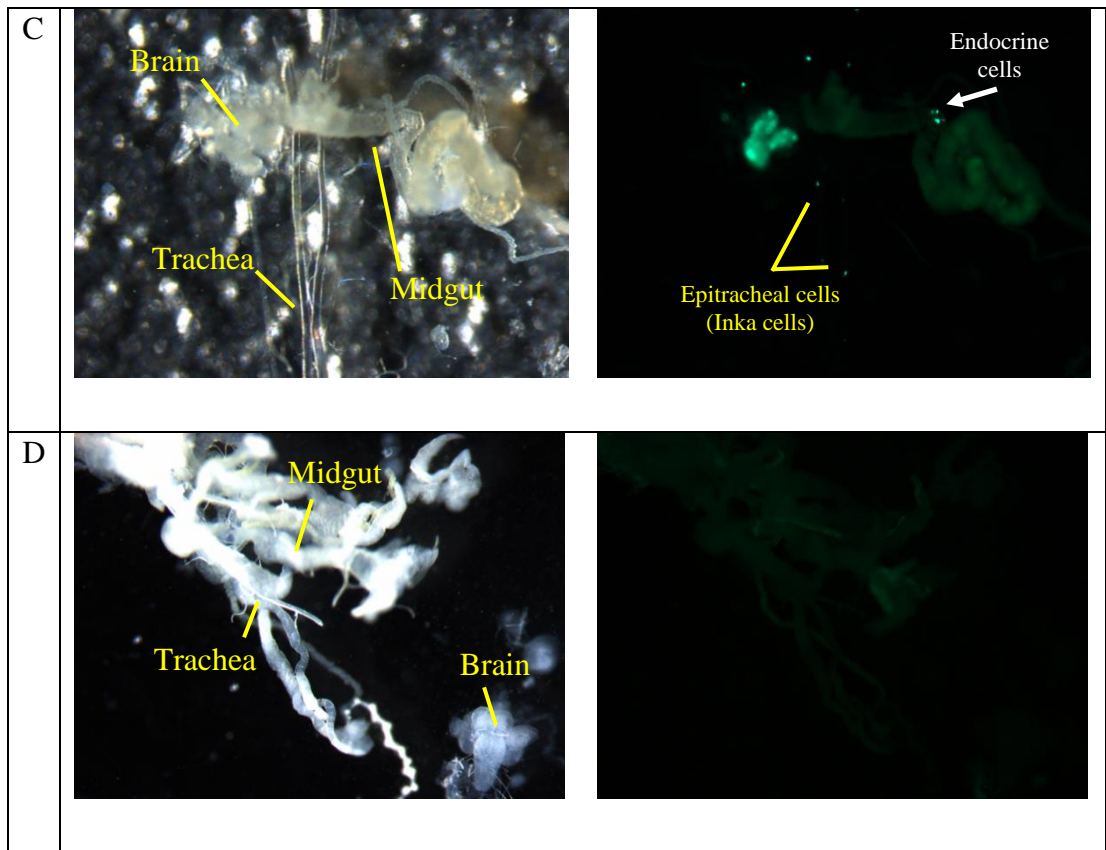


Figure 53 The *DMS-R2* (39399)-*GAL4* transgene generates GFP expression in epitracheal cells, brain, and midgut endocrine cells. All micrographs are from fresh unfixed tissues of the 3rd instar larvae. (A) GFP expressing Inka cells at the junction of the tracheal connectives and the main trunk along the length of the trachea. (A-B) There are a group of five endocrine cells in the midgut area (white arrows) (5x and 10x objective respectively). (C) The GFP expression is also present in the brain and there is (D) no fluorescence seen in wild-type 3rd instar larvae used as a negative control (4x objective).

The *DMS-R2 (46556)>GFP* 3rd instar larvae also had fluorescence in midgut endocrine cells but in this case there was no fluorescence in the epitracheal cells (Figure 54A-B). The absence of GFP in the epitracheal gland was confirmed by double-labelling with anti-GFP and anti-ETH antibodies (Figure 54C-D). Also, there are three GFP cells (white arrows) present at a long and slender tubule (yellow arrow) adjacent to the oesophagus (Figure 55).

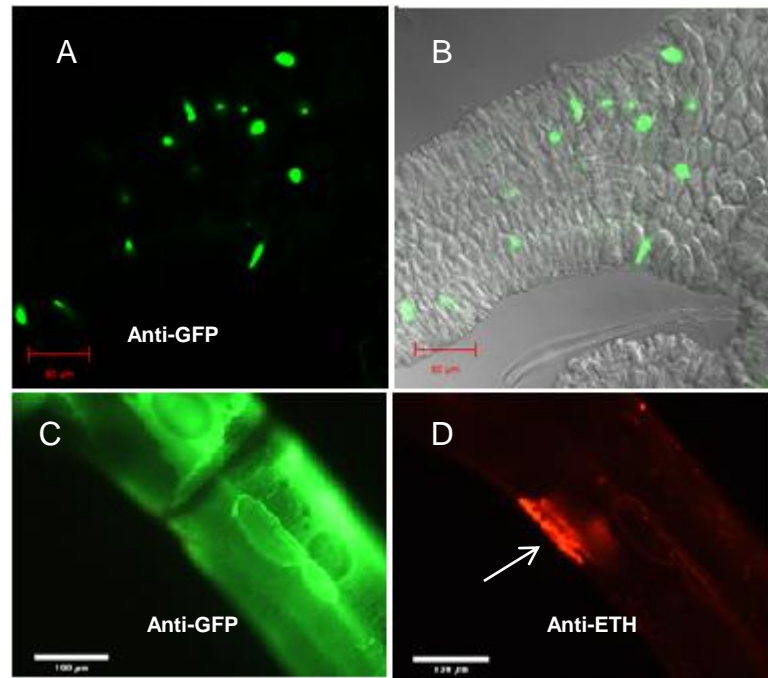


Figure 54 GFP and ETH expression in 3rd instar larvae of *DMS-R2* (46556)>GFP. GFP immunoreactivity in the larval midgut and double-labelling with anti-GFP and anti-ETH antibodies in epitracheal cells of 3rd instar larvae. (A-B) The immunoreactivity in endocrine cells of anterior midgut. (C-D) Double-labelling of GFP (stained in green) and ETH (stained in red) in the larval epitracheal cell of the *DMS-R2* (46556)>*GFP* larvae. The arrow points to the labelled Inka cell detected with anti-ETH; no GFP immunoreactivity was detected in epitracheal cells.

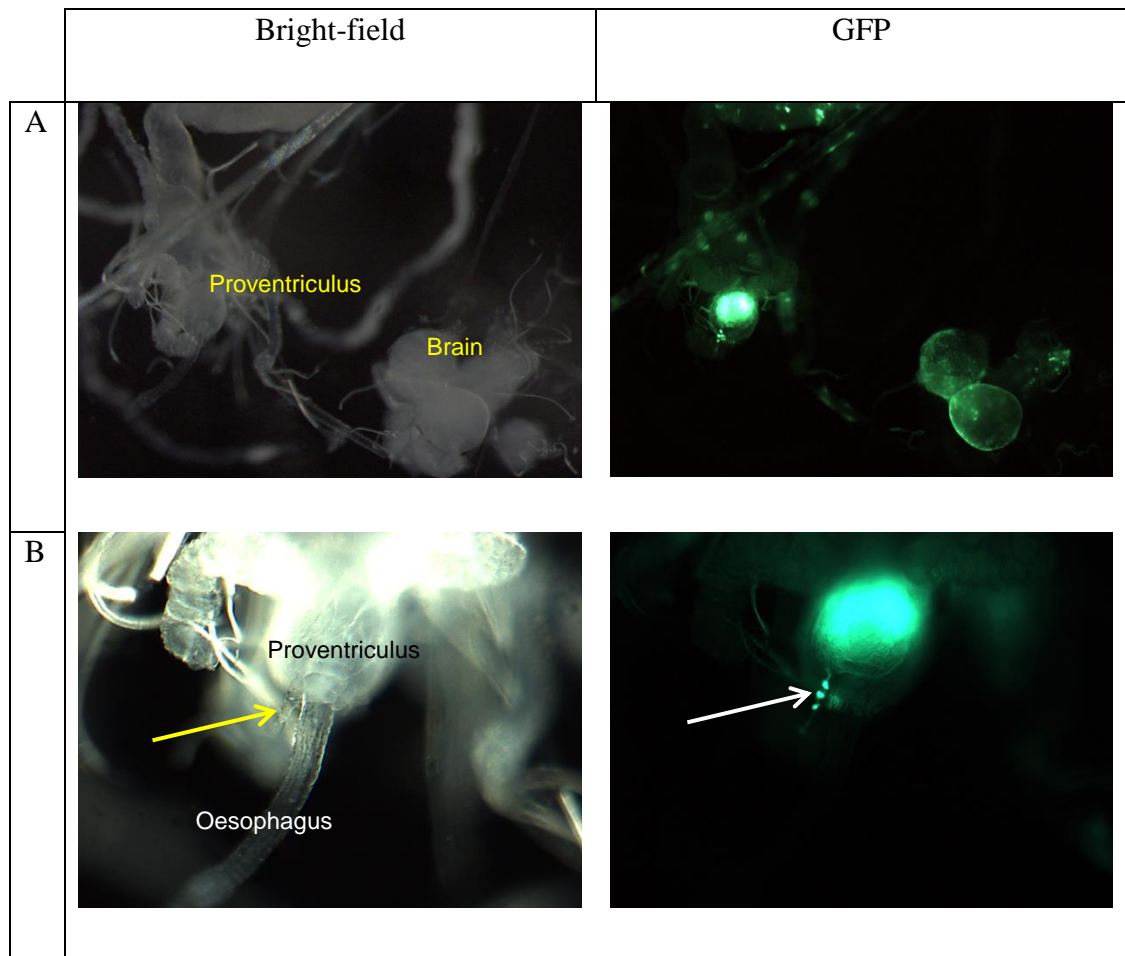
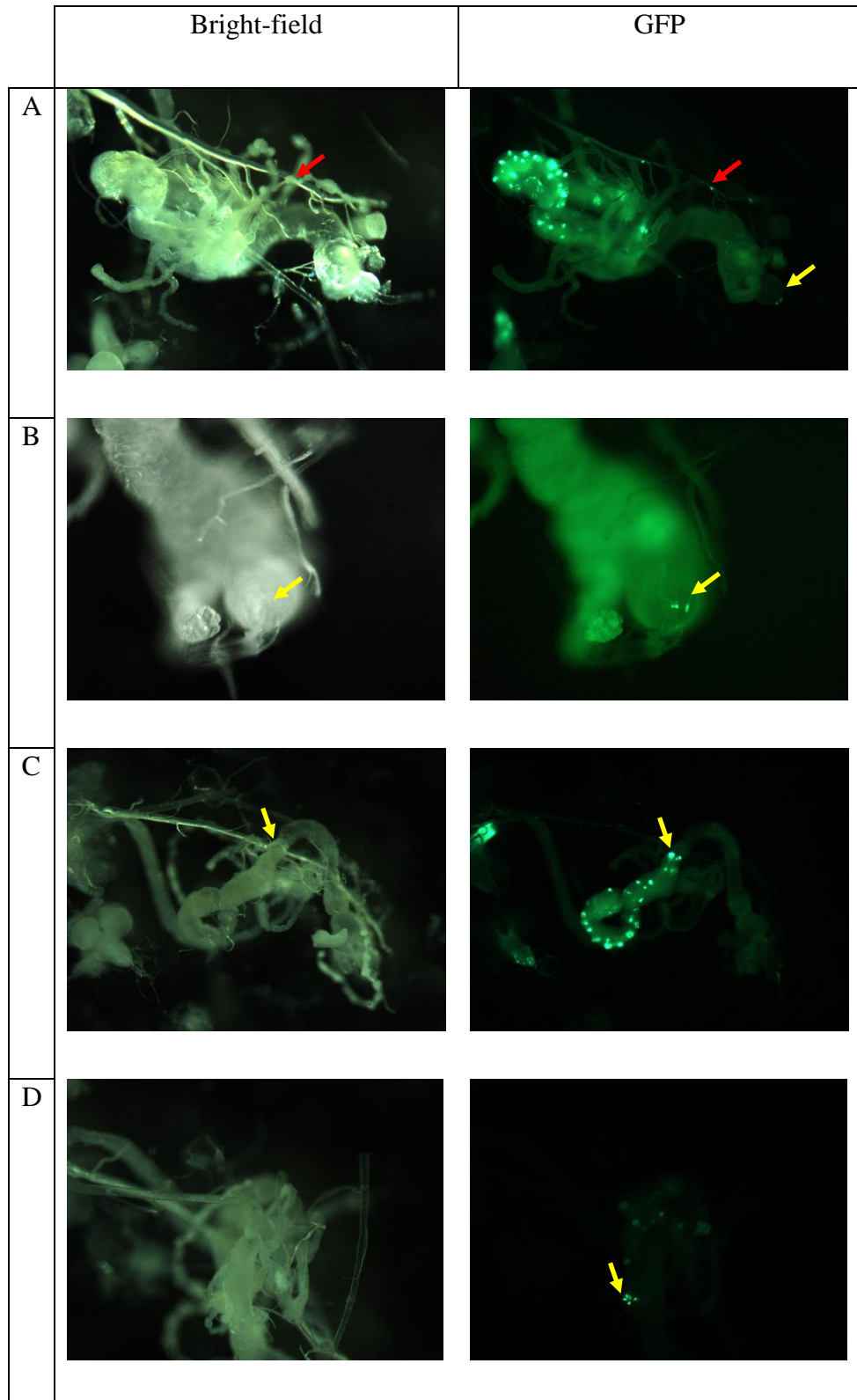


Figure 55 GFP fluorescence in the brain and proventriculus area of *DMS-R2* (46556) $>GFP$ 3rd instar larvae. (A) GFP is present in brain and near the proventriculus (8x objective). (B) By using higher magnification, a long and slender tubule can be seen (yellow arrow) adjacent to the proventriculus. There are three unidentified GFP stained bodies (white arrow) present on this tubule (20x objective).

Towards the end of this study a new *DMS-R2-GAL4* line became available from our collaborator, Dr. Kim Young-Joon at GIST, Republic of Korea. These flies carry a much larger ‘promoter element’ which is likely to provide a more complete expression pattern (Figure 56). This line shows more extensive GFP endocrine expression in the digestive tracts, neuronal expression at the hindgut, and in the CC. The CC expression (yellow arrows) was confirmed by *in-situ* using DMSR cDNA probe (Figure 57C).



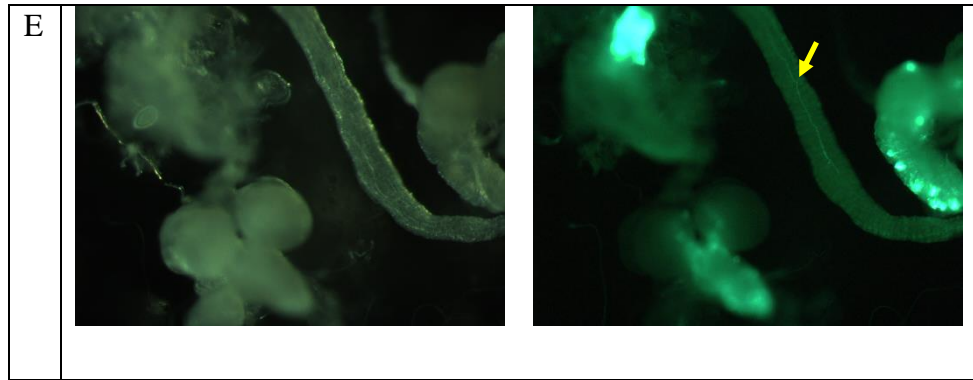


Figure 56 *DMS-R2* localisation in *DMS-R2>GFP* 3rd instar larvae. All micrographs are from fresh sample dissection, and consequently, only part of the tissue with GFP expression is in focus. (A) GFP cells are present at the junction of epitacheal cells throughout the trachea (red arrow) (6.4x objective). (A-B) There are a group of cells at the proventriculus area (yellow arrows) (6.4x and 16x objective respectively). (C) Several endocrine cells are present in the digestive tract (6.4x objective) and (D) five endocrine cells spotted in the midgut area (yellow arrows) (6.3x objective). (E) A neuronal expression is present in the larval hindgut (10x objective).

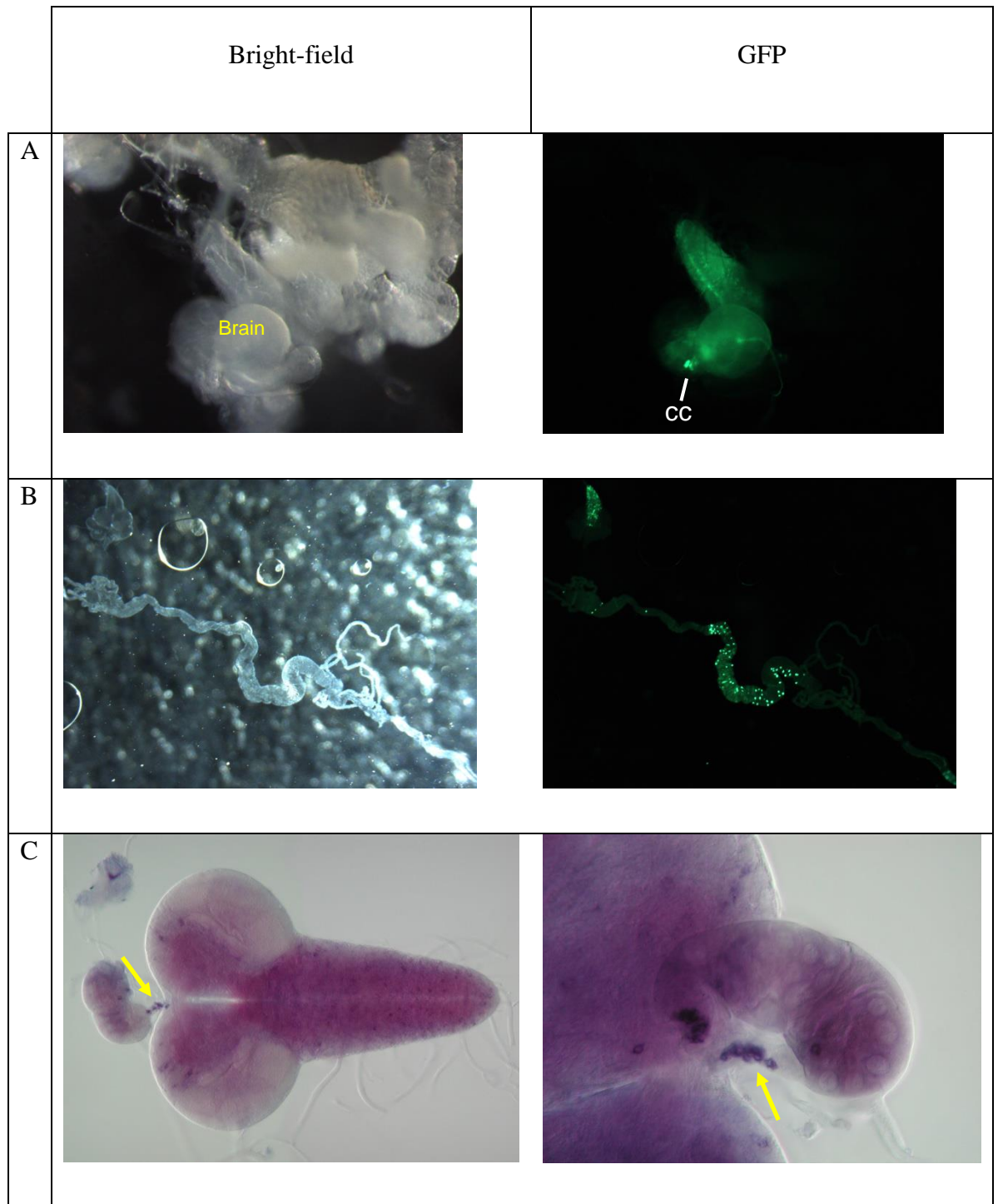


Figure 57 The GFP expression in the corpora cardiaca (CC) of *DMS-R2>GFP* 3rd instar larvae. (A) GFP expression in the CC (12x objective) and (B) complete GFP expression in the brain and digestive tract (2.5x objective). (C) *In-situ* hybridisation using a cDNA probe that cross-hybridises with both DMS-R1 and -2 confirms receptor expression in the CC (yellow arrow) of 3rd instar larva.

5.3 Discussion

This study used the RNAi genetic system in which *DMS* can be silenced when crossed with pan-neuronal *nSyb-GAL4/UAS-dicer2* flies (Dietzl *et al.*, 2007). As Figure 47 shows, the silencing of the *DMS* expression resulted in complete lethality of the adults at day-5 post-emergence. All adults show impaired wing expansion and malformed abdomen. The lethal effect was observed in the KK (*UAS-RNAi* (108760)) lines and not in the GD series (*DMS-RNAi* (12975)). Quantitative RT-PCR was used by Kiss *et al.* to show that the same *DMS-RNAi* (108760) line from VDRC was a strong silencer (Kiss *et al.*, 2013), resulting in lethality. The GD series of *DMS-RNAi* (12975) shows no mortality probably due to a lower level of RNAi effect (Kiss *et al.*, 2013). These results were reported by Kiss *et al.* during the course of this study. All crosses were maintained at a high temperature up to 29°C to increase the effect of the silencing through the GAL4-UAS system. Alongside the lethality, the abnormal wing expansion and malformed abdomen suggested that silencing *DMS* affected the ecdysis processes. Due to 100% mortality at day-5, bioassay contractions on the reproductive tissue and fertility assay could not be done. Several attempts of parental crosses have been done to study the effect of silencing the *DMS* on insect's development (Appendix A).

In insects, the process of shedding the exoskeleton of the previous developmental stage is called ecdysis. There are three major phases of ecdysis: pre-ecdysis, ecdysis proper, and post-ecdysis. Pre-ecdysis consists of swallowing of air or water to raise internal pressure and loosen the old exoskeleton. It is followed by the shedding of the exoskeleton (White and Ewer, 2014). During this phase, ingestion of air and

peristalsis movement is needed to rupture the anterior wall of the exoskeleton leading it to split along the dorsal seam, allowing partial of the animal free from the previous exoskeleton. The subsequent peristalsis movement towards the anterior part of the exoskeleton helps the animal to push out from the old cuticle. Finally, during post-ecdysis stage, the exoskeleton is expanded, hardened, and pigmented. In flies, the abdominal contractions serve to swell the body size accompanied by wing expansion, which involves haemolymph filling the wing veins and unfolding the wings (Kim *et al.*, 2006; Žitňan *et al.*, 2007; White and Ewer, 2014).

The ecdysis behaviours are coordinated by peptidergic cells in both peripheral nervous system and the CNS. The gene encoding *Drosophila* eclosion hormone (EH) shows high sequence similarity to the *Manduca* EH (Horodyski *et al.*, 1993; Park *et al.*, 1999). In the tobacco hornworm, *Manduca sexta*, at least four peptides are involved in activation process of ecdysis process: eclosion hormone (EH), ecdysis-triggering hormone (ETH), pre-ecdysis triggering hormone (PETH), and crustacean cardioactive peptide (CCAP/CAP2b) (Žitňan *et al.*, 1996; Ewer *et al.*, 1997; Gammie and Truman, 1997; Park *et al.*, 1999). The ETH signalling is indeed present in *Drosophila* as shown in a partial impairment of eclosion behaviour in *Drosophila* EH-cell *knockout* (KO) mutant and injection of *Manduca* ETH into *Drosophila* pharate adults which induces premature eclosion behaviour (Horodyski *et al.*, 1993; McNabb *et al.*, 1997; Park *et al.*, 1999). The eclosion phase consists of four sequential events happening within a 3 minute time interval: (1) strong head inflation appears the same as in the pre-eclosion, (2) forward head force, (3) bilateral contracting of the thorax, and (4) strong peristaltic contractions of the abdomen pushing the body forward (Park *et al.*, 1999). As for the CCAP, the presence of this

peptide in *Drosophila* was confirmed by IHC (McNeil *et al.*, 1998; Park *et al.*, 1999). The presence of these peptides in *Drosophila* suggested that the endocrine events leading to ecdysis may be conserved in insect taxa. The effects on ecdysis observed in this study suggest a strong connection between DMS neuropeptide and the classical ecdysis neurohormones.

Successful ecdysis phases require expression of specific genes and release of several regulatory molecules. The expression of the specific gene is controlled by ecdysteroids from prothoracic glands and gonads, while the activation of the ecdysis processes is regulated by ETHs secreted by Inka cells and neuropeptides in the CNS. The increase of haemolymph ecdysteroid level before each ecdysis induces gene expression that is essential for the production of receptors and peptide hormones in the Inka cells and CNS. The humoral signalling between Inka cells and CNS leads to a central release of several neuropeptides and activation of neuronal circuits of ecdysis processes (Žitňan *et al.*, 1999; Kim *et al.*, 2006; Žitňan *et al.*, 2007).

Inka cells are peritracheal endocrine cells that produce the ETH which is an important stimulator of ecdysis motor outputs. From the *DMS-R1>GFP* and *DMS-R2>GFP* screening, GFP expression in the epitracheal cells suggests that the DMS receptors are indeed contributing to the ecdysis process (Table 8). Based from the double-staining of anti-GFP and anti-ETH antibodies, the GFP expression of *DMS-R2* is present in the Inka cells (Figure 52) and *DMS-R1* is present in the second cell that is found beside the Inka cell (Figure 51). These results suggest that DMS and its receptors are involved in the ecdysis process. Closer examination shows that the Inka cells contain cytoplasmic elements that are possibly involved in communicating

between these two cells. Žitňan *et al.* (2003) speculates that these cytoplasmic processes may act as release sites similar to the endocrine cells. The large relative surface area of these processes will produce high concentrations of the product to be transported into the haemolymph, inducing completion of ecdysis (Žitňan *et al.*, 2003). Hence, identification of receptors in these epitracheal cells may contribute to understanding the correlation between neuropeptides released from the central nervous system and Inka cells. Further discussion regarding Inka cells and the second epitracheal cells will be elaborated in the general discussion chapter.

Even though the main source of the neuropeptides are in the CNS neurons, many are also present in other tissues, for example, tachykinin, myoinhibitory peptides, DH31, and sNPF in the enteroendocrine cells of larval midgut. From the screening of the digestive tract and tracheal system of *DMS-R2>GFP* 3rd instar larvae, GFP expression is present in the enteroendocrine cells, CC, and neuronal processes of the HG tissue. In addition, there are a group of cells present at the anterior junction of the midgut, this expression is similar to that reported for DH31 endocrine expression that are responsible for peristalsis function in *Drosophila* larvae midgut (LaJeunesse *et al.*, 2010). This suggests that the CNS might be involved in regulating the release of enteroendocrine peptides from the midgut cells via DMS signalling. In summary, evidence is presented suggesting that DMS and its receptors are important for ecdysis in *D. melanogaster*.

Chapter 6

**The toxicity of angiotensin converting enzyme (ACE) inhibitors to
larvae of the dengue fever mosquito, *Aedes aegypti* and malaria
fever mosquito, *Anopheles gambiae***

6.1 Introduction

6.1.1 Mosquito vectors of disease

The mosquitoes, *Anopheles gambiae* and *Aedes aegypti*, are some of the most deadly animals because of their effectiveness as vectors of malaria and a range of arboviruses, including yellow fever, dengue, chikungunya, and zika. The close association of *Ae. aegypti* with urbanisation in tropical and sub-tropical countries and the ease of trans-global human travel and the mass migrations from war zones presents particular challenges in disrupting the cycle of arbovirus infections transmitted by *Ae. aegypti* in human populations (Johansson *et al.*, 2009; Haddow *et al.*, 2012). The lack of effective vaccines and treatments for dengue, chikungunya, and zika has focused attention on integrated vector control management based on environmental/cultural management, chemical, and biological control (Haddow *et al.*, 2012). The use insecticides from different chemical classes are key components of the integrated strategy against both *An. gambiae* and *Ae. aegypti*, but the ever-increasing problem of insecticide resistance means that new compounds with different modes of action are urgently needed to replace chemicals that fail to control resistant mosquito populations (Enayati and Hemingway, 2010; Hemingway, 2014; Thomsen *et al.*, 2014).

6.1.2 Angiotensin converting enzyme (peptidyl dipeptidase A, ACE)

The peptide-degrading zinc-metalloproteinase, known as angiotensin converting enzyme (ACE) from the role of the mammalian enzyme in the renin-angiotensin systems (Soffer, 1976; Erdös and Skidgel, 1987; Corvol *et al.*, 1995), has been considered as a potential target for new insecticides that interfere with peptide hormone control of insect growth and development (Isaac *et al.*, 2007b; Isaac and Shirras, 2013). The dual role of the enzyme in the processing of the mammalian vasoconstrictor angiotensin II and the inactivation of the vasodilatory bradykinin led to the development of inhibitors of human ACE as anti-hypertensive drugs (Ondetti *et al.*, 1977; Ondetti, 1991; Acharya *et al.*, 2003). The first inhibitors were in fact natural proline-rich peptides (BPPs) with bradykinin-potentiating activity isolated from the venom of the snake *Bothrops jararaca*, but these lacked oral activity (Ferreira *et al.*, 1970; Cushman and Ondetti, 1991; Camargo *et al.*, 2012).

The insect angiotensin converting enzyme (iACE), like the mammalian enzyme, is a promiscuous peptidase that cleaves dipeptides from the carboxyl end of oligopeptides and in some instances can cleave amidated di- or tri-peptides from substrates with an amidated carboxyl terminus (Lamango *et al.*, 1996; Lamango *et al.*, 1997; Siviter *et al.*, 2002; Vandingenen *et al.*, 2002; Macours *et al.*, 2003; Hens *et al.*, 2002; Isaac and Shirras, 2013). iACEs are generally soluble enzymes secreted from cells into the extracellular milieu, where they can degrade peptides by sequential removal of dipeptides, unless a proline is encountered in the C-terminal penultimate position (Isaac and Shirras, 2013). Much of our knowledge of the biochemistry and structural biology of iACE comes from studying the *D.*

melanogaster enzyme known as AnCE (Isaac and Shirras, 2013; Harrison and Acharya, 2014). This peptidyl dipeptidase is strongly expressed as a glycosylated protein of 72 kDa in several tissues, including male reproductive tissues, the larval and adult midgut, larval trachea and adult salivary gland (Chintapalli *et al.*, 2007; Rylett *et al.*, 2007). Other insect species express ACE in male and female reproductive tissues suggesting a broader physiological role for the enzyme in insect reproduction (Wijffels *et al.*, 1996; Vandingenen *et al.*, 2002; Ekbote *et al.*, 1999; Ekbote *et al.*, 2003a; Ekbote *et al.*, 2003b; Vandingenen *et al.*, 2001; Vercruyssen *et al.*, 2004; Isaac *et al.*, 2007a; Xu *et al.*, 2013; Macours *et al.*, 2003). iACE not only resembles the mammalian enzyme in its substrate specificity, but also in susceptibility to inhibitors such as captopril, lisinopril, fosinoprilat, enalapril, andtrandolaprilat, but apart from captopril these inhibitors can be far less potent towards iACE compared with mammalian ACE forms (Cornell *et al.*, 1995; Williams *et al.*, 1996). Nevertheless, the availability of selective ACE inhibitors has been useful in confirming physiological roles for iACE in male and female reproduction in several species (Ekbote *et al.*, 2003a; Vercruyssen *et al.*, 2004; Isaac *et al.*, 2007a). In the mosquito *Anopheles stephensi* females fed with ACE inhibitors in the blood or females mated with males supplied with ACE inhibitors in their sugar diet, lay significantly fewer eggs than normal (Isaac *et al.*, 1999; Ekbote *et al.*, 2003a; Isaac *et al.*, 2007a). A similar effect on egg production was observed when ACE inhibitors were fed to male *An. gambiae*.

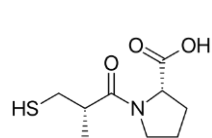
ACE inhibitors can also interfere with insect larval development as was shown by the stunting of larval growth by injection of captopril, lisinopril, and fosinoprilat into 4th instar insects. Injection of the prodrug fosinopril into the same larval stages

resulted in no weight gain and death within a few days. The injection of ACE inhibitors (captopril, lisinopril, and enalapril) combined with the diuretic peptides (helicokinin I, II, and III) into 5th instar larvae of the tobacco budworm (*Heliothis virescens*) resulted in strong lethality, however, the inhibitors on their own had no effect.

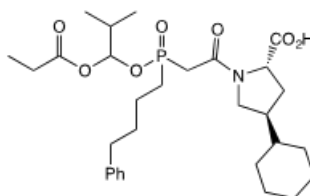
There is much interest in exploiting bioactive natural ACE inhibitors that are present in food sources for the prevention and treatment of hypertension (Huang *et al.*, 2013; Crozier *et al.*, 2009; Yang and Hong, 2013; Ellam and Williamson, 2013; Quiñones *et al.*, 2013). Many of these natural compounds are peptides generated by digestion of food rich in proteins (e.g. milk and meat). There are also a number of reports citing the beneficial effects of plant polyphenols in the management of hypertension and on cardiovascular disease in general. One of the proposed mechanisms of action for polyphenols is the direct inhibition of ACE (Lacaille-Dubois *et al.*, 2001; Kiss *et al.*, 2004; Oh *et al.*, 2004; Persson *et al.*, 2006; Actis-Goretta *et al.*, 2006; Loizzo *et al.*, 2007; Kwon *et al.*, 2009; Persson *et al.*, 2010; Persson, 2012; Hidalgo *et al.*, 2012). In one study 17 polyphenols were tested as ACE inhibitors and of these rutin (IC₅₀, 64 µM), quercetin (IC₅₀, 43 µM), and luteolin (IC₅₀, 23 µM) were shown to be the more potent compounds (Guerrero *et al.*, 2012). There is increasing interest in the application of natural botanicals to control insect pests to minimise off-target toxicity and environmental persistence and therefore it was decided to test one of the polyphenols (luteolin) as an inhibitor of mosquito larval ACE.

6.1.3 Chapter aims

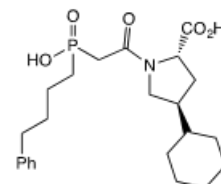
The aim of the work presented in this chapter was to see whether commercially available mammalian ACE inhibitors (Figure 58) are also potent inhibitors of ACE from *Ae. aegypti* and *An. gambiae* and whether they are orally toxic to larvae. The snake venom peptide BPP12b, and the proline-rich trypsin-modulating oostatic factor (TMOF), which is already known to be toxic to *Ae. aegypti* larvae (Borovsky, 2003), were also tested as inhibitors of larval ACE activity. The toxicity testing was designed by Zatul-Iffah Abu Hasan, but because of the loss of mosquito rearing facilities at Leeds University, the toxicity tests were performed in the facilities of the Liverpool School of Tropical Medicine (*An. gambiae*) by Dr. Helen Williams and at the Universiti Kebangsaan Malaysia (*Ae. aegypti*) by Nur Mashitoh Ismail and Dr. Hidayatulfathi Othman.



captopril



fosinopril



fosinoprilat

BPP12b
TMOF

pGlu-Trp-Gly-Arg-Pro-Pro-Gly-Pro-Pro-Ile-Pro-Pro
Tyr-Asp-Pro-Ala-Pro-Pro-Pro-Pro-Pro

Figure 58 Chemical structures of inhibitors of mosquito larval peptidyl dipeptidase activity.

6.2 Results

6.2.1 Inhibition of the soluble peptidyl dipeptidase (iACE) activity from whole larvae of *Ae. aegypti* and *An. gambiae*

Members of the iACE family of peptidyl dipeptidases are generally soluble secreted proteins, whereas mammalian ACEs are mainly membrane tethered. In order to ascertain whether the ACE activity present in homogenates of whole larvae was soluble, a crude homogenate prepared from 3rd instar *Ae. aegypti* and *An. gambiae* was centrifuged at 55,000 g for 1h to sediment all membrane components. By measuring the peptidase activity before and after centrifugation, it was clear that the majority of the enzyme remained in the high-speed supernatant. Most of this soluble peptidyl dipeptidase activity was inhibited by captopril (Figure 59). The soluble larval enzyme from both mosquito species was then used to determine the relative potency of synthetic and natural peptide ACE inhibitors. Apart from the pro-drug fosinopril, all the inhibitors showed a greater degree of potency towards the *Ae. aegypti* activity, with captopril being the most potent (Figure 60 and Figure 61). For enzyme prepared from both species fosinopril was weaker than the non-esterified fosinoprilat in inhibiting the activity of both species (Table 9). The snake venom peptide BPP12b and the mosquito peptide TMOF both inhibited iACE activity, but were much less potent than the synthetic compounds. Of the two peptides BPP12b had IC₅₀ values around two orders of magnitude lower than those of TMOF. Interestingly, both natural peptides were stronger inhibitors of the *Ae. aegypti* iACE compared to *An. gambiae* (Table 9).

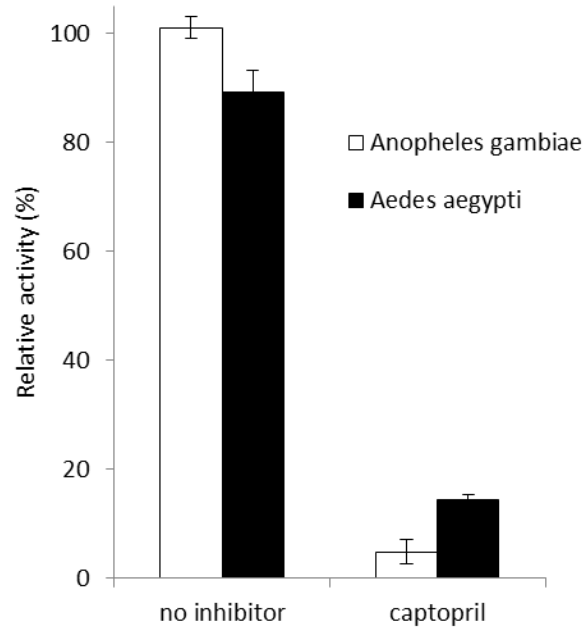


Figure 59 The relative activity of peptidyl dipeptidase in a homogenate of mosquito larvae before and after high-speed centrifugation. Aliquots were removed for activity assay from the homogenate before and after centrifugation at 55,000 *g* for 1 hour. The activity in the high-speed supernatant is expressed relative (%) to the activity of the homogenate prior to centrifugation.

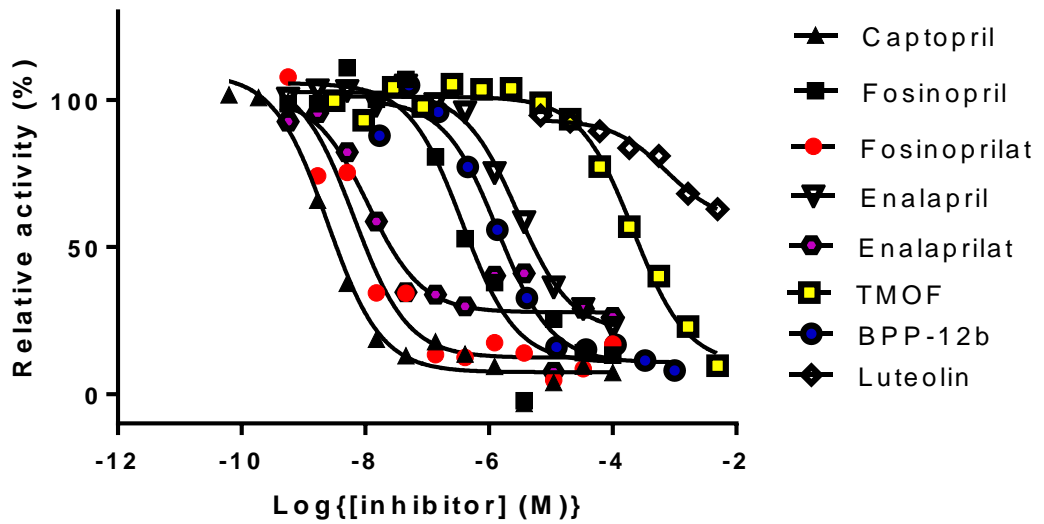


Figure 60 Inhibition of the peptidyl dipeptidase activity of *Ae. aegypti* larvae.

Inhibition curves for captopril, fosinopril, fosinoprilat, enalapril, enalaprilat, TMOF, BPP-12b, and luteolin were generated by assaying peptidyl dipeptidase activity of the high-speed supernatant prepared from a homogenate in the presence of different inhibitor concentrations using the assay described in the materials and methods section. Data is expressed relative to uninhibited activity.

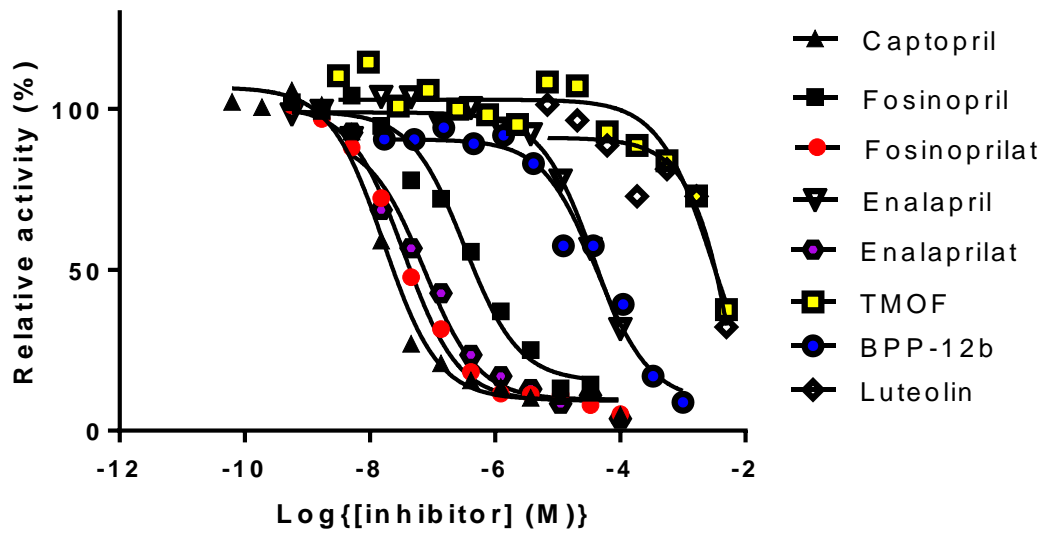


Figure 61 Inhibition of the peptidyl dipeptidase activity of *An. gambiae* larvae.

Inhibition curves for captopril, fosinopril, fosinoprilat, enalapril, enalaprilat, TMOF, BPP-12b, and luteolin were generated by assaying peptidyl dipeptidase activity of the high-speed supernatant prepared from a homogenate in the presence of different inhibitor concentrations using the assay described in the materials and methods section. Data is expressed relative to uninhibited activity.

Table 9 IC₅₀ values for the inhibition of larval peptidyl dipeptidase.

| Inhibitor | <i>Aedes aegypti</i> | <i>Anopheles gambiae</i> |
|------------------|----------------------------|----------------------------|
| | IC₅₀ (M) | IC₅₀ (M) |
| Captopril | 2.47E-09 | 1.67E-08 |
| Fosinopril | 3.73E-07 | 3.26E-07 |
| Fosinoprilat | 6.61E-09 | 3.52E-08 |
| Enalapril | 2.901E-06 | 4.06E-05 |
| Enalaprilat | 1.114E-08 | 7.32E-08 |
| TMOF | 0.0002158 | 0.003095 |
| BPP-12b | 1.40E-06 | 4.23E-05 |
| Luteolin | 5.00E-03 | 0.02423 |

6.2.2 The toxicity of captopril and fosinopril to larval instars of *Ae. aegypti* and *An. gambiae*

The effect of captopril and fosinopril on the development of larval stages of both *Ae. aegypti* and *An. gambiae* was investigated by adding the chemicals at a final concentration of 5 mM to the water environment together with the larval food followed by assessing mortality after 24, 48 and 72 hour (Table 10 and Table 11). High mortality was recorded after the first 24h for all three larval instars (L1, L2, and L3) of *Ae. aegypti* and by 48 hours essentially all L1 and L2 insects were dead. The L3 larvae were slightly more resistant to the chemical, nevertheless by 72 hours mortality of L3 insects had reached around 90%. Very similar results were obtained when L1 and L2 larvae of *An. gambiae* were treated in an identical manner with captopril. The L3 insects were, however, more resistant compared to *Ae. aegypti* at the same stage of development. Even after 72 hours only around 90% of the L3 insects had succumbed to the inhibitor.

High levels of mortality were also recorded for *Ae. aegypti* larvae treated with fosinopril, but this ACE inhibitor appeared to be less effective compared to captopril with the highest mortality occurring when L2 stages were exposed to the inhibitor. On the other hand fosinopril showed high levels of toxicity to all three instars of *An. gambiae* with over 80% mortality within 24 hours and over 95% mortality by 48 hours of treatment (Table 10 and Table 11).

Table 10 Larvicidal activity of captopril and fosinopril against *Aedes aegypti* larvae. Larvae were placed in water containing food with inhibitors. Mortality was assessed every 24 hours. Control and all surviving larvae successfully developed into pupae. Data are expressed as the mean \pm s.e.m., each n= 20, total n= 120.

24 hours

| Percentage of mortality (%) | L1 | L2 | L3 |
|-----------------------------|------------|-------------|-------------|
| Captopril (5 mM) | 99 \pm 2 | 90 \pm 11 | 58 \pm 11 |
| Fosinopril (5 mM) | 51 \pm 7 | 68 \pm 8 | 64 \pm 14 |

48 hours

| Percentage of mortality (%) | L1 | L2 | L3 |
|-----------------------------|------------|------------|-------------|
| Captopril (5 mM) | 100 | 99 \pm 2 | 64 \pm 9 |
| Fosinopril (5 mM) | 56 \pm 6 | 92 \pm 7 | 79 \pm 16 |

72 hours

| Percentage of mortality (%) | L1 | L2 | L3 |
|-----------------------------|------------|------------|-------------|
| Captopril (5 mM) | 100 | 100 | 88 \pm 9 |
| Fosinopril (5 mM) | 65 \pm 8 | 97 \pm 5 | 84 \pm 12 |

Table 11 Larvicidal activity of captopril and fosinopril against *Anopheles gambiae* larvae. Larvae were placed in water containing food with inhibitors. Mortality was assessed every 24 hours. Control and all surviving larvae successfully developed into pupae. Data are expressed as the mean \pm s.e.m., each n= 20, total n= 120.

24 hours

| Percentage of mortality (%) | L1 | L2 | L3 |
|-----------------------------|------------|-------------|-------------|
| Captopril (5 mM) | 96 \pm 9 | 93 \pm 7 | 7 \pm 10 |
| Fosinopril (5 mM) | 87 \pm 8 | 82 \pm 11 | 81 \pm 15 |

48 hours

| Percentage of mortality (%) | L1 | L2 | L3 |
|-----------------------------|------------|------------|------------|
| Captopril (5 mM) | 100 | 91 \pm 9 | 8 \pm 5 |
| Fosinopril (5 mM) | 99 \pm 3 | 99 \pm 3 | 94 \pm 9 |

72 hours

| Percentage of mortality (%) | L1 | L2 | L3 |
|-----------------------------|-----|-------------|-------------|
| Captopril (5 mM) | 100 | 94 \pm 11 | 10 \pm 10 |
| Fosinopril (5 mM) | 100 | 99 \pm 3 | 100 |

6.3 Discussion

ACE inhibitors fed to adult mosquitoes can have profound effects on female fecundity, suggesting that the mosquito peptidyl dipeptidase activity could become a target for the development of novel mosquito control chemicals (Ekbote *et al.*, 1999; Ekbote *et al.*, 2003a). The data reported in this chapter on the effects of ACE inhibitors on the development and survival of larval instars of both *Ae. aegypti* and *An. gambiae* support this view. Captopril was one of the first generation of orally active ACE inhibitors and is also the smallest (Kim *et al.*, 2003; Williams *et al.*, 1996). Key to the design of captopril was the inclusion of a sulfhydryl group that interacts with the active site zinc. Other ACE inhibitors can be of a larger design enabling interaction with more than two enzyme sub-sites and may have a different zinc-binding ligand (Acharya *et al.*, 2003). The pro-drug fosinopril has greater hydrophobicity to improve bioavailability and undergoes metabolic de-esterification to fosinoprilat, the active inhibitor. These chemical properties of fosinopril are likely to be important factors in determining the toxicity of the inhibitor in mosquito larvae.

BPP12b, a member of the BPP family of peptides originally isolated from the venom of the pit viper, *Bothrops jararaca*, was tested as an inhibitor of mosquito peptidyl dipeptidase and showed that the proline-rich peptide was a powerful natural inhibitor of the activity in both species. The presence of Pro-Pro dipeptide at the C-terminus and a pyroglutamate at the N-terminus protects these peptides from metabolic degradation by exo-peptidases (Soffer, 1976). TMOF is a mosquito peptide isolated from the ovaries of adult *Ae. aegypti* that is also proline rich and therefore it was not

surprising that it also inhibits mosquito larval peptidase activity, albeit with reduced potency relative to BPP12b. Luteolin inhibited larval ACE activity from both mosquito species, but was much weaker than both the synthetic and the peptide inhibitors.

The iACE gene family has expanded greatly in mosquitoes to nine and there is evidence that four *An. gambiae* genes (*AnoACE2*, *AnoACE3*, *AnoACE7* and *AnoACE9*) are expressed in larval stages. *AnoACE7* and *AnoACE9* are predicted to have a C-terminal hydrophobic sequence that can form a membrane anchor (Burnham *et al.*, 2005). Since the majority of the peptidyl dipeptidase activity in homogenates of larvae is soluble in nature, it seems likely that the activity results from expression of one or both of *AnoACE2* and *AnoACE3*.

Chapter 7
General Discussion

This Ph. D. project followed on from the earlier discovery that the MAG of the mosquito *Ae. aegypti* contained a high concentration (around 400 μ M) of the so-called head peptide (Aea-HP-1) which is passed to the female in seminal fluid (Naccarati *et al.*, 2012). The only known physiological response to this ‘sex’ peptide is the inhibition of female host-seeking, which suggests that the male can influence the behaviour of the post-mated female mosquito. Aea-HP-1 is a member of the extended RFa family of peptides that are widely distributed in insects. Insect myosuppressins also have a carboxy-terminal RFa (Nässel and Winther, 2010a). FlyAtlas database for the tissue distribution of *D. melanogaster* transcripts indicates strong expression and enrichment of myosuppressin (DMS) in the MAGs of this fruitfly (Chintapalli *et al.*, 2007). This strong expression in the MAGs suggested that the DMS was another ‘sex’ peptide that would be passed to the female during copulation alongside the well-known seminal fluid sex peptide (SP). If this was the case, then we would expect MALDI-MS to detect the peptide in tissue extracts as was the case for the mosquito Aea-HP-1 and *D. melanogaster* SP. Chapter 3 of this thesis indicates that this is not the case because despite extracting a large number of tissues and subjecting the extract to chromatography prior to mass spectrometry, no physical evidence for DMS was found. These results raised a major question regarding the exact location and the site of synthesis of this peptide, as well as its physiological role.

The mosquito Aea-HP-1 was isolated using an antibody that recognised the RFa epitope (Brown *et al.*, 1994). In the present study (Chapter 3), IHC using a similar commercial RFa antibody showed that RFa peptides were localised in neuronal processes innervating the male reproductive tissues in six drosophilid species, but no

evidence was obtained for this type of peptide in the MAG cells themselves. It is, however, difficult to prove the complete absence of a molecule especially from a relatively large structure such as the MAG. The Nichols laboratory using an antibody recognising the N-terminus of DMS had shown intense staining of two cells close to the HG, which were called the rectal cells (McCormick and Nichols, 1993). In chapter 3, not only are the rectal cells stained, but also a previously unreported third cell that is attached to the rectal cells and the ED, which has been called the ejaculatory duct (ED) cell. Difficulty in removing the ED cell and the paired rectal cells during dissection of the MAG might explain the high DMS transcript levels described in FlyAtlas for the MAGs.

Although previous publications reported the myoinhibitory roles of these RFa peptides on different insect tissues, it was important to investigate the role of the peptide in *D. melanogaster* itself. The RFa antibody used in chapter 3 does not distinguish between DMS, DSK, NPF, sNPF, or FMRFa peptides as they all end in RFa. Duttlinger *et al.*, suggest these structurally related peptides do not play redundant functions in the gut (Duttlinger *et al.*, 2002). Thus, it was important to identify individual peptides and determine their neuronal expression pattern to provide reliable information regarding sites of action and biological function. By comparing the RFa immuno-staining of the male reproductive tissues with GFP staining in *DMS>GFP* flies, we conclude that most, but not all, GFP expression in the neurons innervating the male reproductive tract co-stained with RFa and that DMS is an important neuropeptide involved in the control of the muscle of the male reproductive tissues. The DMS was not co-localised with 5-HT, which has been shown to stimulate contractions of the ED muscle and transfer sperm and seminal

fluid to the female. The 5-HT neurons are themselves activated by abdominal ganglion interneurons containing the neuropeptide corazonin (Tayler *et al.*, 2012). Activation of the 5-HT neurons resulted in premature transfer of both sperm and seminal fluid and shortened copulation time. The DMS neurons descend directly from the abdominal ganglion to project onto the MAG and ED.

Based on the single-cell mass spectrum data, DMS and sNPF⁴⁻¹¹ are expressed in the same ED cell in *D. melanogaster*. The question why both DMS and sNPF⁴⁻¹¹ are expressed in the same ED cell is interesting. It is likely that the RFa (DMS) expression in the ED cells of the other drosophilid species reported in Chapter 3 will contain sNPF⁴⁻¹¹ as well. The presence of both DMS and sNPF⁴⁻¹¹ in the same neurons might provide a backup or serve to potentiate each other. DMS is well known to inhibit the muscle contractions in several insects and sNPF⁴⁻¹¹ was reported to be also myoinhibitory on various insect visceral muscle (Nässel *et al.*, 2008; Schoofs *et al.*, 2001). Indeed, the inhibition of male ED and MAG muscle activity by both DMS and sNPF⁴⁻¹¹ as reported in chapter 4 supports this conclusion. In *Drosophila*, we suggest that the DMS and sNPF⁴⁻¹¹ have primary roles in inhibition of the contractions of the male reproductive tissues to manipulate the amount of the sperm and seminal fluid transferred during copulation.

For the reproductive tissues to respond to DMS they must express a cell surface receptor. DMS has been shown to activate two GPCRs (DMS-R1 and -R2) when expressed in mammalian cell lines. Since there were no antibodies available, *DMS-R-GAL4* lines from Janelia Research Campus and latterly from the Young-Joon Kim group were used to drive expression of GFP. The patterns obtained suggested that

DMS-R1 is located in myofibres and neurons, and that DMS-R2 is in endocrine cells and neurons. However, these results must be interpreted with caution as the GAL4-UAS system can generate ectopic expression unfaithful to the real expression pattern. *DMS-R1* and *DMS-R2* knockout flies have recently become available from the Young-Joon Kim group. MAGs and ED tissues from these flies can now be used in contraction assays to confirm which receptor is required for DMS inhibitory activity. DMS also inhibits the spontaneous contractions of the crop of adult *D. melanogaster* and it has been shown recently that the crop muscle from flies lacking *DMS-R1* is 1000-fold less sensitive to applied DMS, compared with crops from *DMS-R2* knockout flies (Petra Pribylova, personal communication). Future work will exploit the availability of these deletion mutants not only in contraction assays, but also to investigate the effect of the receptor mutations on reproduction and general growth and development.

Chapter 5 reports on the phenotypic consequence of a pan-neuronal knock-down of *DMS* expression, which resulted in an abnormal wing phenotype and adult mortality. This outcome suggests that DMS is not only important in inhibiting muscle activity, but may also have a wider role in insect development. Consistent with a role for DMS signalling in adult ecdysis, the *DMS-R2>GFP* flies showed strong GFP expression in the Inka cells, while GFP was in the second and adjacent cell of the epitracheal gland in *DMS-R1>GFP* flies. Inka cells are the source of ETH, the main initiator of ecdysis. The release of ETH from Inka cells in the moth, *Manduca sexta*, is triggered by the peptide hormone corazonin (Kim *et al.*, 2004). The role of the second epitracheal cell is not known (Dusan Zitnan, personal communication). The data reported here suggests that DMS from neuroendocrine cells is also involved in

the control of the release of ETH, at least in *D. melanogaster*. The lack of an ecdysis phenotype in the recently obtained DMSR-1 and DMSR-2 deletion mutants is at first sight problematic, however, there is a possibility that the normal ecdysis seen in these flies is because of functional redundancy or even the existence of a third receptor for DMS, e.g. the receptor for FMRFa (CG 2114) (Egerod *et al.*, 2003; Meeusen *et al.*, 2002).

In addition to the Inka cells, *DMS-R2>GFP* flies labelled cells of the CC endocrine cells and the enteroendocrine cells of the larval midgut (Chapter 5) suggesting that hormonal DMS regulates hormone secretion from these endocrine tissues. The insect gut is divided into foregut, midgut, and hindgut. The midgut is the only region with endocrine cells. The *Drosophila* midgut is separated by three regions; the anterior, middle, and posterior midgut. The posterior midgut is the region presumed to absorb most of the nutrients (Veenstra *et al.*, 2008). Preliminary data not presented in this thesis shows that the GFP expression in the midgut co-localises mainly with endocrine cells in the middle region that contain MIP (non-RFa myoinhibitory peptides) suggesting that MIP secretion is itself under hormonal control (Min *et al.*, 2016). The physiological role of the MIP enteroendocrine cell is not known, but might be related to peristaltic movement of the midgut.

The digestive physiology of insects is coordinated by the enteroendocrine cells and by enteric neurons of the hypercerebral ganglion. DMS fibres from the hypercerebral ganglion descend onto the anterior midgut muscle where they might control peristaltic contractions. They might also release DMS to activate DMS-R2 on the

surface of the midgut enteroendocrine cells. The role of this proposed pathway is currently being investigated (Petra Pribylova, personal communication).

There is a need for new strategies to control mosquito vectors that include chemical control. The novel data reported in chapter 6 provide support for the suggestion made by Isaac *et al.* that mosquito ACE is a potential new target for control chemicals (Isaac *et al.*, 1999). The availability of crystal structures of human and insect ACE proteins provide opportunity to use rational structure-based design to make inhibitors that are selective for the insect enzyme (Harrison and Acharya, 2014). A number of factors will determine the efficacy of the inhibitors as larvicides, including binding affinity to the enzyme, bioavailability, metabolic detoxification as well as chemical stability in the aquatic breeding environment. A particulate formulation and delivery system is probably required for the mosquito larvae feeding on detritus in their natural environment. Work in the School of Chemical and Process Engineering at the University of Leeds is currently developing a ‘smart’ nanoparticle delivery method that will release insecticidal molecules in the alkaline lumen of the gut (Calum Ferguson, personal communication). Such a delivery system will minimise dilution and protect the molecules whether synthetic inhibitors or peptides from degradation in the environment. It was not unexpected from its structure that TMOF would inhibit ACE. TMOF is involved in regulating egg development and blood digestion following a blood meal (Borovsky *et al.*, 1990). It appears to work by inhibiting the biosynthesis of midgut trypsin and not by inhibition of the protease activity (Borovsky, 2003). TMOF also inhibits trypsin biosynthesis in larval instars and has been used as a larvicide against *Ae. aegypti*. It is most effective when used in combination with δ -endotoxins from *Bacillus*

thuringiensis (Misni *et al.*, 2010). TMOF is not a particularly potent inhibitor of larval mosquito ACE, nevertheless this inhibition might contribute in a minor way to the toxicity against *Ae. aegypti* larvae. The evolutionary battle between plants and insects has generated a rich source of insecticidal (e.g. pyrethrum, neem) and deterrent chemicals (e.g. malathion, temephos) to help in the fight against crop and animal arthropod pests. Although the potency of the luteolin was poor, more extensive screening for more potent plant-derived ACE inhibitors might be of value in the search for a sustainable chemical control strategy.

Chapter 8

Conclusion

The work presented in this thesis increases our knowledge and understanding of the role of neuropeptides in the physiology of the male insect reproductive system, especially the role of DMS. Myosuppressin peptide family is widely distributed amongst insects and the information gleaned from working with *D. melanogaster* is likely to be relevant to other insect species, including pest species. There is increasing interest in the development of chemical insecticides targeting neuropeptides and peptide hormones through developing non-peptide mimetics and/or inhibitors of enzymes involved in neuropeptide metabolism. The information reported here on the role of DMS and its receptors on adult eclosion and gut physiology will encourage further studies in these areas. The work on ACE inhibitors as larvicides provides an exciting example of how disrupting neuropeptide/hormone metabolism can lead to new chemical control methods.

The work from this Ph. D. has been presented at the following international conferences: the Seventh International Symposium on Molecular Insect Science, Amsterdam, Netherlands (July, 2014); the 10th European Congress of Entomology, York, (August 2014); the Science@Malaysia Conference, University of Oxford, U.K. (Nov, 2014); the Invertebrate Neuropeptide Conference, Bagan, Myanmar (Feb, 2015); the Invertebrate Neuropeptide Conference, Ouro Preto, Brazil (Feb, 2016); the European Conference of Comparative Endocrinologists, Leuven, Belgium (Aug, 2016); and the Neurofly2016, Chania, Crete (Sep, 2016).

List of References

- Acharya, K.R., Sturrock, E.D., Riordan, J.F. and Ehlers, M.R. 2003. ACE revisited: a new target for structure-based drug design. *Nature Reviews Drug Discovery*. **2**(11), pp.891-902.
- Actis-Goretta, L., Ottaviani, J.I. and Fraga, C.G. 2006. Inhibition of angiotensin converting enzyme activity by flavanol-rich foods. *Journal of agricultural and food chemistry*. **54**(1), pp.229-234.
- Adams, M.D., Celniker, S.E., Holt, R.A., Evans, C.A., Gocayne, J.D., Amanatides, P.G., Scherer, S.E., Li, P.W., Hoskins, R.A. and Galle, R.F. 2000. The genome sequence of *Drosophila melanogaster*. *Science*. **287**(5461), pp.2185-2195.
- Adrion, J.R., Kousathanas, A., Pascual, M., Burrack, H.J., Haddad, N.M., Bergland, A.O., Machado, H., Sackton, T.B., Schlenke, T.A. and Watada, M. 2014. *Drosophila suzukii*: the genetic footprint of a recent, worldwide invasion. *Molecular biology and evolution*. **31**(12), pp.3148-3163.
- Asplen, M.K., Anfora, G., Biondi, A., Choi, D.-S., Chu, D., Daane, K.M., Gibert, P., Gutierrez, A.P., Hoelmer, K.A. and Hutchison, W.D. 2015. Invasion biology of spotted wing *Drosophila* (*Drosophila suzukii*): a global perspective and future priorities. *Journal of Pest Science*. **88**(3), pp.469-494.

- Audsley, N., Matthews, H.J., Down, R.E. and Weaver, R.J. 2011. Neuropeptides associated with the central nervous system of the cabbage root fly, *Delia radicum* (L). *Peptides*. **32**(3), pp.434-440.
- Avila, F.W., Mattei, A.L. and Wolfner, M.F. 2015. Sex peptide receptor is required for the release of stored sperm by mated *Drosophila melanogaster* females. *Journal of Insect Physiology*. **76**(0), pp.1-6.
- Avila, F.W., Sirot, L.K., LaFlamme, B.A., Rubinstein, C.D. and Wolfner, M.F. 2011. Insect seminal fluid proteins: identification and function. *Annual Review of Entomology*. **56**, pp.21-40.
- Baggerman, G., Boonen, K., Verleyen, P., De Loof, A. and Schoofs, L. 2005. Peptidomic analysis of the larval *Drosophila melanogaster* central nervous system by two-dimensional capillary liquid chromatography quadrupole time-of-flight mass spectrometry. *Journal of mass spectrometry*. **40**(2), pp.250-260.
- Baggerman, G., Cerstiaens, A., De Loof, A. and Schoofs, L. 2002. Peptidomics of the larval *Drosophila melanogaster* central nervous system. *Journal of Biological Chemistry*. **277**(43), pp.40368-40374.
- Billeter, J.C. and Goodwin, S.F. 2004. Characterization of *Drosophila fruitless-GAL4* transgenes reveals expression in male-specific fruitless neurons and innervation of male reproductive structures. *The Journal of Comparative Neurology*. **475**(2), pp.270-287.

- Boes, K.E., Ribeiro, J.M.C., Wong, A., Harrington, L.C., Wolfner, M.F. and Sirot, L.K. 2014. Identification and Characterization of Seminal Fluid Proteins in the Asian Tiger Mosquito, *Aedes albopictus*. *PLoS Negl Trop Dis.* **8**(6), pe2946.
- Borovsky, D. 2003. Trypsin-modulating oostatic factor: a potential new larvicide for mosquito control. *Journal of Experimental Biology.* **206**(21), pp.3869-3875.
- Borovsky, D., Carlson, D., Griffin, P., Shabanowitz, J. and Hunt, D. 1990. Mosquito oostatic factor: a novel decapeptide modulating trypsin-like enzyme biosynthesis in the midgut. *The FASEB Journal.* **4**(12), pp.3015-3020.
- Broeck, J.V. 2001. Neuropeptides and their precursors in the fruitfly, *Drosophila melanogaster*. *Peptides.* **22**(2), pp.241-254.
- Brown, M.R., Klowden, M.J., Crim, J.W., Young, L., Shrouder, L.A. and Lea, A.O. 1994. Endogenous regulation of mosquito host-seeking behavior by a neuropeptide. *Journal of insect physiology.* **40**(5), pp.399-406.
- Burnet, B., Connolly, K., Kearney, M. and Cook, R. 1973. Effects of male paragonial gland secretion on sexual receptivity and courtship behaviour of female *Drosophila melanogaster*. *Journal of insect physiology.* **19**(12), pp.2421-2431.
- Burnham, S., Smith, J.A., Lee, A.J., Isaac, R.E. and Shirras, A.D. 2005. The angiotensin-converting enzyme (ACE) gene family of *Anopheles gambiae*. *BMC genomics.* **6**(1), p1.

- Calabria, G., Máca, J., Bächli, G., Serra, L. and Pascual, M. 2012. First records of the potential pest species *Drosophila suzukii* (Diptera: Drosophilidae) in Europe. *Journal of Applied Entomology*. **136**(1-2), pp.139-147.
- Camargo, A.C., Ianzer, D., Guerreiro, J.R. and Serrano, S.M. 2012. Bradykinin-potentiating peptides: beyond captopril. *Toxicon*. **59**(4), pp.516-523.
- Capy, P., Pla, E. and David, J. 1993. Phenotypic and genetic variability of morphometrical traits in natural populations of *Drosophila melanogaster* and *D. simulans*. I. Geographic variations. *Genetics Selection Evolution*. **25**(6), p1.
- Carmel, I., Tram, U. and Heifetz, Y. 2016. Mating induces developmental changes in the insect female reproductive tract. *Current Opinion in Insect Science*. **13**, pp.106-113.
- Carvalho, G.B., Kapahi, P., Anderson, D.J. and Benzer, S. 2006. Allocrine Modulation of Feeding Behavior by the Sex Peptide of *Drosophila*. *Current Biology*. **16**(7), pp.692-696.
- Chapman, T., Liddle, L.F., Kalb, J.M., Wolfner, M.F. and Partridge, L. 1995. Cost of mating in *Drosophila melanogaster* females is mediated by male accessory gland products. *Nature*. **373**(6511), pp.241-244.
- Chen, P. 1984. The functional morphology and biochemistry of insect male accessory glands and their secretions. *Annual Review of Entomology*. **29**(1), pp.233-255.

- Chintapalli, V.R., Wang, J. and Dow, J.A.T. 2007. Using FlyAtlas to identify better *Drosophila melanogaster* models of human disease. *Natural Genetics*. **39**(6), pp.715-720.
- Claeys, I., Poels, J., Simonet, G., Franssens, V., Van Loy, T., Van Hiel, M.B., Breugelmans, B. and Broeck, J.V. 2005. Insect neuropeptide and peptide hormone receptors: current knowledge and future directions. *Vitamins & Hormones*. **73**, pp.217-282.
- Clynen, E., Husson, S.J. and Schoofs, L. 2009. Identification of new members of the (short) neuropeptide F family in locusts and *Caenorhabditis elegans*. *Annals of the New York Academy of Sciences*. **1163**(1), pp.60-74.
- Cornell, M.J., Williams, T.A., Lamango, N.S., Coates, D., Corvol, P., Soubrier, F., Hoheisel, J., Lehrach, H. and Isaac, R.E. 1995. Cloning and expression of an evolutionary conserved single-domain angiotensin converting enzyme from *Drosophila melanogaster*. *Journal of Biological Chemistry*. **270**(23), pp.13613-13619.
- Corvol, P., Michaud, A., Soubrier, F. and Williams, T.A. 1995. Recent advances in knowledge of the structure and function of the angiotensin I converting enzyme. *Journal of Hypertension*. **13**, pp.S3-S10.
- Cottrell, G. S. T. 2012. Aminopeptidase P1. In: N. D. S. Rawlings, G.S., ed. *Handbook of Proteolytic Enzyme*. Amsterdam Elsevier, pp. 1525-1528.

- Crozier, A., Jaganath, I.B. and Clifford, M.N. 2009. Dietary phenolics: chemistry, bioavailability and effects on health. *Natural product reports*. **26**(8), pp.1001-1043.
- Cushman, D.W. and Ondetti, M.A. 1991. History of the design of captopril and related inhibitors of angiotensin converting enzyme. *Hypertension*. **17**(4), pp.589-592.
- Dietzl, G., Chen, D., Schnorrer, F., Su, K., C-Barinova, Y, Fellner, M., Gasser, B., Kinsey, K.Oppel, S. and Scheiblauer, S. 2007. A genome-wide transgenic RNAi library for conditional gene inactivation in *Drosophila*. *Nature*. **448**(7150), pp.151-156.
- Domanitskaya, E.V., Liu, H., Chen, S. and Kubli, E. 2007. The hydroxyproline motif of male sex peptide elicits the innate immune response in *Drosophila* females. *FEBS Journal*. **274**(21), pp.5659-5668.
- Duffy, J.B. 2002. GAL4 system in *Drosophila*: a fly geneticist's Swiss army knife. *genesis*. **34**(1-2), pp.1-15.
- Duttlinger, A., Berry, K. and Nichols, R. 2002. The different effects of three *Drosophila melanogaster* dFMRFamide-containing peptides on crop contractions suggest these structurally related peptides do not play redundant functions in gut. *Peptides*. **23**(11), pp.1953-1957.
- Egerod, K., Reynisson, E., Hauser, F., Cazzamali, G., Williamson, M. and Grimmelikhuijzen, C.J. 2003. Molecular cloning and functional expression

of the first two specific insect myosuppressin receptors. *Proceedings of the National Academy of Sciences*. **100**(17), pp.9808-9813.

Eipper, B.A., Stoffers, D.A. and Mains, R.E. 1992. The biosynthesis of neuropeptides: peptide alpha-amidation. *Annual review of neuroscience*. **15**(1), pp.57-85.

Ekbote, U., Coates, D. and Isaac, R. 1999. A mosquito (*Anopheles stephensi*) angiotensin I-converting enzyme (ACE) is induced by a blood meal and accumulates in the developing ovary. *FEBS letters*. **455**(3), pp.219-222.

Ekbote, U., Looker, M. and Isaac, R.E. 2003a. ACE inhibitors reduce fecundity in the mosquito, *Anopheles stephensi*. *Comparative Biochemistry and Physiology Part B: Biochemistry and Molecular Biology*. **134**(4), pp.593-598.

Ekbote, U., Weaver, R. and Isaac, R. 2003b. Angiotensin I-converting enzyme (ACE) activity of the tomato moth, *Lacanobia oleracea*: changes in levels of activity during development and after copulation suggest roles during metamorphosis and reproduction. *Insect biochemistry and molecular biology*. **33**(10), pp.989-998.

Ellam, S. and Williamson, G. 2013. Cocoa and human health. *Annual review of nutrition*. **33**, pp.105-128.

Enayati, A. and Hemingway, J. 2010. Malaria management: past, present, and future. *Annual review of entomology*. **55**, pp.569-591.

- Erdös, E.G. and Skidgel, R.A. 1987. The angiotensin I-converting enzyme. *Laboratory investigation; a journal of technical methods and pathology*. **56**(4), p345.
- Ewer, J., Gammie, S.C. and Truman, J.W. 1997. Control of insect ecdysis by a positive-feedback endocrine system: roles of eclosion hormone and ecdysis triggering hormone. *Journal of Experimental Biology*. **200**(5), pp.869-881.
- Ferreira, S.H., Bartelt, D.C. and Greene, L.J. 1970. Isolation of bradykinin-potentiating peptides from *Bothrops jararaca* venom. *Biochemistry*. **9**(13), pp.2583-2593.
- Ferro, E.S., Rioli, V., Castro, L.M. and Fricker, L.D. 2014. Intracellular peptides: From discovery to function. *EuPA Open Proteomics*. **3**, pp.143-151.
- French, A.S., Simcock, K.L., Rolke, D., Gartside, S.E., Blenau, W. and Wright, G.A. 2014. The role of serotonin in feeding and gut contractions in the honeybee. *Journal of insect physiology*. **61**, pp.8-15.
- Fuchs, M. and Hiss, E. 1970. The partial purification and separation of the protein components of matrone from *Aedes aegypti*. *Journal of insect physiology*. **16**(5), pp.931-939.
- Gäde, G. and Kellner, R. 1992. Primary structures of the hypertrehalosemic peptides from corpora cardiaca of the primitive cockroach *Polyphaga aegyptiaca*. *General and comparative endocrinology*. **86**(1), pp.119-127.

- Gammie, S.C. and Truman, J.W. 1997. Neuropeptide hierarchies and the activation of sequential motor behaviors in the hawkmoth, *Manduca sexta*. *The Journal of neuroscience*. **17**(11), pp.4389-4397.
- Garbutt, J.S., Bellés, X., Richards, E.H. and Reynolds, S.E. 2013. Persistence of double-stranded RNA in insect hemolymph as a potential determiner of RNA interference success: evidence from *Manduca sexta* and *Blattella germanica*. *Journal of insect physiology*. **59**(2), pp.171-178.
- Gasque, G., Conway, S., Huang, J., Rao, Y. and Vosshall, L.B. 2013. Small molecule drug screening in *Drosophila* identifies the 5HT2A receptor as a feeding modulation target. *Scientific reports*. **3**. srep02120.
- Goodwin, S.F. 1999. Molecular neurogenetics of sexual differentiation and behaviour. *Current opinion in neurobiology*. **9**(6), pp.759-765.
- Griffith, L.C. 2012. Identifying behavioral circuits in *Drosophila melanogaster*: moving targets in a flying insect. *Current opinion in neurobiology*. **22**(4), pp.609-614.
- Guerrero, L., Castillo, J., Quinones, M., Garcia-Vallve, S., Arola, L., Pujadas, G. and Muguerza, B. 2012. Inhibition of angiotensin-converting enzyme activity by flavonoids: structure-activity relationship studies. *PLoS One*. **7**(11), pe49493.
- Haddow, A.D., Schuh, A.J., Yasuda, C.Y., Kasper, M.R., Heang, V., Huy, R., Guzman, H., Tesh, R.B. and Weaver, S.C. 2012. Genetic characterization of

Zika virus strains: geographic expansion of the Asian lineage. *PLoS Negl Trop Dis.* **6**(2), pe1477.

Harrison, C. and Acharya, K.R. 2014. ACE for all—a molecular perspective. *Journal of cell communication and signaling.* **8**(3), pp.195-210.

Hauser, F., Cazzamali, G., Williamson, M., Park, Y., Li, B., Tanaka, Y., Predel, R., Neupert, S., Schachtner, J. and Verleyen, P. 2008. A genome-wide inventory of neurohormone GPCRs in the red flour beetle *Tribolium castaneum*. *Frontiers in neuroendocrinology.* **29**(1), pp.142-165.

Hemingway, J. 2014. The role of vector control in stopping the transmission of malaria: threats and opportunities. *Phil. Trans. R. Soc. B.* **369**(1645), p20130431.

Hens, K., Vandingenen, A., Macours, N., Baggerman, G., Karaoglanovic, A.C., Schoofs, L., De Loof, A. and Huybrechts, R. 2002. Characterization of four substrates emphasizes kinetic similarity between insect and human C-domain angiotensin-converting enzyme. *European Journal of Biochemistry.* **269**(14), pp.3522-30.

Hidalgo, M., Martin-Santamaria, S., Recio, I., Sanchez-Moreno, C., de Pascual-Teresa, B., Rimbach, G. and de Pascual-Teresa, S. 2012. Potential anti-inflammatory, anti-adhesive, anti/estrogenic, and angiotensin-converting enzyme inhibitory activities of anthocyanins and their gut metabolites. *Genes & nutrition.* **7**(2), pp.295-306.

- Holman, G., Cook, B. and Nachman, R. 1986. Isolation, primary structure and synthesis of leucomyosuppressin, an insect neuropeptide that inhibits spontaneous contractions of the cockroach hindgut. *Comparative Biochemistry and Physiology Part C: Comparative Pharmacology*. **85**(2), pp.329-333.
- Horodyski, F.M., Ewer, J., Riddiford, L.M. and Truman, J.W. 1993. Isolation, characterization and expression of the eclosion hormone gene of *Drosophila melanogaster*. *European journal of biochemistry*. **215**(2), pp.221-228.
- Huang, W.Y., Davidge, S.T. and Wu, J. 2013. Bioactive natural constituents from food sources—potential use in hypertension prevention and treatment. *Critical reviews in food science and nutrition*. **53**(6), pp.615-630.
- Huang, Y., Liu, Z. and Rong, Y.S. 2016. Genome Editing: From *Drosophila* to Non-Model Insects and Beyond. *Journal of Genetics and Genomics*. **43**(5), pp.263-272.
- Isaac, R.E., Ekbote, U., Coates, D. and Shirras, A.D. 1999. Insect Angiotensin-converting Enzyme: A Processing Enzyme with Broad Substrate Specificity and a Role in Reproduction. *Annals of the New York Academy of Sciences*. **897**(1), pp.342-347.
- Isaac, R.E., Lamango, N.S., Ekbote, U., Taylor, C.A., Hurst, D., Weaver, R.J., Carhan, A., Burnham, S. and Shirras, A.D. 2007a. Angiotensin-converting enzyme as a target for the development of novel insect growth regulators. *Peptides*. **28**(1), pp.153-162.

- Isaac, R.E., Li, C., Leedale, A.E. and Shirras, A.D. 2010. *Drosophila* male sex peptide inhibits siesta sleep and promotes locomotor activity in the post-mated female. *Proceedings of the Royal Society B: Biological Sciences*. **277**(1678), pp.65-70.
- Isaac, R.E. and Shirras, A.D. 2013. Peptidyl-Dipeptidase A (Invertebrate). *Handbook of Proteolytic Enzymes, Vols 1 and 2, 3rd Edition*. pp.494-498.
- Ito, K., Okada, R., Tanaka, N.K. and Awasaki, T. 2003. Cautionary observations on preparing and interpreting brain images using molecular biology-based staining techniques. *Microscopy research and technique*. **62**(2), pp.170-186.
- Jenett, A., Rubin, G.M., Ngo, T.T., Shepherd, D., Murphy, C., Dionne, H., Pfeiffer, B.D., Cavallaro, A., Hall, D. and Jeter, J. 2012. A GAL4-driver line resource for *Drosophila* neurobiology. *Cell reports*. **2**(4), pp.991-1001.
- Johansson, M.A., Dominici, F. and Glass, G.E. 2009. Local and global effects of climate on dengue transmission in Puerto Rico. *PLoS Negl Trop Dis*. **3**(2), pe382.
- Johnson, O., Becnel, J. and Nichols, C.D. 2009. Serotonin 5-HT1A-like, 5-HT2, and 5-HT7 receptors modulate learning and memory in *Drosophila*. *The FASEB Journal*. **23**(1_MeetingAbstracts), p586.11.
- Johnson, O., Becnel, J. and Nichols, C.D. 2011. Serotonin receptor activity is necessary for olfactory learning and memory in *Drosophila melanogaster*. *Neuroscience*. **192**, pp.372-381.

- Kim, H.M., Shin, D.R., Yoo, O.J., Lee, H. and Lee, J.-O. 2003. Crystal structure of *Drosophila* angiotensin I-converting enzyme bound to captopril and lisinopril 1. *FEBS letters*. **538**(1-3), pp.65-70.
- Kim, Y.-J., Spalovská-Valachová, I., Cho, K.-H., Zitnanova, I., Park, Y., Adams, M.E. and Žitňan, D. 2004. Corazonin receptor signaling in ecdysis initiation. *Proceedings of the National Academy of Sciences of the United States of America*. **101**(17), pp.6704-6709.
- Kim, Y.-J., Žitňan, D., Galizia, C.G., Cho, K.-H. and Adams, M.E. 2006. A command chemical triggers an innate behavior by sequential activation of multiple peptidergic ensembles. *Current Biology*. **16**(14), pp.1395-1407.
- Kingan, T., Shabanowitz, J., Hunt, D. and Witten, J. 1996. Characterization of two myotrophic neuropeptides in the FMRFamide family from the segmental ganglia of the moth *Manduca sexta*: candidate neurohormones and neuromodulators. *Journal of Experimental Biology*. **199**(5), pp.1095-1104.
- Kiss, A., Kowalski, J. and Melzig, M.F. 2004. Compounds from *Epilobium angustifolium* inhibit the specific metallopeptidases ACE, NEP and APN. *Planta medica*. **70**(10), pp.919-923.
- Kiss, B., Szlanka, T., Zvara, Á., Žurovec, M., Sery, M., Kakaš, Š., Ramasz, B., Hegedűs, Z., Lukacsovich, T. and Puskás, L. 2013. Selective elimination/RNAi silencing of FMRF-related peptides and their receptors decreases the locomotor activity in *Drosophila melanogaster*. *General and comparative endocrinology*. **191**, pp.137-145.

- Klowden, M.J. 1999. The check is in the male: male mosquitoes affect female physiology and behavior. *Journal of the American Mosquito Control Association*. **15**(2), pp.213-220.
- Kubli, E. 2003. Sex-peptides: seminal peptides of the *Drosophila* male. *Cellular and Molecular Life Sciences CMLS*. **60**(8), pp.1689-1704.
- Kwon, E.-K., Lee, D.-Y., Lee, H., Kim, D.-O., Baek, N.-I., Kim, Y.-E. and Kim, H.-Y. 2009. Flavonoids from the buds of *Rosa damascena* inhibit the activity of 3-hydroxy-3-methylglutaryl-coenzyme a reductase and angiotensin I-converting enzyme. *Journal of agricultural and food chemistry*. **58**(2), pp.882-886.
- Lacaille-Dubois, M., Franck, U. and Wagner, H. 2001. Search for potential angiotensin converting enzyme (ACE)-inhibitors from plants. *Phytomedicine*. **8**(1), pp.47-52.
- LaJeunesse, D.R., Johnson, B., Presnell, J.S., Catignas, K.K. and Zapotoczny, G. 2010. Peristalsis in the junction region of the *Drosophila* larval midgut is modulated by DH31 expressing enteroendocrine cells. *BMC physiology*. **10**(1), p1.
- Lamango, N., Nachman, R., Hayes, T., Strey, A. and Isaac, R. 1997. Hydrolysis of insect neuropeptides by an angiotensin-converting enzyme from the housefly, *Musca domestica*. *Peptides*. **18**(1), pp.47-52.

- Lamango, N.S., Sajid, M. and Isaac, R.E. 1996. The endopeptidase activity and the activation by Cl⁻ of angiotensin-converting enzyme is evolutionarily conserved: purification and properties of an an angiotensin-converting enzyme from the housefly, *Musca domestica*. *Biochemical Journal*. **314**(2), pp.639-646.
- Lee, G., Vilella, A., Taylor, B.J. and Hall, J.C. 2001. New reproductive anomalies in fruitless-mutant *Drosophila* males: Extreme lengthening of mating durations and infertility correlated with defective serotonergic innervation of reproductive organs. *Journal of Neurobiology*. **47**(2), pp.121-149.
- Lee, J.J. and Klowden, M.J. 1999. A male accessory gland protein that modulates female mosquito (Diptera: Culicidae) host-seeking behavior. *Journal of the American Mosquito Control Association*. **15**(1), pp.4-7.
- Lee, T. and Luo, L. 1999. Mosaic analysis with a repressible cell marker for studies of gene function in neuronal morphogenesis. *Neuron*. **22**(3), pp.451-461.
- Leopold, R., Terranova, A., Thorson, B. and Degrugillier, M. 1971. The biosynthesis of the male housefly accessory secretion and its fate in the mated female. *Journal of Insect Physiology*. **17**(6), pp.987-1003.
- Liu, H. and Kubli, E. 2003. Sex-peptide is the molecular basis of the sperm effect in *Drosophila melanogaster*. *Proceedings of the National Academy of Sciences*. **100**(17), pp.9929-9933.

- Loizzo, M.R., Said, A., Tundis, R., Rashed, K., Statti, G.A., Hufner, A. and Menichini, F. 2007. Inhibition of angiotensin converting enzyme (ACE) by flavonoids isolated from *Ailanthus excelsa* (Roxb)(Simaroubaceae). *Phytotherapy Research*. **21**(1), pp.32-36.
- Lung, O., Tram, U., Finnerty, C.M., Eipper-Mains, M.A., Kalb, J.M. and Wolfner, M.F. 2002. The *Drosophila melanogaster* seminal fluid protein Acp62F is a protease inhibitor that is toxic upon ectopic expression. *Genetics*. **160**(1), pp.211-224.
- Luo, J., Becnel, J., Nichols, C.D. and Nässel, D.R. 2012. Insulin-producing cells in the brain of adult *Drosophila* are regulated by the serotonin 5-HT1A receptor. *Cellular and Molecular Life Sciences*. **69**(3), pp.471-484.
- Macours, N., Vandingenen, A., Gielens, C., Hens, K., Baggerman, G., Schoofs, L. and Huybrechts, R. 2003. Isolation of angiotensin converting enzyme from the testes of *Locusta migratoria* (Orthoptera). *European Journal of Entomology*. **100**, pp.467-474.
- Matsumoto, S., Brown, M.R., Crim, J.W., Vigna, S.R. and Lea, A.O. 1989. Isolation and primary structure of neuropeptides from the mosquito, *Aedes aegypti*, immunoreactive to FMRFamide antiserum. *Insect biochemistry*. **19**(3), pp.277-283.
- Matsumura, S. 1931. 6000 illustrated insects of Japan-Empire.

- McCormick, J. and Nichols, R. 1993. Spatial and temporal expression identify dromyosuppressin as a brain-gut peptide in *Drosophila melanogaster*. *Journal of Comparative Neurology*. **338**(2), pp.279-288.
- McNabb, S.L., Baker, J.D., Agapite, J., Steller, H., Riddiford, L.M. and Truman, J.W. 1997. Disruption of a behavioral sequence by targeted death of peptidergic neurons in *Drosophila*. *Neuron*. **19**(4), pp.813-823.
- McNeil, G.P., Zhang, X., Genova, G. and Jackson, F.R. 1998. A molecular rhythm mediating circadian clock output in *Drosophila*. *Neuron*. **20**(2), pp.297-303.
- Meeusen, T., Mertens, I., Clynen, E., Baggerman, G., Nichols, R., Nachman, R.J., Huybrechts, R., De Loof, A. and Schoofs, L. 2002. Identification in *Drosophila melanogaster* of the invertebrate G protein-coupled FMRFamide receptor. *Proceedings of the National Academy of Sciences*. **99**(24), pp.15363-15368.
- Min, S., Chae, H.-S., Jang, Y.-H., Choi, S., Lee, S., Jeong, Y.T., Jones, W.D., Moon, S.J., Kim, Y.-J. and Chung, J. 2016. Identification of a peptidergic pathway critical to satiety responses in *Drosophila*. *Current Biology*. **26**(6), pp.814-820.
- Misni, N., Othman, H. and Sulaiman, S. 2010. Larvicidal effect of trypsin modulating oostatic factor (TMOF) formulations on *Aedes aegypti* larvae in the Laboratory. *J Trop Med Parasitol*. **33**, pp.69-76.

- Moffat, K.G., Gould, J.H., Smith, H.K. and O'Kane, C.J. 1992. Inducible cell ablation in *Drosophila* by cold-sensitive ricin A chain. *Development*. **114**(3), pp.681-687.
- Naccarati, C., Audsley, N., Keen, J.N., Kim, J.-H., Howell, G.J., Kim, Y.-J. and Isaac, R.E. 2012. The host-seeking inhibitory peptide, Aea-HP-1, is made in the male accessory gland and transferred to the female during copulation. *Peptides*. **34**(1), pp.150-157.
- Nässel, D.R. 1993. Neuropeptides in the insect brain: a review. *Cell and tissue research*. **273**(1), pp.1-29.
- Nässel, D.R. 2000. Functional roles of neuropeptides in the insect central nervous system. *Naturwissenschaften*. **87**(10), pp.439-449.
- Nässel, D.R. 2002. Neuropeptides in the nervous system of *Drosophila* and other insects: multiple roles as neuromodulators and neurohormones. *Progress in neurobiology*. **68**(1), pp.1-84.
- Nässel, D.R., Enell, L.E., Santos, J.G., Wegener, C. and Johard, H.A. 2008. A large population of diverse neurons in the *Drosophila* central nervous system expresses short neuropeptide F, suggesting multiple distributed peptide functions. *BMC neuroscience*. **9**(1), p90.
- Nässel, D.R. and Winther, Å.M. 2010b. *Drosophila* neuropeptides in regulation of physiology and behavior. *Progress in neurobiology*. **92**(1), pp.42-104.

- Neckameyer, W.S. 2010. A trophic role for serotonin in the development of a simple feeding circuit. *Developmental neuroscience*. **32**(3), pp.217-237.
- Neupert, S., Johard, H.A., Nässel, D.R. and Predel, R. 2007. Single-cell peptidomics of *Drosophila melanogaster* neurons identified by GAL4-driven fluorescence. *Analytical chemistry*. **79**(10), pp.3690-3694.
- Nichols, R. 1992a. Isolation and expression of the *Drosophila* drosulfakinin neural peptide gene product, DSK-I. *Molecular and Cellular Neuroscience*. **3**(4), pp.342-347.
- Nichols, R. 1992b. Isolation and structural characterization of *Drosophila* TDVDHVFLRFamide and FMRFamide-containing neural peptides. *Journal of molecular neuroscience: MN*. **3**(4), p213.
- Nichols, R., McCormick, J. and Lim, I. 1999. Structure, Function, and Expression of *Drosophila melanogaster* FMRFamide-related Peptides. *Annals of the New York Academy of Sciences*. **897**(1), pp.264-272.
- Norville, K., Sweeney, S.T. and Elliott, C.J.H. 2010. Postmating Change in Physiology of Male *Drosophila* Mediated by Serotonin (5-HT). *Journal of Neurogenetics*. **24**(1), pp.27-32.
- Oh, H., Kang, D.-G., Kwon, J.-W., Kwon, T.-O., Lee, S.-Y., Lee, D.-B. and Lee, H.-S. 2004. Isolation of angiotensin converting enzyme (ACE) inhibitory flavonoids from *Sedum sarmentosum*. *Biological and Pharmaceutical Bulletin*. **27**(12), pp.2035-2037.

- Ondetti, M. 1991. Angiotensin converting enzyme inhibitors. An overview. *Hypertension*. **18**(5 Suppl), pIII134.
- Ondetti, M.A., Rubin, B. and Cushman, D.W. 1977. Design of specific inhibitors of angiotensin-converting enzyme: new class of orally active antihypertensive agents. *Science*. **196**(4288), pp.441-444.
- Park, Y., Zitnan, D., Gill, S.S. and Adams, M.E. 1999. Molecular cloning and biological activity of ecdysis-triggering hormones in *Drosophila melanogaster*. *FEBS Letters*. **463**(1), pp.133-138.
- Pauls, D., Chen, J., Reiher, W., Vanselow, J.T., Schlosser, A., Kahnt, J. and Wegener, C. 2014. Peptidomics and processing of regulatory peptides in the fruit fly *Drosophila*. *EuPA Open Proteomics*. **3**(0), pp.114-127.
- Peeff, N.M., Orchard, I. and Lange, A.B. 1994. Isolation, sequence, and bioactivity of PDVDHVFLRFamide and ADVGHVFLRFamide peptides from the locust central nervous system. *peptides*. **15**(3), pp.387-392.
- Persson, I.A.L., Dong, L. and Persson, K. 2006. Effect of Panax ginseng extract (G115) on angiotensin-converting enzyme (ACE) activity and nitric oxide (NO) production. *Journal of ethnopharmacology*. **105**(3), pp.321-325.
- Persson, I.A.L., Persson, K., Hägg, S. and Andersson, R.G. 2010. Effects of green tea, black tea and Rooibos tea on angiotensin-converting enzyme and nitric oxide in healthy volunteers. *Public health nutrition*. **13**(05), pp.730-737.

- Persson, I.A.L. 2012. The Pharmacological Mechanism of Angiotensin-converting Enzyme Inhibition by Green Tea, Rooibos and Enalaprilat—A Study on Enzyme Kinetics. *Phytotherapy Research*. **26**(4), pp.517-521.
- Pfeiffer, B.D., Jenett, A., Hammonds, A.S., Ngo, T.T.B., Misra, S., Murphy, C., Scully, A., Carlson, J.W., Wan, K.H. and Lavery, T.R. 2008. Tools for neuroanatomy and neurogenetics in *Drosophila*. *Proceedings of the National Academy of Sciences*. **105**(28), pp.9715-9720.
- Pfeiffer, B.D., Ngo, T.T.B., Hibbard, K.L., Murphy, C., Jenett, A., Truman, J.W. and Rubin, G.M. 2010. Refinement of Tools for Targeted Gene Expression in *Drosophila*. *Genetics*. **186**(2), pp.735-755.
- Pfeiffer, B.D., Truman, J.W. and Rubin, G.M. 2012. Using translational enhancers to increase transgene expression in *Drosophila*. *Proceedings of the National Academy of Sciences*. **109**(17), pp.6626-6631.
- Poels, J., Verlinden, H., Fichna, J., Van Loy, T., Franssens, V., Studzian, K., Janecka, A., Nachman, R.J. and Broeck, J.V. 2007. Functional comparison of two evolutionary conserved insect neurokinin-like receptors. *Peptides*. **28**(1), pp.103-108.
- Poiani, A. 2006. Complexity of seminal fluid: a review. *Behavioral Ecology and Sociobiology*. **60**(3), pp.289-310.

- Pooryasin, A. and Fiala, A. 2015. Identified serotonin-releasing neurons induce behavioral quiescence and suppress mating in *Drosophila*. *The Journal of Neuroscience*. **35**(37), pp.12792-12812.
- Predel, R., Nachman, R.J. and Gäde, G. 2001. Myostimulatory neuropeptides in cockroaches: structures, distribution, pharmacological activities, and mimetic analogs. *Journal of insect physiology*. **47**(4), pp.311-324.
- Predel, R., Wegener, C., Russell, W.K., Tichy, S.E., Russell, D.H. and Nachman, R.J. 2004. Peptidomics of CNS-associated neurohemal systems of adult *Drosophila melanogaster*: A mass spectrometric survey of peptides from individual flies. *Journal of Comparative Neurology*. **474**(3), pp.379-392.
- Price, D.A. and Greenberg, M.J. 1977. Structure of a molluscan cardioexcitatory neuropeptide. *Science*. **197**(4304), pp.670-671.
- Quiñones, M., Miguel, M. and Aleixandre, A. 2013. Beneficial effects of polyphenols on cardiovascular disease. *Pharmacological Research*. **68**(1), pp.125-131.
- Ram, K.R. and Wolfner, M.F. 2007. Sustained Post-Mating Response in *Drosophila melanogaster* Requires Multiple Seminal Fluid Proteins. *PLoS Genet*. **3**(12), pe238.
- Reid, W. and O'Brochta, D.A. 2016. Applications of genome editing in insects. *Current Opinion in Insect Science*. **13**, pp.43-54.

- Reiher, W., Shirras, C., Kahnt, J.R., Baumeister, S., Isaac, R.E. and Wegener, C. 2011. Peptidomics and peptide hormone processing in the *Drosophila* midgut. *Journal of proteome research*. **10**(4), pp.1881-1892.
- Richer, S., Stoffolano Jr, J.G., Yin, C.M. and Nichols, R. 2000. Innervation of dromyosuppressin (DMS) immunoreactive processes and effect of DMS and benzethonium chloride on the *Phormia regina* (Meigen) crop. *The Journal of Comparative Neurology*. **421**(1), pp.136-142.
- Robb, S. and Evans, P. 1994. The modulatory effect of SchistoFLRFamide on heart and skeletal muscle in the locust *Schistocerca gregaria*. *Journal of Experimental Biology*. **197**(1), pp.437-442.
- Robb, S., Packman, L.C. and Evans, P.D. 1989. Isolation, primary structure and bioactivity of SchistoFLRF-amide, a FMRF-amide-like neuropeptide from the locust, *Schistocerca gregaria*. *Biochemical and biophysical research communications*. **160**(2), pp.850-856.
- Röser, C., Jordan, N., Balfanz, S., Baumann, A., Walz, B., Baumann, O. and Blenau, W. 2012. Molecular and pharmacological characterization of serotonin 5-HT_{2α} and 5-HT₇ receptors in the salivary glands of the blowfly *Calliphora vicina*. *PLoS One*. **7**(11), pe49459.
- Rylett, C.M., Walker, M.J., Howell, G.J., Shirras, A.D. and Isaac, R.E. 2007. Male accessory glands of *Drosophila melanogaster* make a secreted angiotensin I-converting enzyme (ANCE), suggesting a role for the peptide-processing

enzyme in seminal fluid. *Journal of Experimental Biology*. **210**(20), pp.3601-3606.

Ryner, L.C., Goodwin, S.F., Castrillon, D.H., Anand, A., Vilella, A., Baker, B.S., Hall, J.C., Taylor, B.J. and Wasserman, S.A. 1996. Control of male sexual behavior and sexual orientation in *Drosophila* by the fruitless gene. *Cell*. **87**(6), pp.1079-1089.

Schaffer, M.H., Noyes, B.E., Slaughter, C.A., Thorne, G. and Gaskell, S. 1990. The fruitfly *Drosophila melanogaster* contains a novel charged adipokinetic-hormone-family peptide. *Biochemical Journal*. **269**(2), pp.315-320.

Schoofs, L., Clynen, E., Cerstiaens, A., Baggerman, G., Wei, Z., Vercammen, T., Nachman, R., De Loof, A. and Tanaka, S. 2001. Newly discovered functions for some myotropic neuropeptides in locusts. *Peptides*. **22**(2), pp.219-227.

Schoofs, L., Veelaert, D., Broeck, J.V. and De Loof, A. 1997. Peptides in the locusts, *Locusta migratoria* and *Schistocerca gregaria*. *Peptides*. **18**(1), pp.145-156.

Silva, B., Goles, N.I., Varas, R. and Campusano, J.M. 2014. Serotonin receptors expressed in *Drosophila* mushroom bodies differentially modulate larval locomotion. *PloS one*. **9**(2), pe89641.

Sirot, L.K., Poulson, R.L., Caitlin McKenna, M., Girnary, H., Wolfner, M.F. and Harrington, L.C. 2008. Identity and transfer of male reproductive gland proteins of the dengue vector mosquito, *Aedes aegypti*: Potential tools for

control of female feeding and reproduction. *Insect Biochemistry and Molecular Biology*. **38**(2), pp.176-189.

Siviter, R.J., Nachman, R.J., Dani, M.P., Keen, J.N., Shirras, A.D. and Isaac, R.E. 2002. Peptidyl dipeptidases (Ance and Acer) of *Drosophila melanogaster*: major differences in the substrate specificity of two homologs of human angiotensin I-converting enzyme. *Peptides*. **23**(11), pp.2025-2034.

Soffer, R.L. 1976. Angiotensin-converting enzyme and the regulation of vasoactive peptides. *Annual review of biochemistry*. **45**(1), pp.73-94.

Sturtevant, A. 1920. Genetic studies on *Drosophila simulans*. I. Introduction. Hybrids with *Drosophila melanogaster*. *Genetics*. **5**(5), p488.

Susic-Jung, L., Hornbruch-Freitag, C., Kuckwa, J., Rexer, K.-H., Lammel, U. and Renkawitz-Pohl, R. 2012. Multinucleated smooth muscles and mononucleated as well as multinucleated striated muscles develop during establishment of the male reproductive organs of *Drosophila melanogaster*. *Developmental Biology*. **370**(1), pp.86-97.

Taylor, T.D., Pacheco, D.A., Hergarden, A.C., Murthy, M. and Anderson, D.J. 2012. A neuropeptide circuit that coordinates sperm transfer and copulation duration in *Drosophila*. *Proceedings of the National Academy of Sciences*. **109**(50), pp.20697-20702.

Terhzaz, S., O'Connell, F.C., Pollock, V.P., Kean, L., Davies, S.A., Veenstra, J.A. and Dow, J.A. 1999. Isolation and characterization of a leucokinin-like

peptide of *Drosophila melanogaster*. *Journal of Experimental Biology*. **202**(24), pp.3667-3676.

Thomsen, E.K., Strode, C., Hemmings, K., Hughes, A.J., Chanda, E., Musapa, M., Kamuliwo, M., Phiri, F.N., Muzia, L. and Chanda, J. 2014. Underpinning sustainable vector control through informed insecticide resistance management. *PloS one*. **9**(6), pe99822.

Tinoco, A.D. and Saghatelian, A. 2011. Investigating endogenous peptides and peptidases using peptidomics. *Biochemistry*. **50**(35), pp.7447-7461.

Vandingenen, A., Hens, K., Macours, N., Schoofs, L., De Loof, A. and Huybrechts, R. 2002. Presence of angiotensin converting enzyme (ACE) interactive factors in ovaries of the grey fleshfly *Neobellieria bullata*. *Comparative Biochemistry and Physiology Part B: Biochemistry and Molecular Biology*. **132**(1), pp.27-35.

Vandingenen, A., Hens, K., Macours, N., Zhu, W., Janssen, I., Breuer, M., De Loof, A. and Huybrechts, R. 2001. Captopril, a specific inhibitor of angiotensin converting enzyme, enhances both trypsin and vitellogenin titers in the grey fleshfly *Neobellieria bullata*. *Archives of insect biochemistry and physiology*. **47**(3), pp.161-167.

Veenstra, J.A. 1999. Isolation and identification of three RFamide-immunoreactive peptides from the mosquito *Aedes aegypti*. *Peptides*. **20**(1), pp.31-38.

- Veenstra, J.A. 2016. Neuropeptide evolution: Chelicerate neurohormone and neuropeptide genes may reflect one or more whole genome duplications. *General and comparative endocrinology*. **229**, pp.41-55.
- Veenstra, J.A., Agricola, H.-J. and Sellami, A. 2008. Regulatory peptides in fruit fly midgut. *Cell and Tissue Research*. **334**(3), pp.499-516.
- Veenstra, J.A. and Hagedorn, H.H. 1995. Isolation of two AKH-related peptides from cicadas. *Archives of insect biochemistry and physiology*. **29**(4), pp.391-396.
- Venken, K.J., Simpson, J.H. and Bellen, H.J. 2011. Genetic manipulation of genes and cells in the nervous system of the fruit fly. *Neuron*. **72**(2), pp.202-230.
- Vercruyse, L., Gelman, D., Raes, E., Hooghe, B., Vermeirssen, V., Van Camp, J. and Smagghe, G. 2004. The angiotensin converting enzyme inhibitor captopril reduces oviposition and ecdysteroid levels in Lepidoptera. *Archives of insect biochemistry and physiology*. **57**(3), pp.123-132.
- Wegener, C., Neupert, S. and Predel, R. 2010. Direct MALDI-TOF mass spectrometric peptide profiling of neuroendocrine tissue of *Drosophila*. *Peptidomics: Methods and Protocols*. pp.117-127.
- Wegener, C., Reinl, T., Jansch, L. and Predel, R. 2006. Direct mass spectrometric peptide profiling and fragmentation of larval peptide hormone release sites in *Drosophila melanogaster* reveals tagma-specific peptide expression and differential processing. *Journal of neurochemistry*. **96**(5), pp.1362-1374.

- White, B.H. and Ewer, J. 2014. Neural and hormonal control of postecdysial behaviors in insects. *Annual review of entomology*. **59**, pp.363-381.
- White, K., Hurteau, T. and Punsal, P. 2004. Neuropeptide-Fmrfamide-Like immunoreactivity in *Drosophila*: Development and distribution. *The Journal of Comparative Neurology*. **247**(4), pp.430-438.
- Wijffels, G., Fitzgerald, C., Gough, J., Riding, G., Elvin, C., Kemp, D. and Willadsen, P. 1996. Cloning and Characterisation of Angiotensin-Converting Enzyme from the Dipteran Species, *Haematobia irritans exigua*, and Its Expression in the Maturing Male Reproductive System. *European journal of biochemistry*. **237**(2), pp.414-423.
- Williams, D.W., Tyrer, M. and Shepherd, D. 2000. Tau and tau reporters disrupt central projections of sensory neurons in *Drosophila*. *Journal of Comparative Neurology*. **428**(4), pp.630-640.
- Williams, T.A., Michaud, A., Houard, X., Chauvet, M.-T., Soubrier, F. and Corvol, P. 1996. *Drosophila melanogaster* angiotensin I-converting enzyme expressed in *Pichia pastoris* resembles the C domain of the mammalian homologue and does not require glycosylation for secretion and enzymic activity. *Biochemical Journal*. **318**(1), pp.125-131.
- Winther, A. and Nassel, D. 2001. Intestinal peptides as circulating hormones: release of tachykinin-related peptide from the locust and cockroach midgut. *Journal of Experimental Biology*. **204**(7), pp.1269-1280.

- Winther, Å.M., Siviter, R.J., Isaac, R.E., Predel, R. and Nässel, D.R. 2003. Neuronal expression of tachykinin-related peptides and gene transcript during postembryonic development of *Drosophila*. *Journal of Comparative Neurology*. **464**(2), pp.180-196.
- Wolfner, M.F. 1997. Tokens of love: functions and regulation of *Drosophila* male accessory gland products. *Insect Biochemistry and Molecular Biology*. **27**(3), pp.179-192.
- Wu, W.-H. and Cooper, R.L. 2012. Serotonin and synaptic transmission at invertebrate neuromuscular junctions. *Experimental neurobiology*. **21**(3), pp.101-112.
- Xu, J., Baulding, J. and Palli, S.R. 2013. Proteomics of *Tribolium castaneum* seminal fluid proteins: Identification of an angiotensin-converting enzyme as a key player in regulation of reproduction. *Journal of Proteomics*. **78**, pp.83-93.
- Yang, C.S. and Hong, J. 2013. Prevention of chronic diseases by tea: possible mechanisms and human relevance. *Annual review of nutrition*. **33**, pp.161-181.
- Yew, J.Y., Wang, Y., Barteneva, N., Dikler, S., Kutz-Naber, K.K., Li, L. and Kravitz, E.A. 2009. Analysis of neuropeptide expression and localization in adult *Drosophila melanogaster* central nervous system by affinity cell-capture mass spectrometry. *Journal of proteome research*. **8**(3), pp.1271-1284.

- Yuan, Q., Joiner, W.J. and Sehgal, A. 2006. A sleep-promoting role for the *Drosophila* serotonin receptor 1A. *Current Biology*. **16**(11), pp.1051-1062.
- Zhou, L., Schnitzler, A., Agapite, J., Schwartz, L., Steller, H. and Nambu, J. 1997. Cooperative functions of the reaper and head involution defective genes in the programmed cell death of *Drosophila* central nervous system midline cells. *Proceedings of the National Academy of Sciences*. **94**(10), pp.5131-5136.
- Zitnan, D. and Adams, M.E. 2000. Excitatory and inhibitory roles of central ganglia in initiation of the insect ecdysis behavioural sequence. *Journal of Experimental Biology*. **203**(8), pp.1329-1340.
- Žitňan, D., Kim, Y.-J., Žitňanová, I., Roller, L. and Adams, M. 2007. Complex steroid-peptide-receptor cascade controls insect ecdysis. *General and comparative endocrinology*. **153**(1), pp.88-96.
- Žitňan, D., Kingan, T.G., Hermesman, J.L. and Adams, M.E. 1996. Identification of ecdysis-triggering hormone from an epitracheal endocrine system. *Science*. **271**(5245), pp.88-91.
- Žitňan, D., Žitňanová, I., Spalovska, I., Takáč, P., Park, Y. and Adams, M. 2003. Conservation of ecdysis-triggering hormone signalling in insects. *Journal of experimental biology*. **206**(8), pp.1275-1289.

Žitňan, D., Ross, L.S., Žitňanová, I., Hermesman, J.L., Gill, S.S. and Adams, M.E.

1999. Steroid induction of a peptide hormone gene leads to orchestration of a defined behavioral sequence. *Neuron*. **23**(3), pp.523-535.

Appendix A

Attempted crosses

Several attempts of parental crosses have been done to study the effect of silencing the DMS on insect's development (Appendix A).

| Genetic combinations | F1 phenotype |
|---|--------------|
| <i>DMS-GAL4</i> (39278)> <i>DMS-RNAi</i> (108760) | Wild-type |
| <i>nSyb-GAL4/UAS-dicr2</i> >VDRC 9370 CG 8985, <i>DMSR-1</i> | Wild-type |
| <i>nSyb-GAL4/UAS-dicr2</i> >VDRC 9369 CG 8985, <i>DMSR-1</i> | Wild-type |
| <i>nSyb-GAL4/UAS-dicr2</i> >VDRC 101845 <i>DMSR-1</i> | Wild-type |
| <i>nSyb-GAL4/UAS-dicr2</i> >IR-1-128, VDRC GD 42304, <i>DMSR-2-RNAi-1</i> (II) | Wild-type |
| <i>nSyb-GAL4/UAS-dicr2</i> >IR-1-129. VDRC GD 49952, <i>DMSR-2-RNAi-2</i> (II) | Wild-type |
| <i>nSyb-GAL4/UAS-dicr2</i> >IR-1-130, VDRC GD 49953, <i>DMSR-2-RNAi-2</i> (III) | Wild-type |
| <i>ETH GAL4 -1</i> (II)>IR-1-128, VDRC GD 42304, <i>DMSR-2-RNAi-1</i> (II) | Wild-type |
| <i>ETH-GAL4 -1</i> (II)>IR-1-129. VDRC GD 49952, <i>DMSR-2-RNAi-2</i> (II) | Wild-type |
| <i>ETH-GAL4 -1</i> (II)>IR-1-130, VDRC GD 49953, <i>DMSR-2-RNAi-2</i> (III) | Wild-type |
| <i>ETH-GAL4 -2</i> (II)>IR-1-128, VDRC GD 42304, <i>DMSR-2-</i> | Wild-type |

| | |
|--|-----------|
| RNAi-1(II) | |
| <i>ETH-GAL4 -2(II)>IR-1-129</i> . VDRC GD 49952, <i>DMSR-2-</i> | Wild-type |
| RNAi-2(II) | |
| <i>ETH-GAL4 -2(II)>IR-1-130</i> , VDRC GD 49953, <i>DMSR-2-</i> | Wild-type |
| RNAi-2(III) | |
| <i>ETH-GAL4 -1(II)>VDRC 9370 CG 8985</i> , <i>DMSR-1</i> | Wild-type |
| <i>ETH-GAL4 -1(II)>VDRC 9369 CG 8985</i> , <i>DMSR-1</i> | Wild-type |
| <i>ETH-GAL4 -1(II)>VDRC 101845</i> <i>DMSR-1</i> | Wild-type |
| <i>ETH-GAL4 -2 (II)>VDRC 9370 CG 8985</i> , <i>DMSR-1</i> | Wild-type |
| <i>ETH-GAL4 -2(II)>VDRC 9369 CG 8985</i> , <i>DMSR-1</i> | Wild-type |
| <i>ETH-GAL4 -2(II)>VDRC 101845</i> , <i>DMSR-1</i> | Wild-type |
| <i>Actin 5C-GAL4 >IR-1-128</i> , VDRC GD 42304, <i>DMSR-2-RNAi-</i> | Wild-type |
| 1(II) | |
| <i>Actin 5C-GAL4 >IR-1-129</i> . VDRC GD 49952, <i>DMSR-2-RNAi-</i> | Wild-type |
| 2(II) | |
| <i>Actin 5C-GAL4 >IR-1-130</i> , VDRC GD 49953, <i>DMSR-2-RNAi-</i> | Wild-type |
| 2(III) | |
| <i>Actin 5C-GAL4 >VDRC 9370 CG 8985</i> , <i>DMSR-1</i> | Wild-type |
| <i>Actin 5C-GAL4 >VDRC 9369 CG 8985</i> , <i>DMSR-1</i> | Wild-type |
| <i>Actin 5C-GAL4 >VDRC 101845</i> <i>DMSR-1</i> | Wild-type |
| <i>DMSR-2 (39399)>IR-1-128</i> , VDRC GD 42304, <i>DMSR-2-</i> | Wild-type |
| RNAi-1(II) | |
| <i>DMSR-2 (39399)>IR-1-129</i> . VDRC GD 49952, <i>DMSR-2-</i> | Wild-type |
| RNAi-2(II) | |
| <i>DMSR-2 (39399)>IR-1-130</i> , VDRC GD 49953, <i>DMSR-2-</i> | Wild-type |

RNAi-2(III)

| | |
|--|-----------|
| <i>DMSR-1</i> (48230)>VDRC 9370 CG 8985, <i>DMSR-1</i> | Wild-type |
| <i>DMSR-1</i> (48230)>VDRC 9369 CG 8985, <i>DMSR-1</i> | Wild-type |
| <i>DMSR-1</i> (48230)>VDRC 101845 <i>DMSR-1</i> | Wild-type |
